

Many-Body Superconductivity in Topological Flat Bands

Jonah Herzog-Arbeitman¹, Aaron Chew¹, Kukka-Emilia Huhtinen², Päivi Törmä², and B. Andrei Bernevig^{1,3,4}

¹*Department of Physics, Princeton University, Princeton, NJ 08544*

²*Department of Applied Physics, Aalto University School of Science, FI-00076 Aalto, Finland*

³*Donostia International Physics Center, P. Manuel de Lardizabal 4, 20018 Donostia-San Sebastian, Spain and*

⁴*IKERBASQUE, Basque Foundation for Science, Bilbao, Spain*

(Dated: September 2, 2022)

In a flat band superconductor, bosonic excitations can disperse while unpaired electrons are immobile. To study this strongly interacting system, we construct a family of multi-band Hubbard models with exact eta-pairing ground states in all space groups. We analytically compute their many-body excitations and find that the Cooper pair bound states and density excitations obey an effective single-particle Hamiltonian written in terms of the non-interacting wavefunctions. These bound states possess a unique zero-energy excitation whose quadratic dispersion is determined by the minimal quantum metric. The rest of the bound state spectrum is classified by topological quantum chemistry, which we use to identify Cooper pairs with Weyl nodes, higher angular momentum pairing, and fragile topology. We also add electron kinetic energy as a perturbation to show that the strongest pairing occurs at half filling and not at the highest density of states. This is similar in spirit to the superconductivity observed in twisted bilayer graphene.

Attractive interactions among electrons can lead to a pairing instability at the Fermi surface and create a superconducting ground state at low temperatures. Both the weakly and strongly interacting limits of these systems can be described by attractive Hubbard models. Such models, however, are rarely exactly solvable. Recent work^{1–14} has generated great interest in flat band superconductivity where electrons are completely immobile without interactions. A mean-field calculation in the multiband Hubbard model shows¹⁵ that the superfluid weight can be non-zero due to quantum geometry¹⁶, indicating mobile Cooper pairs despite the infinite effective mass of the unpaired electrons. Lower bounds on the superfluid weight have been obtained from topology^{15,17,18} and symmetry¹⁹. While numerical beyond-mean-field work exists^{3,8,19–24} and confirms the mean-field picture, the few exact approaches on the attractive Hubbard model governing flat band superconductivity have been limited to ground state properties¹⁸ or one dimension⁵. In this Letter, we show that the *many-body* problem is analytically tractable in any dimension subject to a simple requirement called the uniform pairing condition^{15,18}. Our exact results characterize not only the superconducting ground state, but also its excitations which control the low-temperature behavior.

We consider tight-binding models with electron operators $c_{\mathbf{k},\alpha,\sigma}^\dagger$ with spin $\sigma = \uparrow, \downarrow$, orbital $\alpha = 1, \dots, N_{orb}$, and momentum \mathbf{k} in the Brillouin zone (BZ). Throughout, we assume S_z spin conservation, e.g. no spin-orbit coupling. We consider kinetic terms with flat bands at zero energy labeled by $m = 1, \dots, N_f$ separated by a large gap to the other bands (see Fig. 1b for example). We assume the gap is much larger than the interaction strength $|U|$. Under this approximation, the kinetic term is completely characterized by the single-particle eigenvectors of the flat bands which form the $N_{orb} \times N_f$ matrix $[U_\sigma(\mathbf{k})]_{\alpha m}$. By orthonormality, $U_\sigma^\dagger(\mathbf{k})U_\sigma(\mathbf{k}) = \mathbb{1}_{N_f}$, and $P_{\alpha\beta}^\sigma(\mathbf{k}) = [U_\sigma(\mathbf{k})U_\sigma^\dagger(\mathbf{k})]_{\alpha\beta}$ is a rank N_f projector, or \mathbf{k} -

space correlation function²⁵. The gap to the other bands can be sent adiabatically to infinity so all operators can be projected into the flat bands spanned by

$$\bar{c}_{\mathbf{k},\alpha,\sigma}^\dagger = \sum_\beta c_{\mathbf{k},\beta,\sigma}^\dagger P_{\beta\alpha}^\sigma(\mathbf{k}), \quad \{\bar{c}_{\mathbf{k}',\alpha,\sigma}, \bar{c}_{\mathbf{k},\beta,\sigma}^\dagger\} = \delta_{\mathbf{k}\mathbf{k}'} P_{\alpha\beta}^\sigma(\mathbf{k}) \quad (1)$$

which form an overcomplete basis due to the projection (App. A). The canonical flat band operators $\gamma_{\mathbf{k},m,\sigma}^\dagger = \sum_\alpha c_{\mathbf{k},\alpha,\sigma}^\dagger U_{\alpha,m}^\sigma(\mathbf{k})$ alternatively form a complete basis of the projected Hilbert space. For brevity, we define $P(\mathbf{k}) = P^\dagger(\mathbf{k})$. We assume S_z conservation and spinful time-reversal symmetry \mathcal{T} which yields $P^\dagger(\mathbf{k}) = P(-\mathbf{k})^*$.

Hamiltonian. The N_f flat bands have zero kinetic energy and the remaining bands are projected out, so the kinetic term is zero and only interactions remain. We study an attractive Hubbard model proposed in Ref.¹⁸,

$$H = \frac{|U|}{2} \sum_{\mathbf{R}\alpha} (\bar{n}_{\mathbf{R},\alpha,\uparrow} - \bar{n}_{\mathbf{R},\alpha,\downarrow})^2, \quad \bar{n}_{\mathbf{R},\alpha,\sigma} = \bar{c}_{\mathbf{R},\alpha,\sigma}^\dagger \bar{c}_{\mathbf{R},\alpha,\sigma} \quad (2)$$

where $\bar{c}_{\mathbf{R},\alpha,\sigma}^\dagger$ is the Fourier transform of $\bar{c}_{\mathbf{k},\alpha,\sigma}^\dagger$. If we impose the uniform pairing condition (UPC)^{15,18}

$$\frac{1}{\mathcal{N}} \sum_{\mathbf{k}} P_{\alpha\alpha}(\mathbf{k}) = \frac{N_f}{N_{orb}} \equiv \epsilon \leq 1 \quad (3)$$

where the α -independent constant ϵ is fixed by $\text{Tr } P(\mathbf{k}) = N_f$, and \mathcal{N} is the number of unit cells, then we find

$$H = \frac{\epsilon|U|}{2} \bar{N} - \sum_{\mathbf{R}\alpha} \bar{n}_{\mathbf{R},\alpha,\uparrow} \bar{n}_{\mathbf{R},\alpha,\downarrow} \quad (4)$$

which is the usual Hubbard model up to a chemical potential (note that $\bar{N} = \sum_{\mathbf{R}\alpha\sigma} \bar{n}_{\mathbf{R},\alpha,\sigma}$ is the projected number operator). The UPC thus allows to relate the flat band Hubbard Hamiltonian to the positive-definite

Hamiltonian Eq. (2), which is crucial to analytically solving the ground states and excitations.

Intuitively, if the orbitals are related by symmetry, the UPC should hold¹⁸. Indeed, we prove that Eq. (3) is enforced by symmetry. Our proof (App. A 2) uses Schur's lemma and some basic facts from topological quantum chemistry^{26–30}. We show that if the orbitals of the model can all be related by a symmetry operator (technically, if they form an irrep of a Wyckoff position), then the UPC holds. Thus the class of flat bands with the UPC is very large, and encompasses existing examples^{4,5,8,10,19,31–33}.

There is a generalization¹⁸ of Eq. (3): if the flat band wavefunction $[U_\sigma(\mathbf{k})]_{\alpha m}$ vanishes on some orbitals $\tilde{\alpha}$, then $\bar{n}_{\mathbf{R},\tilde{\alpha},\sigma} = 0$ and the UPC is only required on $\alpha \neq \tilde{\alpha}$. Calugaru et al.³⁴ construct models with $N_f = N_L - N_{\tilde{L}}$ perfectly flat bands on bipartite lattices consisting of two sublattices L, \tilde{L} with $[U_\sigma(\mathbf{k})]_{\tilde{\alpha} m} = 0$ where N_L ($N_{\tilde{L}}$) is the number of orbitals in L (\tilde{L}) per unit cell. Choosing the L lattice to have the UPC, their method constructs exactly flat bands with the UPC in all space groups. In this case, Eq. (3) holds with $\epsilon = N_f/N_L$. In this manner, we construct a 10 band model (see Fig. 1) with the momentum space irreps of twisted bilayer graphene (TBG)^{35–37} and the UPC (see Fig. 1), but with Wilson loop winding^{38–40} 2 (instead of 1 as in TBG).

Superconducting Ground States. Originally, H in Eq. (2) was proposed to exhibit an exact BCS-type groundstate despite the ill-defined Fermi surface of the flat band¹⁸. In this work, we instead focus on the more physical ground states at *fixed* particle number. We define the local spin operator $\tilde{S}_{\mathbf{R},\alpha}^z = \bar{n}_{\mathbf{R},\alpha,\uparrow} - \bar{n}_{\mathbf{R},\alpha,\downarrow}$ appearing in Eq. (2). Because of the projection, $\tilde{c}_{\mathbf{R},\alpha,\sigma}^\dagger$ is extended on the scale of the correlation length, which cannot be adiabatically sent to zero (the atomic limit) if the bands are topological or obstructed¹⁹. This is crucial for superconductivity in transport since trivial flat bands in the atomic limit would make $H = \frac{|U|}{2} \sum_{\mathbf{R},\alpha} (\tilde{S}_{\mathbf{R},\alpha}^z)^2$ a sum of commuting local terms with trivial dynamics and macroscopic degeneracies. Away from the trivial limit, H retains a single nontrivial symmetry operator η

$$[\eta^\dagger, \tilde{S}_{\mathbf{R},\alpha}^z] = 0, \quad \eta^\dagger = \sum_{\mathbf{k}\alpha} \tilde{c}_{\mathbf{k},\alpha,\uparrow}^\dagger \tilde{c}_{-\mathbf{k},\alpha,\downarrow}^\dagger = \sum_{\mathbf{R}\alpha} \tilde{c}_{\mathbf{R},\alpha,\uparrow}^\dagger \tilde{c}_{\mathbf{R},\alpha,\downarrow}^\dagger. \quad (5)$$

This result relies on the UPC, global S_z conservation, and \mathcal{T} (App. B). Here η^\dagger is simply the creation operator of a zero-momentum s -wave Cooper pair, and it forms an $su(2)$ algebra, $[\tilde{N}, \eta^\dagger] = 2\eta^\dagger$, which extends $U(1)$ charge conservation¹⁸. We define the states $|n\rangle \propto \eta^{\dagger n} |0\rangle$ which have fixed particle number $\tilde{N} |n\rangle = 2n |n\rangle$ for $n = 0, \dots, \mathcal{N}N_f$. Yang first introduced similar eta-pairing states⁴¹ on the square lattice, which is also bipartite. However, his operators carried momentum π and were not ground states. In contrast, $|n\rangle$ must be ground states because H is positive semi-definite, and $H |n\rangle \propto \eta^{\dagger n} H |0\rangle = 0$.

Because $|n\rangle$ differs from the BCS-BEC^{42,43} states $e^{z\eta^\dagger} |0\rangle$ (which are also exact ground states¹⁸), it may

not be apparent that they describe a bosonic condensate. To establish this, we show that $|n\rangle$ has off-diagonal long-range order in the two-particle density matrix⁴⁴; this is intuitive since the η pairs are superpositions of pairs on *all* sites. In the states $|n\rangle$, a generalized Wick's theorem^{45–47} holds for the correlators of the Wannier state operators $w_{\mathbf{R}m\sigma}^\dagger = \frac{1}{\sqrt{\mathcal{N}}} \sum_{\mathbf{k}\alpha} e^{i\mathbf{R}\cdot\mathbf{k}} \gamma_{\mathbf{k},m,\sigma}^\dagger$ obeying $\{w_{\mathbf{R},m,\sigma}, w_{\mathbf{R}',m',\sigma'}^\dagger\} = \delta_{\mathbf{R},\mathbf{R}'} \delta_{m,m'} \delta_{\sigma,\sigma'}$. We find (App. C)

$$\lim_{|\mathbf{R}-\mathbf{R}'| \rightarrow \infty} \langle n | w_{\mathbf{R}'m'\downarrow}^\dagger w_{\mathbf{R}'m'\uparrow}^\dagger w_{\mathbf{R}m\uparrow} w_{\mathbf{R}m\downarrow} | n \rangle = \nu(1-\nu) \quad (6)$$

in the thermodynamic limit where $\nu = n/N_f\mathcal{N}$ is the filling. Clearly the strongest condensate appears at half-filling of the flat bands. Similar dependence on the filling appears in mean-field results on the multi-band Hubbard model¹⁵ which also indicate half-filling is favorable for the superconductor. We remark that the Wannier operators have a gauge freedom corresponding to the redefinition of eigenvectors $U_\sigma(\mathbf{k}) \rightarrow U_\sigma(\mathbf{k})\mathcal{W}_\sigma(\mathbf{k})$ where $\mathcal{W}_\sigma(\mathbf{k}) \in U(N_f)$ ^{48–56}. Nevertheless, Eq. (6) shows that the resulting correlator is gauge-invariant. This condensate ground state is a universal result in all UPC lattices.

Electron Excitations. The presence of an enlarged symmetry algebra and exact ground states suggests that more features of H may be accessible. We now show that the electron (and hole) excitations above the $|n\rangle$ ground states are exactly solvable. Our procedure^{57–60} is to add a single electron $\gamma_{\mathbf{k},m,\sigma}^\dagger$ to the ground state and calculate

$$H \gamma_{\mathbf{k},m,\sigma}^\dagger |n\rangle = [H, \gamma_{\mathbf{k},m,\sigma}^\dagger] |n\rangle = \sum_{m'} \gamma_{\mathbf{k},m',\sigma}^\dagger |n\rangle [R^\sigma(\mathbf{k})]_{m'm} \quad (7)$$

since $H |n\rangle = 0$. Diagonalizing $R^\sigma(\mathbf{k})$, one obtains the charge +1 (electron) excitation spectrum and the eigenstates. Using $H = \frac{|U|}{2} \sum_{\mathbf{q}\alpha} \tilde{S}_{-\mathbf{q},\alpha}^z \tilde{S}_{\mathbf{q},\alpha}^z$ where $\tilde{S}_{\mathbf{q},\alpha}^z$ is the Fourier transform of $\tilde{S}_{\mathbf{R},\alpha}^z$ and $\tilde{S}_{\mathbf{q},\alpha}^z |n\rangle = 0$, we find

$$\begin{aligned} [H, \gamma_{\mathbf{k},m,\sigma}^\dagger] |n\rangle &= \frac{|U|}{2} \sum_{\mathbf{q}\alpha} [\tilde{S}_{-\mathbf{q},\alpha}^z, [\tilde{S}_{\mathbf{q},\alpha}^z, \gamma_{\mathbf{k},m,\sigma}^\dagger]] |n\rangle \\ &= \frac{|U|}{2\mathcal{N}} \sum_{\mathbf{q}\alpha, m'l} M_{\sigma,\alpha}^{m'l}(\mathbf{k} + \mathbf{q}, -\mathbf{q}) M_{\sigma,\alpha}^{lm}(\mathbf{k}, \mathbf{q}) \gamma_{\mathbf{k},m',\sigma}^\dagger |n\rangle \end{aligned} \quad (8)$$

defining $M_{\alpha,\sigma}^{mn}(\mathbf{k}, \mathbf{q}) = U_{\alpha m}^{\sigma*}(\mathbf{k} + \mathbf{q}) U_{\alpha n}^\sigma(\mathbf{k})$ as the orbital-resolved form factors (App. D 1). Matching Eq. (8) to Eq. (7) and simplifying the form factors yields

$$\begin{aligned} [R^\sigma(\mathbf{k})]_{m'm} &= \frac{|U|}{2\mathcal{N}} \sum_{\mathbf{q}\alpha} U_{\alpha m'}^{\sigma*}(\mathbf{k}) P_{\alpha\alpha}^\sigma(\mathbf{k} + \mathbf{q}) U_{\alpha m}^\sigma(\mathbf{k}) \\ &= \frac{\epsilon|U|}{2} \sum_{\alpha} U_{\alpha m'}^{\sigma*}(\mathbf{k}) U_{\alpha m}^\sigma(\mathbf{k}) = \frac{\epsilon|U|}{2} \delta_{m'm} \end{aligned} \quad (9)$$

where the UPC, Eq. (3), was crucial to compute the \mathbf{q} sum. Hence, the electron excitations are independent of ν , N_f -degenerate per spin, and exactly flat meaning that the single-electron excitations are immobile. Indeed,

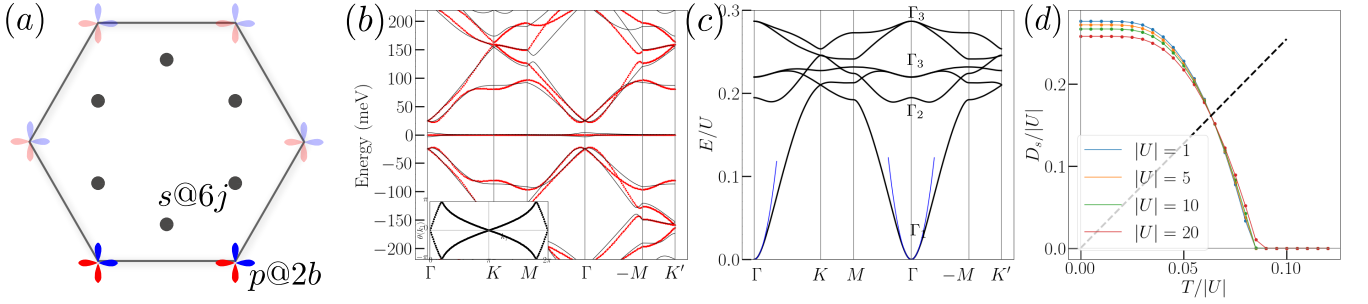


FIG. 1. Ten band model inspired by TBG. (a) A bipartite lattice of s (p) orbitals at the $6j$ ($2b$) Wyckoff positions reproduces the momentum space irreps^{36–38} of the Bistritzer-MacDonald (BM) model³⁵ with uniform pairing. (b) Band structure of the 10-band model (red) and BM model (black) with Wilson loop inset. (c) Cooper pair spectrum with the minimal quantum metric approximation in blue. p -wave pairing Leggett modes appear above the zero-energy s -wave mode (App. F). (d) Superfluid weight D_s from mean-field theory in units where $e, \hbar, k_B = 1$. The BKT temperature $T_c = \frac{\pi}{8} D_s(T_c)$ is estimated at $T_c \approx 0.06|U|$.

a mean-field treatment assuming a \mathbf{k} -independent pairing gap reproduces the $\epsilon|U|/2$ s -wave gap⁶¹. The temperature scale $\epsilon|U|$ describes the onset of pairing, but is expected to be somewhat above the superconducting critical temperature with a pseudogap intervening^{5,62–64}.

The electronic excitations characterize the stability of the superconducting phase, as in BCS theory. When dispersion is added to the flat bands, as in realistic systems, we determine the filling where superconductivity is strongest through the Richardson criterion^{57,65,66} $E_\Delta(N+2) = E(N+2) - 2E(N+1) + E(N)$ where $E(N)$ is the ground state energy at particle number N . Here E_Δ is an estimate of the Cooper pair binding energy: $E_\Delta < 0$ indicates the favorability of pair formation (at $T = 0$). We can compute $E_\Delta(N)$ perturbatively when dispersion $\tilde{E}_n(\mathbf{k})$ is added to the flat bands. For convenience, we assume $\sum_{\mathbf{k},n} \tilde{E}_n(\mathbf{k}) = 0$ in which case (App. D 2)

$$-E_\Delta(\nu) = \epsilon|U| - |1 - 2\nu|\tilde{E}_\nu \quad (10)$$

where $\tilde{E}_\nu > 0$ is $\max_{\mathbf{k},n} \tilde{E}_n(\mathbf{k})$ ($|\min_{\mathbf{k},n} \tilde{E}_n(\mathbf{k})|$) for $\nu \geq 1/2$ ($\nu < 1/2$). Hence the strongest Cooper pair binding occurs at $\nu = \frac{1}{2}$, where the condensate is also strongest (see Eq. (6)) in agreement with multi-band mean-field results¹⁵, but in contrast to conventional BCS theory where pairing is maximized at the highest density of states. This echoes the phenomenology of twisted bilayer graphene where critical temperature is highest *not* at the van Hove singularities of the flat bands^{67–71}. Eq. (10) is not valid when spin-orbit coupling is added, but we provide a general formula in App. D 2.

Cooper Pair Excitations and Bound States. We now show that the two-particle excitations, containing the Cooper pair and density excitation spectrum, are analytically solvable. We will also find a set of excitations (Leggett modes⁷²) in other pairing channels. We find that these modes can carry higher angular momentum, e.g. d -wave symmetry, and fragile topology. Our calculation shows in microscopic detail the formation of bosons from the underlying fermion bands.

The two-body excitations are characterized by their

global quantum numbers, S_z spin and charge. We start in the charge $+2$ sector and compute the scattering matrix

$$\begin{aligned} & [H, \gamma_{\mathbf{p}+\mathbf{k},m,\sigma}^\dagger \gamma_{-\mathbf{k},n,\sigma'}^\dagger] |n\rangle \\ &= \sum_{\mathbf{k}'m'n'} \gamma_{\mathbf{p}+\mathbf{k}',m',\sigma}^\dagger \gamma_{-\mathbf{k}',n',\sigma'}^\dagger |n\rangle [R^{\sigma\sigma'}(\mathbf{p})]_{\mathbf{k}'m'n',\mathbf{k}mn} \end{aligned} \quad (11)$$

which is a function of the total momentum \mathbf{p} . The commutator can be computed since $\tilde{S}_{\mathbf{R},\alpha}^z |n\rangle = 0$. The full scattering matrix can be written (App. D 3)

$$R^{\sigma\sigma'}(\mathbf{p}) = \epsilon|U| \mathbb{1} + s_\sigma^z s_{\sigma'}^z \frac{|U|}{N} \mathcal{U}_{\sigma\sigma'}(\mathbf{p}) \mathcal{U}_{\sigma\sigma'}^\dagger(\mathbf{p}) \quad (12)$$

where $s_{\uparrow/\downarrow}^z = \pm 1$ and $[\mathcal{U}_{\sigma\sigma'}(\mathbf{p})]_{\mathbf{k}mn,\alpha} = U_{m\alpha}^{\sigma*}(\mathbf{p} + \mathbf{k}) U_{n\alpha}^{\sigma'}(-\mathbf{k})$ is a $\mathcal{N}N_f^2 \times N_L$ matrix (\mathcal{N} is the number of \mathbf{k} points). If $\sigma = \sigma'$, then $\mathcal{U}_{\sigma\sigma}(\mathbf{p})$ is symmetric under $\mathbf{p} + \mathbf{k}, m \leftrightarrow -\mathbf{k}, n$ whereas the fermion operators in Eq. (11) are anti-symmetric. Hence the anti-symmetrization of the fermions annihilates the $\mathcal{U}_{\sigma\sigma}(\mathbf{p}) \mathcal{U}_{\sigma\sigma}^\dagger(\mathbf{p})$ term, so all spin-aligned states have energy $\epsilon|U|$ for all \mathbf{p} and are completely unpaired.

We now consider $\sigma = -\sigma'$. Denote $R^{\uparrow\downarrow}(\mathbf{p}) = \epsilon|U| \mathbb{1} - \mathcal{U}(\mathbf{p}) \mathcal{U}^\dagger(\mathbf{p}) / \mathcal{N}$, dropping spin labels for brevity. First, note that $\text{rank } \mathcal{U} \mathcal{U}^\dagger \leq \text{rank } \mathcal{U} \leq N_L$ and hence $\mathcal{U} \mathcal{U}^\dagger$ has a very large kernel of dimension at least $\mathcal{N}N_f^2 - N_L$, corresponding to the particle-particle continuum. Its nonzero eigenvalues are identical to the eigenvalues of the $N_L \times N_L$ matrix $h(\mathbf{p}) = \mathcal{U}^\dagger(\mathbf{p}) \mathcal{U}(\mathbf{p}) / \mathcal{N}$. This pairing Hamiltonian takes the universal form (App. D 3)

$$h_{\alpha\beta}(\mathbf{p}) = \frac{1}{\mathcal{N}} \sum_{\mathbf{k}} P_{\alpha\beta}(\mathbf{k} + \mathbf{p}) P_{\beta\alpha}(\mathbf{k}) \quad (13)$$

which can be interpreted as the effective single-particle Hamiltonian describing the hopping of a tightly bound Cooper pair (App. E 2). However, we emphasize that the Eq. (13) derives from an exact many-body calculation, and its eigenvalues are precisely the binding energies of the various pairing channels.

We denote the eigen-decomposition of Eq. (13) as $h(\mathbf{p}) u_\mu(\mathbf{p}) = \epsilon_\mu(\mathbf{p}) u_\mu(\mathbf{p})$ for $\mu = 0, \dots, N_L - 1$. The

many-body energies of $R^{\uparrow\downarrow}(\mathbf{p})$ are $\epsilon|U|$ for the $\mathcal{N}N_f^2 - N_L$ unpaired states and $E_\mu(\mathbf{p}) = |U|(\epsilon - \epsilon_\mu(\mathbf{p}))$ for the N_L bound states (Fig. 1c). Returning to Eq. (11), the pair excitations can be written as $\eta_{\mathbf{p},\mu}^\dagger |n\rangle$ where (App. D 3)

$$\eta_{\mathbf{p},\mu}^\dagger = \frac{1}{\sqrt{N}} \sum_{\mathbf{k}\alpha} \frac{u_\mu^\alpha(\mathbf{p})}{\sqrt{\epsilon_\mu(\mathbf{p})}} \bar{c}_{\mathbf{p}+\mathbf{k},\alpha,\uparrow}^\dagger \bar{c}_{-\mathbf{k},\alpha,\downarrow}^\dagger \quad (14)$$

which is the many-body analogue of the BCS pairing, with μ enumerating the pairing channels. We will show that $\eta_{\mathbf{p},\mu}^\dagger$ can carry nontrivial topology protected by G .

We remark that the charge-0 density excitations are also exactly solvable. We determine (App. D 5) that the spin ± 1 density excitations are gapped with energies above the $\epsilon|U|$ pairing threshold. The two spin-0 density excitations, of the form $\gamma_{\mathbf{p}+\mathbf{k},\sigma}^\dagger \gamma_{\mathbf{k},\sigma}$, in fact have a spectrum *identical* to the spin-0 Cooper pairs. We will show momentarily that there is guaranteed to be a gapless Goldstone mode in this spectrum, similar to the Anderson-Bogoliubov phonon^{73–75}. However our calculation shows this Goldstone mode is quadratic (App. E 3), whereas the Anderson-Bogoliubov phonon typically has linear dispersion. The quadratic dispersion can be attributed to the breaking of the η, η^\dagger generators by fixing the particle number^{63,76}.

Boson Bands and Topology. We have reduced the two-body scattering matrix to an effective band theory problem given by the Hamiltonian in Eq. (13). Notably, this result is generic: it is valid for all lattices with the UPC. We now prove a number of universal features of $h(\mathbf{p})$.

First, $\epsilon_\mu(\mathbf{p}) \geq 0$. This can be proved from the Schur product theorem⁷⁷, which states that the Hadamard product $[A \circ B]_{\alpha\beta} = A_{\alpha\beta} B_{\alpha\beta}$ of positive semi-definite matrices is positive semi-definite. Therefore $h(\mathbf{p})$ is the sum of positive semi-definite terms, and is also positive semi-definite. Secondly, $\epsilon_\mu(\mathbf{p}) \leq \epsilon$ follows since Eq. (2) is the sum of squares and hence $E_\mu(\mathbf{p}) = |U|(\epsilon - \epsilon_\mu(\mathbf{p})) > 0$. Note that the largest eigenvalue of $h(\mathbf{p})$, i.e. the strongest pairing, corresponds to the lowest energy many-body state. We number the bands such that $\epsilon_0(\mathbf{p}) \geq \epsilon_\mu(\mathbf{p})$.

Because η^\dagger is a zero-energy, s -wave, two-body excitation with $E_0(\mathbf{0}) = 0$, it follows that $\epsilon_0(\mathbf{0}) = \epsilon$ (App. E 2). To study the small \mathbf{p} behavior around $\epsilon_0(\mathbf{0}) = \epsilon$, we apply perturbation theory. The result is $E_0(\mathbf{p}) = \frac{|U|}{N_L} g_{ij} p_i p_j + O(p^4)$ where g_{ij} is the integrated minimal quantum metric⁶¹ (App. E 3). This amounts to a many-body proof of the result first reported in mean-field¹⁵ and by a two-body calculation⁴. Notably, the bipartite construction³⁴ produces many examples of fragile or obstructed single-particle bands, for which g_{ij} is lower bounded^{19,40}. Hence, the low-energy spectrum is universally governed by the quantum geometry of the flat bands. The presence of tightly bound pairs with quadratic dispersion suggests these models are in the Bose-Einstein condensate regime of superconductivity^{42,43,75,78}. Transport in the superconductor can be characterized by the $T = 0$ mean-field superfluid weight D_s , shown in

Fig. 1(d). For degenerate flat bands, a mean-field calculation shows (App. G)

$$[D_s]_{ij} = 8 \frac{\epsilon|U|}{V_c} \nu(1-\nu) g_{ij}, \quad g_{ij} = \frac{1}{N} \sum_{\mathbf{k}} g_{ij}(\mathbf{k}) \quad (15)$$

where V_c is the volume of a unit cell and $g_{ij}(\mathbf{k})$ is the minimal quantum metric of the degenerate bands^{17,19,61,79}. Eq. (15) predicts $D_s/|U| \approx 0.277$ for our model, in good agreement with Fig. 1d.

The eigenvalues of $h_{\alpha\beta}(\mathbf{p})$ correspond to the pairing channels, with s -wave pairing at low energies, but higher energy modes with nontrivial pairing symmetries appear (see Fig. 1c) and contribute to the finite temperature behavior. Although the zero-energy s -wave mode is universal across all space groups G , the higher energy spectrum varies. Nevertheless, we can use topological quantum chemistry to determine all possible Cooper pair band connectivities^{80–84} and topology for each G (App. E).

The pairing Hamiltonian $h(\mathbf{p})$ in an effective tight-binding model which inherits *bosonic* single-particle symmetries from the underlying electron space group G . Eq. (13) shows $h_{\alpha\beta}(\mathbf{p}) = h_{\alpha\beta}^*(-\mathbf{p})$ so $h(\mathbf{p})$ has a spinless time-reversal symmetry. We can also show (App. E 4) that $h(\mathbf{p})$ inherits the space group G but in the real representation $|D_{\alpha\beta}[g]|, g \in G$, where $D_{\alpha\beta}[g]$ is the representation of the spin- \uparrow electrons⁸⁵. The possible band structures with these orbitals are highly constrained by topological quantum chemistry since, by enforcing the UPC within our construction, the orbitals of $h(\mathbf{p})$ form a single Wyckoff position²⁷ and are symmetry-related. If the orbitals are at low-symmetry (non-maximal Wyckoff) positions, then the bands of $h(\mathbf{p})$ are composite and can be deformed into disconnected atomic representations⁸⁶. If the orbitals are located at high-symmetry (maximal Wyckoff) positions, the bands are either all connected through high-symmetry points of the BZ or decomposable into *topological* bands^{87,88}. However, because $h(\mathbf{p})$ has a spinless time-reversal symmetry, no stable topology is possible^{49,89}. Instead, a non-zero symmetry indicator^{26,84,90,91} identifies the presence of topologically protected Weyl nodes^{92,93}. In 2D, we check exhaustively that the only groups with fragile topological Cooper pairs are $G = p6, p6mm$. In $p6mm$, placing s or p orbitals at the kagome (3c) position induces a unique decomposition: the low-energy branch is a topologically trivial s -wave Cooper pair, and there is a gap to two connected bands with fragile topology where the Cooper pair wavefunction interpolates between d -wave and p -wave character across the BZ (App. D 4). This decomposition is also possible in $p6$, but there is also a second decomposition with a nonzero symmetry indicator $\theta_2 \in \mathbb{Z}_2$. In this case, the Cooper pair bands are connected by Weyl nodes. An exhaustive search of the 3D Wyckoff positions with the UPC yields 22 space groups with decomposable bands (App. E 5). We find instances where the low-energy branch is fragile topological. All 22 are kagome/pyrochlore groups where many promising

flat band candidates⁹⁴ have been identified. Our classification identifies flat band superconductors which host topological Cooper pairs and higher angular momentum spin-singlet pairing due to the multi-orbital lattice.

Conclusions. Although the BCS paradigm is successful in describing weakly-coupled superconductors, the numerous unresolved questions in high- T_c materials^{95–97} and moiré heterostructures^{1,63,98–103} demonstrate a pressing need for a strong-coupling theory of superconductivity^{63,104–108}. To this end, we introduced a broad family of flat band Hubbard models constructed within the framework of topological quantum chemistry. Their groundstates are bosonic condensates featuring maximal off-diagonal long-range order at half-filling and a linear-in- $|U|$ pairing gap. Computing the mass of the condensing Cooper pair, we established that symmetry-protected wavefunction topology coheres the superconductor with a nonzero superfluid weight. We also found exact Cooper pair bound states with p, d, \dots -wave symmetries below the pairing gap and completely

classified Cooper pair bands with fragile topology. Finally, we solved the Goldstone and gapped spin-wave excitations which hint at BEC-like behavior. Further study of these exactly solvable models may provide a new route to high-temperature superconductivity.

B.A.B. and A.C. were supported by the European Research Council (ERC) under the European Union's Horizon 2020 research and innovation programme (grant agreement No. 101020833), the ONR Grant No. N00014-20-1-2303, the Schmidt Fund for Innovative Research, Simons Investigator Grant No. 404513, the Packard Foundation, the Gordon and Betty Moore Foundation through the EPIQS Initiative, Grant GBMF11070 and Grant No. GBMF8685 towards the Princeton theory program. Further support was provided by the NSF-MRSEC Grant No. DMR-2011750, BSF Israel US foundation Grant No. 2018226, and the Princeton Global Network Funds. J.H. is supported by a Hertz Fellowship. P.T. and K-E.H. acknowledge support by the Academy of Finland under project numbers 303351 and 327293. K-E.H. acknowledges support from the Magnus Ehrnrooth Foundation.

-
- ¹ Päivi Törmä, Sebastiano Peotta, and Bogdan A. Bernevig. Superconductivity, superfluidity and quantum geometry in twisted multilayer systems. *Nature Reviews Physics*, pages 1–15, 2022.
 - ² N. B. Kopnin, T. T. Heikkilä, and G. E. Volovik. High-temperature surface superconductivity in topological flat-band systems. *Phys. Rev. B*, 83:220503, Jun 2011. doi: 10.1103/PhysRevB.83.220503. URL <https://link.aps.org/doi/10.1103/PhysRevB.83.220503>.
 - ³ Aleksi Julku, Sebastiano Peotta, Tuomas I. Vanhala, Dong-Hee Kim, and Päivi Törmä. Geometric Origin of Superfluidity in the Lieb-Lattice Flat Band. *Phys. Rev. Lett.*, 117(4):045303, July 2016. doi: 10.1103/PhysRevLett.117.045303.
 - ⁴ P. Törmä, L. Liang, and S. Peotta. Quantum metric and effective mass of a two-body bound state in a flat band. *Phys. Rev. B*, 98(22):220511, December 2018. doi: 10.1103/PhysRevB.98.220511.
 - ⁵ Murad Tovmasyan, Sebastiano Peotta, Long Liang, Päivi Törmä, and Sebastian D. Huber. Preformed pairs in flat Bloch bands. *Phys. Rev. B*, 98(13):134513, October 2018. doi:10.1103/PhysRevB.98.134513.
 - ⁶ A. Julku, T. J. Peltonen, L. Liang, T. T. Heikkilä, and P. Törmä. Superfluid weight and Berezinskii-Kosterlitz-Thouless transition temperature of twisted bilayer graphene. *Phys. Rev. B*, 101(6):060505, February 2020. doi:10.1103/PhysRevB.101.060505.
 - ⁷ Haidong Tian, Shi Che, Tianyi Xu, Patrick Cheung, Kenji Watanabe, Takashi Taniguchi, Mohit Randeria, Fan Zhang, Chun Ning Lau, and Marc W. Bockrath. Evidence for Flat Band Dirac Superconductor Originating from Quantum Geometry. *arXiv e-prints*, art. arXiv:2112.13401, December 2021.
 - ⁸ Valerio Peri, Zhi-Da Song, B. Andrei Bernevig, and Sebastian D. Huber. Fragile Topology and Flat-Band Superconductivity in the Strong-Coupling Regime. *Phys. Rev. Lett.*, 126(2):027002, January 2021. doi: 10.1103/PhysRevLett.126.027002.
 - ⁹ Xiang Hu, Timo Hyart, Dmitry I. Pikulin, and Enrico Rossi. Geometric and conventional contribution to the superfluid weight in twisted bilayer graphene. *Phys. Rev. Lett.*, 123:237002, Dec 2019. doi: 10.1103/PhysRevLett.123.237002. URL <https://link.aps.org/doi/10.1103/PhysRevLett.123.237002>.
 - ¹⁰ Kukka-Emilia Huhtinen and Päivi Törmä. Possible insulator-pseudogap crossover in the attractive Hubbard model on the Lieb lattice. *Phys. Rev. B*, 103(22):L220502, June 2021. doi:10.1103/PhysRevB.103.L220502.
 - ¹¹ Jie Wang, Jennifer Cano, Andrew J. Millis, Zhao Liu, and Bo Yang. Exact Landau Level Description of Geometry and Interaction in a Flatband. *Phys. Rev. Lett.*, 127(24):246403, December 2021. doi: 10.1103/PhysRevLett.127.246403.
 - ¹² M. Iskin. Two-body problem in a multiband lattice and the role of quantum geometry. *Phys. Rev. A*, 103:053311, May 2021. doi:10.1103/PhysRevA.103.053311. URL <https://link.aps.org/doi/10.1103/PhysRevA.103.053311>.
 - ¹³ Rok Žitko and Luka Pavešić. Yu-shiba-rusinov states, the bcs-bec crossover, and the exact solution in the flat-band limit, 2022. URL <https://arxiv.org/abs/2204.12610>.
 - ¹⁴ Taisei Kitamura, Tatsuya Yamashita, Jun Ishizuka, Akito Daido, and Youichi Yanase. Superconductivity in monolayer FeSe enhanced by quantum geometry. *Physical Review Research*, 4(2):023232, June 2022. doi: 10.1103/PhysRevResearch.4.023232.
 - ¹⁵ Sebastiano Peotta and Päivi Törmä. Superfluidity in topologically nontrivial flat bands. *Nature Communications*, 6:8944, November 2015. doi:10.1038/ncomms9944.
 - ¹⁶ R. Resta. The insulating state of matter: a geometrical theory. *European Physical Journal B*, 79(2):121–137, January 2011. doi:10.1140/epjb/e2010-10874-4.
 - ¹⁷ Fang Xie, Zhida Song, Biao Lian, and B. Andrei Bernevig. Topology-Bounded Superfluid Weight in Twisted Bilayer

- Graphene. *Phys. Rev. Lett.*, 124(16):167002, April 2020. doi:10.1103/PhysRevLett.124.167002.
- ¹⁸ Murad Tovmasyan, Sebastiano Peotta, Päivi Törmä, and Sebastian D. Huber. Effective theory and emergent SU(2) symmetry in the flat bands of attractive hubbard models. *Phys. Rev. B*, 94:245149, Dec 2016. doi:10.1103/PhysRevB.94.245149. URL <https://link.aps.org/doi/10.1103/PhysRevB.94.245149>.
 - ¹⁹ Jonah Herzog-Arbeitman, Valerio Peri, Frank Schindler, Sebastian D. Huber, and B. Andrei Bernevig. Superfluid Weight Bounds from Symmetry and Quantum Geometry in Flat Bands. *Phys. Rev. Lett.*, 128(8):087002, February 2022. doi:10.1103/PhysRevLett.128.087002.
 - ²⁰ Si Min Chan, B. Grémaud, and G. G. Batrouni. Pairing and superconductivity in quasi-one-dimensional flat-band systems: Creutz and sawtooth lattices. *Phys. Rev. B*, 105:024502, Jan 2022. doi:10.1103/PhysRevB.105.024502. URL <https://link.aps.org/doi/10.1103/PhysRevB.105.024502>.
 - ²¹ Si Min Chan, B. Grémaud, and G. G. Batrouni. Designer Flat Bands: Topology and Enhancement of Superconductivity. *arXiv e-prints*, art. arXiv:2206.10651, June 2022.
 - ²² Johannes S. Hofmann, Erez Berg, and Debanjan Chowdhury. Superconductivity, charge density wave, and super-solidity in flat bands with tunable quantum metric. *arXiv e-prints*, art. arXiv:2204.02994, April 2022.
 - ²³ Johannes S. Hofmann, Erez Berg, and Debanjan Chowdhury. Superconductivity, pseudogap, and phase separation in topological flat bands. *Phys. Rev. B*, 102(20):201112, November 2020. doi:10.1103/PhysRevB.102.201112.
 - ²⁴ Giuliano Orso and Manpreet Singh. Pairs, trimers, and bcs-bec crossover near a flat band: Sawtooth lattice. *Phys. Rev. B*, 106:014504, Jul 2022. doi:10.1103/PhysRevB.106.014504. URL <https://link.aps.org/doi/10.1103/PhysRevB.106.014504>.
 - ²⁵ B. Andrei Bernevig and Taylor L. Hughes. *Topological Insulators and Topological Superconductors*. Princeton University Press, student edition edition, 2013. ISBN 9780691151755. URL <http://www.jstor.org/stable/j.ctt19cc2gc>.
 - ²⁶ Barry Bradlyn, L. Elcoro, Jennifer Cano, M. G. Vergniory, Zhijun Wang, C. Felser, M. I. Aroyo, and B. Andrei Bernevig. Topological quantum chemistry. *Nature (London)*, 547(7663):298–305, Jul 2017. doi:10.1038/nature23268.
 - ²⁷ Jennifer Cano and Barry Bradlyn. Band Representations and Topological Quantum Chemistry. *arXiv e-prints*, art. arXiv:2006.04890, June 2020.
 - ²⁸ H Bacry, L Michel, and J Zak. Symmetry and classification of energy bands in crystals. In *Group Theoretical Methods in Physics*, pages 289–308. Springer, 1988.
 - ²⁹ MI Aroyo, JM Perez-Mato, Cesar Capillas, Eli Kroumova, Svetoslav Ivantchev, Gotzon Madariaga, Asen Kirov, and Hans Wondratschek. Bilbao crystallographic server: I. databases and crystallographic computing programs. *ZEITSCHRIFT FÜR KRISTALLOGRAPHIE*, 221:15–27, 01 2006. doi:10.1524/zkri.2006.221.1.15.
 - ³⁰ Mois I. Aroyo, Asen Kirov, Cesar Capillas, J. M. Perez-Mato, and Hans Wondratschek. Bilbao Crystallographic Server. II. Representations of crystallographic point groups and space groups. *Acta Crystallographica Section A*, 62(2):115–128, Mar 2006. doi:10.1107/S0108767305040286. URL <https://doi.org/10.1107/S0108767305040286>.
 - ³¹ Doron L. Bergman, Congjun Wu, and Leon Balents. Band touching from real-space topology in frustrated hopping models. *Phys. Rev. B*, 78:125104, Sep 2008. doi:10.1103/PhysRevB.78.125104. URL <https://link.aps.org/doi/10.1103/PhysRevB.78.125104>.
 - ³² Jun-Won Rhim and Bohm-Jung Yang. Classification of flat bands according to the band-crossing singularity of bloch wave functions. *Phys. Rev. B*, 99:045107, Jan 2019. doi:10.1103/PhysRevB.99.045107. URL <https://link.aps.org/doi/10.1103/PhysRevB.99.045107>.
 - ³³ Zhi-Da Song, Luis Elcoro, and B. Andrei Bernevig. Twisted bulk-boundary correspondence of fragile topology. *Science*, 367(6479):794–797, February 2020. doi:10.1126/science.aaz7650.
 - ³⁴ Dumitru Călugăru, Aaron Chew, Luis Elcoro, Yuanfeng Xu, Nicolas Regnault, Zhi-Da Song, and B. Andrei Bernevig. General construction and topological classification of crystalline flat bands. *Nature Physics*, 18(2):185–189, December 2021. doi:10.1038/s41567-021-01445-3.
 - ³⁵ Rafi Bistritzer and Allan H. MacDonald. Moiré bands in twisted double-layer graphene. *Proceedings of the National Academy of Science*, 108(30):12233–12237, Jul 2011. doi:10.1073/pnas.1108174108.
 - ³⁶ Zhi-Da Song, Zhijun Wang, Wujun Shi, Gang Li, Chen Fang, and B. Andrei Bernevig. All Magic Angles in Twisted Bilayer Graphene are Topological. *Phys. Rev. Lett.*, 123(3):036401, Jul 2019. doi:10.1103/PhysRevLett.123.036401.
 - ³⁷ Hoi Chun Po, Liujun Zou, T. Senthil, and Ashvin Vishwanath. Faithful Tight-binding Models and Fragile Topology of Magic-angle Bilayer Graphene. *arXiv e-prints*, art. arXiv:1808.02482, Aug 2018.
 - ³⁸ J. Ahn, S. Park, and B.-J. Yang. Failure of Nielsen-Ninomiya Theorem and Fragile Topology in Two-Dimensional Systems with Space-Time Inversion Symmetry: Application to Twisted Bilayer Graphene at Magic Angle. *Physical Review X*, 9(2):021013, April 2019. doi:10.1103/PhysRevX.9.021013.
 - ³⁹ Adrien Bouhon, Annica M. Black-Schaffer, and Robert-Jan Slager. Wilson loop approach to metastable topology of split elementary band representations and topological crystalline insulators with time reversal symmetry. *arXiv e-prints*, art. arXiv:1804.09719, Apr 2018.
 - ⁴⁰ Jiabin Yu, Ming Xie, Fengcheng Wu, and Sankar Das Sarma. Euler Obstructed Cooper Pairing in Twisted Bilayer Graphene: Nematic Nodal Superconductivity and Bounded Superfluid Weight. *arXiv e-prints*, art. arXiv:2202.02353, February 2022.
 - ⁴¹ Chen Ning Yang. η pairing and off-diagonal long-range order in a hubbard model. *Phys. Rev. Lett.*, 63:2144–2147, Nov 1989. doi:10.1103/PhysRevLett.63.2144. URL <https://link.aps.org/doi/10.1103/PhysRevLett.63.2144>.
 - ⁴² Qijin Chen, Jelena Stajic, Shina Tan, and K. Levin. BCS BEC crossover: From high temperature superconductors to ultracold superfluids. *Physics Reports*, 412(1):1–88, June 2005. doi:10.1016/j.physrep.2005.02.005.
 - ⁴³ Mohit Randeria and Edward Taylor. BCS-BEC Crossover and the Unitary Fermi Gas. *arXiv e-prints*, art. arXiv:1306.5785, June 2013.
 - ⁴⁴ C. N. Yang. Concept of off-diagonal long-range order and the quantum phases of liquid he and of supercon-

- ductors. *Rev. Mod. Phys.*, 34:694–704, Oct 1962. doi: 10.1103/RevModPhys.34.694. URL <https://link.aps.org/doi/10.1103/RevModPhys.34.694>.
- ⁴⁵ Sebastiano Peotta. Superconductivity, generalized random phase approximation and linear scaling methods. *arXiv e-prints*, art. arXiv:2204.12163, April 2022.
- ⁴⁶ Luca Guido Molinari. Notes on Wick’s theorem in many-body theory. *arXiv e-prints*, art. arXiv:1710.09248, October 2017.
- ⁴⁷ Alexander L. Fetter and John Dirk Walecka. *Quantum theory of many-particle systems*. Courier Corporation, 2003, 1971.
- ⁴⁸ Nicola Marzari, Arash A. Mostofi, Jonathan R. Yates, Ivo Souza, and David Vanderbilt. Maximally localized Wannier functions: Theory and applications. *Reviews of Modern Physics*, 84(4):1419–1475, October 2012. doi: 10.1103/RevModPhys.84.1419.
- ⁴⁹ Christian Brouder, Gianluca Panati, Matteo Calandra, Christophe Mourougane, and Nicola Marzari. Exponential localization of wannier functions in insulators. *Phys. Rev. Lett.*, 98:046402, Jan 2007. doi: 10.1103/PhysRevLett.98.046402. URL <https://link.aps.org/doi/10.1103/PhysRevLett.98.046402>.
- ⁵⁰ B. Andrei Bernevig, Taylor L. Hughes, and Shou-Cheng Zhang. Quantum Spin Hall Effect and Topological Phase Transition in HgTe Quantum Wells. *Science*, 314(5806): 1757, Dec 2006. doi:10.1126/science.1133734.
- ⁵¹ Domenico Monaco, Gianluca Panati, Adriano Pisante, and Stefan Teufel. Optimal Decay of Wannier functions in Chern and Quantum Hall Insulators. *Communications in Mathematical Physics*, January 2018. doi:10.1007/s00220-017-3067-7.
- ⁵² D. Monaco, G. Panati, A. Pisante, and S. Teufel. The Localization Dichotomy for gapped periodic quantum systems. *arXiv e-prints*, art. arXiv:1612.09557, December 2016.
- ⁵³ Georg W. Winkler, Alexey A. Soluyanov, and Matthias Troyer. Smooth gauge and Wannier functions for topological band structures in arbitrary dimensions. *Phys. Rev. B*, 93(3):035453, January 2016. doi: 10.1103/PhysRevB.93.035453.
- ⁵⁴ Alexey A. Soluyanov and David Vanderbilt. Wannier representation of z_2 topological insulators. *Phys. Rev. B*, 83:035108, Jan 2011. doi:10.1103/PhysRevB.83.035108. URL <https://link.aps.org/doi/10.1103/PhysRevB.83.035108>.
- ⁵⁵ Zhi-Da Song, Luis Elcoro, Yuan-Feng Xu, Nicolas Regnault, and B. Andrei Bernevig. Fragile Phases as Affine Monoids: Classification and Material Examples. *Physical Review X*, 10(3):031001, July 2020. doi: 10.1103/PhysRevX.10.031001.
- ⁵⁶ Zhi-Da Song, Luis Elcoro, and B. Andrei Bernevig. Twisted bulk-boundary correspondence of fragile topology. *Science*, 367(6479):794–797, February 2020. doi: 10.1126/science.aaz7650.
- ⁵⁷ B. Andrei Bernevig, Biao Lian, Aditya Cowsik, Fang Xie, Nicolas Regnault, and Zhi-Da Song. Twisted bilayer graphene. V. Exact analytic many-body excitations in Coulomb Hamiltonians: Charge gap, Goldstone modes, and absence of Cooper pairing. *Phys. Rev. B*, 103(20): 205415, May 2021. doi:10.1103/PhysRevB.103.205415.
- ⁵⁸ Jian Kang, B. Andrei Bernevig, and Oskar Vafek. Cascades between Light and Heavy Fermions in the Normal State of Magic-Angle Twisted Bilayer Graphene. *Phys. Rev. Lett.*, 127(26):266402, December 2021. doi: 10.1103/PhysRevLett.127.266402.
- ⁵⁹ Jonah Herzog-Arbeitman, Aaron Chew, Dmitri K Efetov, and B Andrei Bernevig. Reentrant correlated insulators in twisted bilayer graphene at 25 t (2π flux). *Physical Review Letters*, 129(7):076401, 2022.
- ⁶⁰ Jian Kang and Oskar Vafek. Strong coupling phases of partially filled twisted bilayer graphene narrow bands. *Phys. Rev. Lett.*, 122:246401, Jun 2019. doi: 10.1103/PhysRevLett.122.246401. URL <https://link.aps.org/doi/10.1103/PhysRevLett.122.246401>.
- ⁶¹ Kukka-Emilia Huhtinen, Jonah Herzog-Arbeitman, Aaron Chew, Bogdan A. Bernevig, and Päivi Törmä. Revisiting flat band superconductivity: Dependence on minimal quantum metric and band touchings. *Phys. Rev. B*, 106(1):014518, July 2022. doi:10.1103/PhysRevB.106.014518.
- ⁶² Zhiqiang Wang, Gaurav Chaudhary, Qijin Chen, and K. Levin. Quantum geometric contributions to the BKT transition: Beyond mean field theory. *Phys. Rev. B*, 102(18):184504, November 2020. doi: 10.1103/PhysRevB.102.184504.
- ⁶³ Xu Zhang, Kai Sun, Heqiu Li, Gaopei Pan, and Zi Yang Meng. Superconductivity and bosonic fluid emerging from Moiré flat bands. *arXiv e-prints*, art. arXiv:2111.10018, November 2021.
- ⁶⁴ Makoto Hashimoto, Inna M. Vishik, Rui-Hua He, Thomas P. Devereaux, and Zhi-Xun Shen. Energy gaps in high-transition-temperature cuprate superconductors. *Nature Physics*, 10(7):483–495, July 2014. doi: 10.1038/nphys3009.
- ⁶⁵ R. W. Richardson and N. Sherman. Exact eigenstates of the pairing-force Hamiltonian. *Nuclear Physics*, 52:221–238, April 1964. doi:10.1016/0029-5582(64)90687-X.
- ⁶⁶ R. W. Richardson. Pairing in the limit of a large number of particles. *Journal of Mathematical Physics*, 18(9):1802–1811, September 1977. doi:10.1063/1.523493.
- ⁶⁷ Yuan Cao, Valla Fatemi, Shiang Fang, Kenji Watanabe, Takashi Taniguchi, Efthimios Kaxiras, and Pablo Jarillo-Herrero. Unconventional superconductivity in magic-angle graphene superlattices. *Nature (London)*, 556(7699):43–50, April 2018. doi:10.1038/nature26160.
- ⁶⁸ Myungchul Oh, Kevin P. Nuckolls, Dillon Wong, Ryan L. Lee, Xiaomeng Liu, Kenji Watanabe, Takashi Taniguchi, and Ali Yazdani. Evidence for unconventional superconductivity in twisted bilayer graphene. *Nature (London)*, 600(7888):240–245, October 2021. doi:10.1038/s41586-021-04121-x.
- ⁶⁹ Jeong Min Park, Yuan Cao, Kenji Watanabe, Takashi Taniguchi, and Pablo Jarillo-Herrero. Flavour Hund’s Coupling, Correlated Chern Gaps, and Diffusivity in Moiré Flat Bands. *arXiv e-prints*, art. arXiv:2008.12296, August 2020.
- ⁷⁰ Petr Stepanov, Ipsita Das, Xiaobo Lu, Ali Fahimniya, Kenji Watanabe, Takashi Taniguchi, Frank H. L. Koppen, Johannes Lischner, Leonid Levitov, and Dmitri K. Efetov. Untying the insulating and superconducting orders in magic-angle graphene. *Nature (London)*, 583(7816):375–378, July 2020. doi:10.1038/s41586-020-2459-6.
- ⁷¹ Yonglong Xie, Biao Lian, Berthold Jäck, Xiaomeng Liu, Cheng-Li Chiu, Kenji Watanabe, Takashi Taniguchi, B. Andrei Bernevig, and Ali Yazdani. Spectroscopic signatures of many-body correlations in magic-angle twisted

- bilayer graphene. *Nature (London)*, 572(7767):101–105, Jul 2019. doi:10.1038/s41586-019-1422-x.
- ⁷² A. J. Leggett. Number-Phase Fluctuations in Two-Band Superconductors. *Progress of Theoretical Physics*, 36(5): 901–930, November 1966. doi:10.1143/PTP.36.901.
- ⁷³ Lev P Pitaevskii, Sandro Stringari, and Sandro Stringari. *Bose-einstein condensation*. Number 116. Oxford University Press, 2003.
- ⁷⁴ R. P. Feynman. Atomic theory of the two-fluid model of liquid helium. *Phys. Rev.*, 94:262–277, Apr 1954. doi: 10.1103/PhysRev.94.262. URL <https://link.aps.org/doi/10.1103/PhysRev.94.262>.
- ⁷⁵ Wilhelm Zwerger. *The BCS-BEC crossover and the unitary Fermi gas*, volume 836. Springer Science & Business Media, 2011.
- ⁷⁶ Haruki Watanabe. Counting Rules of Nambu-Goldstone Modes. *arXiv e-prints*, art. arXiv:1904.00569, April 2019.
- ⁷⁷ Viktor Vasil'evich Prasolov. *Problems and theorems in linear algebra*, volume 134. American Mathematical Soc., 1994.
- ⁷⁸ Aleksi Julku, Georg M. Bruun, and Päivi Törmä. Quantum geometry and flat band bose-einstein condensation. *Phys. Rev. Lett.*, 127:170404, Oct 2021. doi: 10.1103/PhysRevLett.127.170404. URL <https://link.aps.org/doi/10.1103/PhysRevLett.127.170404>.
- ⁷⁹ Bruno Mera and Johannes Mitscherling. Nontrivial quantum geometry of degenerate flat bands. *arXiv e-prints*, art. arXiv:2205.07900, May 2022.
- ⁸⁰ Barry Bradlyn, L. Elcoro, M. G. Vergniory, Jennifer Cano, Zhijun Wang, C. Felser, M. I. Aroyo, and B. Andrei Bernevig. Band connectivity for topological quantum chemistry: Band structures as a graph theory problem. *Phys. Rev. B*, 97:035138, Jan 2018. doi: 10.1103/PhysRevB.97.035138. URL <https://link.aps.org/doi/10.1103/PhysRevB.97.035138>.
- ⁸¹ Thomas Christensen, Hoi Chun Po, John D. Joannopoulos, and Marin Soljačić. Location and topology of the fundamental gap in photonic crystals. *arXiv e-prints*, art. arXiv:2106.10267, June 2021.
- ⁸² Luis Elcoro, Zhida Song, and B. Andrei Bernevig. Application of induction procedure and Smith decomposition in calculation and topological classification of electronic band structures in the 230 space groups. *Phys. Rev. B*, 102(3):035110, July 2020. doi: 10.1103/PhysRevB.102.035110.
- ⁸³ Haruki Watanabe, Hoi Chun Po, and Ashvin Vishwanath. Structure and topology of band structures in the 1651 magnetic space groups. *Science Advances*, 4(8):eaat8685, August 2018. doi:10.1126/sciadv.aat8685.
- ⁸⁴ Jorrit Kruthoff, Jan de Boer, Jasper van Wezel, Charles L. Kane, and Robert-Jan Slager. Topological Classification of Crystalline Insulators through Band Structure Combinatorics. *Physical Review X*, 7(4):041069, October 2017. doi:10.1103/PhysRevX.7.041069.
- ⁸⁵ A. Alexandradinata, J. Höller, Chong Wang, Hengbin Cheng, and Ling Lu. Crystallographic splitting theorem for band representations and fragile topological photonic crystals. *Phys. Rev. B*, 102:115117, Sep 2020. doi:10.1103/PhysRevB.102.115117. URL <https://link.aps.org/doi/10.1103/PhysRevB.102.115117>.
- ⁸⁶ Jennifer Cano, Barry Bradlyn, Zhijun Wang, L. Elcoro, M. G. Vergniory, C. Felser, M. I. Aroyo, and B. Andrei Bernevig. Building blocks of topological quantum chemistry: Elementary band representations. *Phys. Rev. B*, 97(3):035139, Jan 2018. doi:10.1103/PhysRevB.97.035139.
- ⁸⁷ Barry Bradlyn, Zhijun Wang, Jennifer Cano, and B. Andrei Bernevig. Disconnected Elementary Band Representations, Fragile Topology, and Wilson Loops as Topological Indices: An Example on the Triangular Lattice. *arXiv e-prints*, art. arXiv:1807.09729, July 2018.
- ⁸⁸ Jennifer Cano, Barry Bradlyn, Zhijun Wang, L. Elcoro, M. G. Vergniory, C. Felser, M. I. Aroyo, and B. Andrei Bernevig. Topology of Disconnected Elementary Band Representations. *Phys. Rev. Lett.*, 120(26):266401, June 2018. doi:10.1103/PhysRevLett.120.266401.
- ⁸⁹ Chen Fang, Matthew J. Gilbert, and B. Andrei Bernevig. Bulk topological invariants in noninteracting point group symmetric insulators. *Phys. Rev. B*, 86(11):115112, September 2012. doi:10.1103/PhysRevB.86.115112.
- ⁹⁰ Hoi Chun Po. Symmetry indicators of band topology. *Journal of Physics Condensed Matter*, 32(26):263001, June 2020. doi:10.1088/1361-648X/ab7adb.
- ⁹¹ Hoi Chun Po, Ashvin Vishwanath, and Haruki Watanabe. Complete theory of symmetry-based indicators of band topology. *Nature Communications*, 8:50, June 2017. doi: 10.1038/s41467-017-00133-2.
- ⁹² Taylor L. Hughes, Emil Prodan, and B. Andrei Bernevig. Inversion-symmetric topological insulators. *Phys. Rev. B*, 83(24):245132, Jun 2011. doi: 10.1103/PhysRevB.83.245132.
- ⁹³ Luis Elcoro, Benjamin J. Wieder, Zhida Song, Yuanfeng Xu, Barry Bradlyn, and B. Andrei Bernevig. Magnetic Topological Quantum Chemistry. *arXiv e-prints*, art. arXiv:2010.00598, October 2020.
- ⁹⁴ Nicolas Regnault, Yuanfeng Xu, Ming-Rui Li, Da-Shuai Ma, Milena Jovanovic, Ali Yazdani, Stuart S. P. Parkin, Claudia Felser, Leslie M. Schoop, N. Phuan Ong, Robert J. Cava, Luis Elcoro, Zhi-Da Song, and B. Andrei Bernevig. Catalogue of flat-band stoichiometric materials. *Nature (London)*, 603(7903):824–828, March 2022. doi:10.1038/s41586-022-04519-1.
- ⁹⁵ Robert Joynt and Louis Taillefer. The superconducting phases of Upt_3 . *Rev. Mod. Phys.*, 74:235–294, Mar 2002. doi:10.1103/RevModPhys.74.235. URL <https://link.aps.org/doi/10.1103/RevModPhys.74.235>.
- ⁹⁶ Manfred Sgrist and Kazuo Ueda. Phenomenological theory of unconventional superconductivity. *Rev. Mod. Phys.*, 63:239–311, Apr 1991. doi: 10.1103/RevModPhys.63.239. URL <https://link.aps.org/doi/10.1103/RevModPhys.63.239>.
- ⁹⁷ Patrick A. Lee, Naoto Nagaosa, and Xiao-Gang Wen. Doping a mott insulator: Physics of high-temperature superconductivity. *Rev. Mod. Phys.*, 78:17–85, Jan 2006. doi:10.1103/RevModPhys.78.17. URL <https://link.aps.org/doi/10.1103/RevModPhys.78.17>.
- ⁹⁸ Leon Balents, Cory R. Dean, Dmitri K. Efetov, and Andrea F. Young. Superconductivity and strong correlations in moiré flat bands. *Nature Physics*, 16(7):725–733, May 2020. doi:10.1038/s41567-020-0906-9.
- ⁹⁹ Yiran Zhang, Robert Polski, Cyprian Lewandowski, Alex Thomson, Yang Peng, Youngjoon Choi, Hyunjin Kim, Kenji Watanabe, Takashi Taniguchi, Jason Alicea, Felix von Oppen, Gil Refael, and Stevan Nadj-Perge. Ascendance of Superconductivity in Magic-Angle Graphene Multilayers. *arXiv e-prints*, art. arXiv:2112.09270, December 2021.
- ¹⁰⁰ Jeong Min Park, Yuan Cao, Liqiao Xia, Shuwen Sun, Kenji Watanabe, Takashi Taniguchi, and Pablo Jarillo-

- Herrero. Magic-Angle Multilayer Graphene: A Robust Family of Moiré Superconductors. *arXiv e-prints*, art. arXiv:2112.10760, December 2021.
- ¹⁰¹ Ethan Lake, Adarsh S. Patri, and T. Senthil. Pairing symmetry of twisted bilayer graphene: a phenomenological synthesis, 2022. URL <https://arxiv.org/abs/2204.12579>.
- ¹⁰² Yuxuan Wang, Jian Kang, and Rafael M. Fernandes. Topological and nematic superconductivity mediated by ferro-SU(4) fluctuations in twisted bilayer graphene. *Phys. Rev. B*, 103(2):024506, January 2021. doi:10.1103/PhysRevB.103.024506.
- ¹⁰³ Biao Lian, Zhijun Wang, and B. Andrei Bernevig. Twisted Bilayer Graphene: A Phonon-Driven Superconductor. *Phys. Rev. Lett.*, 122(25):257002, June 2019. doi:10.1103/PhysRevLett.122.257002.
- ¹⁰⁴ Matthew F. Lapa and Michael Levin. Rigorous Results on Topological Superconductivity with Particle Number Conservation. *Phys. Rev. Lett.*, 124(25):257002, June 2020. doi:10.1103/PhysRevLett.124.257002.
- ¹⁰⁵ Matthew F. Lapa. Topology of superconductors beyond mean-field theory. *Physical Review Research*, 2(3):033309, August 2020. doi:10.1103/PhysRevResearch.2.033309.
- ¹⁰⁶ RW Richardson. A restricted class of exact eigenstates of the pairing-force hamiltonian. 1963.
- ¹⁰⁷ Miguel Ibañez, Jon Links, Germán Sierra, and Shao-You Zhao. Exactly solvable pairing model for superconductors with $p_x + ip_y$ -wave symmetry. *Phys. Rev. B*, 79(18):180501, May 2009. doi:10.1103/PhysRevB.79.180501.
- ¹⁰⁸ Pieter W. Claeys, Stijn De Baerdemacker, and Dimitri Van Neck. Read-green resonances in a topological superconductor coupled to a bath. *Phys. Rev. B*, 93:220503, Jun 2016. doi:10.1103/PhysRevB.93.220503. URL <https://link.aps.org/doi/10.1103/PhysRevB.93.220503>.
- ¹⁰⁹ Benjamin J. Wieder, Barry Bradlyn, Zhijun Wang, Jennifer Cano, Youngkuk Kim, Hyeong-Seok D. Kim, Andrew M. Rappe, C. L. Kane, and B. Andrei Bernevig. Wallpaper fermions and the nonsymmorphic Dirac insulator. *Science*, 361(6399):246–251, July 2018. doi:10.1126/science.aan2802.
- ¹¹⁰ Elliott H. Lieb. Two theorems on the hubbard model. *Phys. Rev. Lett.*, 62:1201–1204, Mar 1989. doi:10.1103/PhysRevLett.62.1201. URL <https://link.aps.org/doi/10.1103/PhysRevLett.62.1201>.
- ¹¹¹ Wladimir A. Benalcazar, B. Andrei Bernevig, and Taylor L. Hughes. Electric multipole moments, topological multipole moment pumping, and chiral hinge states in crystalline insulators. *Phys. Rev. B*, 96(24):245115, Dec 2017. doi:10.1103/PhysRevB.96.245115.
- ¹¹² Wladimir A. Benalcazar, B. Andrei Bernevig, and Taylor L. Hughes. Quantized electric multipole insulators. *Science*, 357(6346):61766, Jul 2017. ISSN 1095-9203. doi:10.1126/science.aah6442. URL <http://dx.doi.org/10.1126/science.aah6442>.
- ¹¹³ Oskar Vafek, Nicolas Regnault, and B. Andrei Bernevig. Entanglement of exact excited eigenstates of the Hubbard model in arbitrary dimension. *SciPost Physics*, 3(6):043, December 2017. doi:10.21468/SciPostPhys.3.6.043.
- ¹¹⁴ Jiacheng Gao, Zhaopeng Guo, Hongming Weng, and Zhijun Wang. Magnetic band representations, Fu-Kane-like symmetry indicators and magnetic topological materials. *arXiv e-prints*, art. arXiv:2204.10556, April 2022.
- ¹¹⁵ A. Alexandradinata, Xi Dai, and B. Andrei Bernevig. Wilson-Loop Characterization of Inversion-Symmetric Topological Insulators. *Phys. Rev.*, B89(15):155114, 2014. doi:10.1103/PhysRevB.89.155114.
- ¹¹⁶ Zhi-Da Song, Biao Lian, Nicolas Regnault, and B. Andrei Bernevig. Twisted bilayer graphene. II. Stable symmetry anomaly. *Phys. Rev. B*, 103(20):205412, May 2021. doi:10.1103/PhysRevB.103.205412.
- ¹¹⁷ Long Liang, Tuomas I. Vanhala, Sebastiano Peotta, Topi Siro, Ari Harju, and Päivi Törmä. Band geometry, berry curvature, and superfluid weight. *Phys. Rev. B*, 95:024515, Jan 2017. doi:10.1103/PhysRevB.95.024515. URL <https://link.aps.org/doi/10.1103/PhysRevB.95.024515>.

CONTENTS

A. Single-Particle Symmetry and Topology	10
1. Projected Bands	10
2. Uniform Pairing Condition from the Space group	12
a. Spin	15
B. Hubbard Model and Eta-pairing Symmetry	15
1. Attractive Hubbard Models	16
2. Eta Operators	16
3. Symmetry Algebra	18
C. Off-diagonal Long Range Order in the Ground State and Generating Functions	19
1. ODLRO	20
2. Wick's theorem	21
D. Charge excitations	23
1. Charge +1	24
2. Richardson Criterion	26
3. Charge +2 Excitations	29
4. Examples of the Cooper Pair Spectrum	31
a. SSH Chain	32
b. $p3$ Compact Obstructed atomic Insulator	33
c. $p6mm$ Fragile S -matrix Bands	33
5. Density Excitations	35
E. Spectrum and Topology of the Cooper Pairs	37
1. Momentum Space Conventions	37
2. Cooper Pair Hamiltonian and Spectrum	38
3. Cooper Pair mass and Minimal Quantum Metric	40
4. Space Group Symmetry and Representations of the Boson Bands	43
5. Topology of the Boson Bands	45
F. Ten Band Model for Twisted Bilayer Graphene	50
G. Mean-field superfluid weight in degenerate flat bands	52

Appendix A: Single-Particle Symmetry and Topology

In this section, we define the notation used in the rest of the work for the single-particle projectors, projected many-body operators, and space group symmetries (App. A 1). We prove that the uniform pairing condition can be symmetry enforced by choosing orbitals to transform as irreps of a single Wyckoff positions (App. A 2), and extend this result to bipartite lattices where perfectly flat bands can be systematically constructed.

1. Projected Bands

Our problem projects the main electronic degrees of freedom into the quasi-flat bands of the non-interacting Hamiltonian. In a strong coupling approximation, the quasi-flat bands are set to zero energy and the remaining bands are sent to infinite energy and projected out. As such, the physics depends entirely on the flat band wavefunctions.

We now introduce our notation which differs slightly from Ref. [18] where only nondegenerate flat bands (doubly degenerate when including spin) were considered. Let \mathbf{R} index the unit cells and $\alpha = 1, \dots, N_{orb}$ index the orbitals at positions \mathbf{r}_α . For now we neglect spin, but it will be introduced later with $\sigma = \uparrow, \downarrow$. The electron operators (obeying canonical anti-commutation relations) are

$$c_{\mathbf{k},\alpha}^\dagger = \frac{1}{\sqrt{N}} \sum_{\mathbf{R}} e^{-i\mathbf{k} \cdot (\mathbf{R} + \mathbf{r}_\alpha)} c_{\mathbf{R},\alpha}^\dagger, \quad c_{\mathbf{R},\alpha}^\dagger = \frac{1}{\sqrt{N}} \sum_{\mathbf{k}} e^{i\mathbf{k} \cdot (\mathbf{R} + \mathbf{r}_\alpha)} c_{\mathbf{k},\alpha}^\dagger \quad (\text{A1})$$

where \mathcal{N} is the total number of unit cells, which is the number of terms in the \mathbf{R}, \mathbf{k} sums. The general single-particle Hamiltonian reads

$$\tilde{H} = \sum_{\mathbf{k}, \alpha\beta} c_{\mathbf{k},\alpha}^\dagger \tilde{h}_{\alpha\beta}(\mathbf{k}) c_{\mathbf{k},\beta} = \sum_{\mathbf{k}, n} \tilde{E}_n(\mathbf{k}) \gamma_{\mathbf{k},n}^\dagger \gamma_{\mathbf{k},n}, \quad \gamma_{\mathbf{k},n} = \sum_{\alpha} [\tilde{U}^\dagger(\mathbf{k})]_{n,\alpha} c_{\mathbf{k},\alpha} \quad (\text{A2})$$

and $\tilde{h}(\mathbf{k}) = \tilde{U} \tilde{E} \tilde{U}^\dagger$ where \tilde{E} is the diagonal matrix of energies, \tilde{U} is the $N_{orb} \times N_{orb}$ eigenvector matrix, and the diagonalized electron operators obey $\{\gamma_{\mathbf{k},m}, \gamma_{\mathbf{k}',n}^\dagger\} = \delta_{\mathbf{k},\mathbf{k}'} [\tilde{U}^\dagger \tilde{U}]_{mn} = \delta_{\mathbf{k},\mathbf{k}'} \delta_{mn}$. For brevity, we often suppress the \mathbf{k} dependence.

We assume there is a gap around the N_f quasi-flat bands, which we will refer to as the flat bands; in the strong coupling approximation, we do not require them to be exactly flat. We project all operators into the flat bands by setting $\gamma_{\mathbf{k},n} = 0$ if n is not one of the flat bands. Now denote $U(\mathbf{k})$ as the $N_{orb} \times N_f$ occupied eigenstate matrix which obeys $U^\dagger(\mathbf{k})U(\mathbf{k}) = \mathbb{1}_{N_f}$ and $U(\mathbf{k})U^\dagger(\mathbf{k}) = P(\mathbf{k})$ where P is the $N_{orb} \times N_{orb}$ projector matrix obeying $P^2 = P, P^\dagger = P, \text{Tr } P = N_f$. We recall that in the exactly flat case, the eigenstates are degenerate and hence are only defined up to the gauge freedom $U(\mathbf{k}) \rightarrow U(\mathbf{k})\mathcal{W}(\mathbf{k})$ where $\mathcal{W}(\mathbf{k}) \in U(N_f)$ is a unitary matrix with arbitrary \mathbf{k} dependence [19]. Both $U^\dagger(\mathbf{k})U(\mathbf{k})$ and $U(\mathbf{k})U^\dagger(\mathbf{k})$ are invariant under this gauge freedom. The projector $P(\mathbf{k})$ encodes the topology and quantum geometry of the bulk bands. It will play an essential role in the many-body problem, highlighting the interplay of topology and interactions.

We now define the projected operators. Because we have set all $\gamma_{\mathbf{k},n}$ to zero other than the flat band operators, an (over)complete basis of the projected states is given by

$$\bar{c}_{\mathbf{k},\alpha} \equiv \sum_{n=1}^{N_{orb}} [\tilde{U}(\mathbf{k})]_{\alpha,n} \gamma_{\mathbf{k},n} = \sum_{n=1}^{N_f} [U(\mathbf{k})]_{\alpha,n} \gamma_{\mathbf{k},n} = \sum_{\beta} [U(\mathbf{k})U^\dagger(\mathbf{k})]_{\alpha\beta} c_{\mathbf{k},\beta} = \sum_{\beta} [P(\mathbf{k})]_{\alpha\beta} c_{\mathbf{k},\beta} \quad (\text{A3})$$

using Eq. (A2). Because the projector $P(\mathbf{k})$ is Hermitian, we have

$$\bar{c}_{\mathbf{k},\alpha}^\dagger = \sum_{\beta} c_{\mathbf{k},\beta}^\dagger P_{\alpha\beta}^*(\mathbf{k}) = \sum_{\beta} c_{\mathbf{k},\beta}^\dagger P_{\beta\alpha}(\mathbf{k}). \quad (\text{A4})$$

The $\bar{c}_{\mathbf{k},\alpha}^\dagger$ basis is invariant under the eigenvector gauge freedom (unlike the $\gamma_{\mathbf{k},n}^\dagger$ operators). However, the barred operators do not obey canonical anti-commutation relations because they are an overcomplete basis, whereas the $\gamma_{\mathbf{k},n}^\dagger$ operators form a complete basis. We compute

$$\{\bar{c}_{\mathbf{k},\alpha}, \bar{c}_{\mathbf{k}',\beta}^\dagger\} = \sum_{\alpha'\beta'} P_{\alpha\alpha'}(\mathbf{k}) \{c_{\mathbf{k},\alpha'}, c_{\mathbf{k}',\beta'}^\dagger\} P_{\beta'\beta}(\mathbf{k}') = \delta_{\mathbf{k}\mathbf{k}'} [P(\mathbf{k})^2]_{\alpha\beta} = \delta_{\mathbf{k}\mathbf{k}'} P_{\alpha\beta}(\mathbf{k}). \quad (\text{A5})$$

We now need the projected position operators in real space. They are defined in analogy to Eq. (A1) as

$$\begin{aligned} \bar{c}_{\mathbf{R},\alpha} &= \frac{1}{\sqrt{\mathcal{N}}} \sum_{\mathbf{k}} e^{-i\mathbf{k}\cdot(\mathbf{R}+\mathbf{r}_\alpha)} \bar{c}_{\mathbf{k},\alpha} \\ &= \frac{1}{\sqrt{\mathcal{N}}} \sum_{\mathbf{k}\beta} e^{-i\mathbf{k}\cdot(\mathbf{R}+\mathbf{r}_\alpha)} P_{\alpha\beta}(\mathbf{k}) c_{\mathbf{k},\beta} \\ &= \frac{1}{\sqrt{\mathcal{N}}} \sum_{\mathbf{R}'} \left(\frac{1}{\sqrt{\mathcal{N}}} \sum_{\mathbf{k}\beta} e^{-i\mathbf{k}\cdot(\mathbf{R}+\mathbf{r}_\alpha-\mathbf{R}'-\mathbf{r}_\beta)} P_{\alpha\beta}(\mathbf{k}) \right) c_{\mathbf{R}',\beta} \\ &= \sum_{\mathbf{R}'\beta} p_{\alpha\beta}(\mathbf{R}-\mathbf{R}') c_{\mathbf{R}',\beta} \end{aligned} \quad (\text{A6})$$

where we defined the Fourier transform of the projector, i.e. the real-space correlation function of the non-interacting flat bands, as

$$p_{\alpha\beta}(\mathbf{R}-\mathbf{R}') = \frac{1}{\mathcal{N}} \sum_{\mathbf{k}} e^{-i\mathbf{k}\cdot(\mathbf{R}+\mathbf{r}_\alpha-\mathbf{R}'-\mathbf{r}_\beta)} P_{\alpha\beta}(\mathbf{k}) = \frac{1}{\mathcal{N}} \sum_{\mathbf{k}} e^{-i\mathbf{k}\cdot(\mathbf{R}-\mathbf{R}')} [V(\mathbf{k})P(\mathbf{k})V^\dagger(\mathbf{k})]_{\alpha\beta}, \quad [V(\mathbf{k})]_{\alpha\beta} = e^{-i\mathbf{k}\cdot\mathbf{r}_\alpha} \delta_{\alpha\beta}. \quad (\text{A7})$$

The embedding matrix $V(\mathbf{k})$ defined in Eq. (A7) is a unitary diagonal matrix. Although it is sometimes useful [19] to take the thermodynamic limit $\mathcal{N} \rightarrow \infty$, we will keep \mathcal{N} finite throughout this work.

We prove some properties about $p(\mathbf{R})$. It is obvious that $p(\mathbf{R}) = p^\dagger(-\mathbf{R})$ by Hermiticity of $P(\mathbf{k})$ and $\text{Tr } p(\mathbf{R}) = N_f \delta_{\mathbf{R},0}$ follows from $\text{Tr } P(\mathbf{k}) = N_f$. We also have the Fourier inversion

$$P(\mathbf{k}) = \sum_{\mathbf{R}} e^{i\mathbf{k}\cdot\mathbf{R}} V^\dagger(\mathbf{k}) p(\mathbf{R}) V(\mathbf{k}). \quad (\text{A8})$$

From the projector property $P^2 = P$, we find the convolution identity[19]

$$p(\mathbf{R}) = \sum_{\mathbf{R}'} p(\mathbf{R} - \mathbf{R}') p(\mathbf{R}') \quad (\text{A9})$$

which we use to derive the real space anti-commutation relations (and can also be recovered from Eq. A5). We compute

$$\begin{aligned} \{\bar{c}_{\mathbf{R},\alpha}, \bar{c}_{\mathbf{R}',\beta}^\dagger\} &= \sum_{\mathbf{S}, \mathbf{S}', \alpha', \beta'} p_{\alpha\alpha'}(\mathbf{R} - \mathbf{S}) [p^\dagger(\mathbf{R}' - \mathbf{S}')]_{\beta'\beta} \{c_{\mathbf{S},\alpha'}, c_{\mathbf{S}',\beta'}^\dagger\} \\ &= \sum_{\mathbf{S}} [p(\mathbf{R} - \mathbf{S}) p^\dagger(\mathbf{R}' - \mathbf{S})]_{\alpha\beta} \\ &= \sum_{\mathbf{S}} [p(\mathbf{R} - \mathbf{R}' + \mathbf{S}) p^\dagger(\mathbf{S})]_{\alpha\beta} \\ &= p_{\alpha\beta}(\mathbf{R} - \mathbf{R}'). \end{aligned} \quad (\text{A10})$$

In the thermodynamic limit where $\mathcal{N} \rightarrow \infty$, the flat bands are gapped so $P(\mathbf{k})$ is continuous on the BZ and the real space correlation function $p(\mathbf{R})$ decays at least exponentially fast.

We now look at the projected density operators $\bar{n}_{\mathbf{k},\alpha} = \bar{c}_{\mathbf{k},\alpha}^\dagger \bar{c}_{\mathbf{k},\alpha}$. We use the anti-commutation relations Eq. (A5), finding

$$\bar{n}_{\mathbf{k},\alpha}^2 = \bar{c}_{\mathbf{k},\alpha}^\dagger \bar{c}_{\mathbf{k},\alpha} \bar{c}_{\mathbf{k},\alpha}^\dagger \bar{c}_{\mathbf{k},\alpha} = \bar{c}_{\mathbf{k},\alpha}^\dagger P_{\alpha\alpha}(\mathbf{k}) \bar{c}_{\mathbf{k},\alpha} - \bar{c}_{\mathbf{k},\alpha}^\dagger \bar{c}_{\mathbf{k},\alpha}^\dagger \bar{c}_{\mathbf{k},\alpha} \bar{c}_{\mathbf{k},\alpha} = P_{\alpha\alpha}(\mathbf{k}) \bar{n}_{\mathbf{k},\alpha} \quad (\text{A11})$$

where the second term vanishes because $\bar{c}_{\mathbf{k},\alpha}^\dagger$ anti-commutes with itself. In real space, the density $\bar{n}_{\mathbf{R},\alpha} = \bar{c}_{\mathbf{R},\alpha}^\dagger \bar{c}_{\mathbf{R},\alpha}$ obeys

$$\bar{n}_{\mathbf{R},\alpha}^2 = \bar{c}_{\mathbf{R},\alpha}^\dagger \bar{c}_{\mathbf{R},\alpha} \bar{c}_{\mathbf{R},\alpha}^\dagger \bar{c}_{\mathbf{R},\alpha} = \bar{c}_{\mathbf{R},\alpha}^\dagger p_{\alpha\alpha}(\mathbf{R} - \mathbf{R}) \bar{c}_{\mathbf{R},\alpha} - \bar{c}_{\mathbf{R},\alpha}^\dagger \bar{c}_{\mathbf{R},\alpha}^\dagger \bar{c}_{\mathbf{R},\alpha} \bar{c}_{\mathbf{R},\alpha} = p_{\alpha\alpha}(0) \bar{n}_{\mathbf{R},\alpha} \quad (\text{A12})$$

using Eq. (A10). The correlation function elements $p_{\alpha\alpha}(0)$ are onsite and measure local density of each orbital. They will play an important role in the many-body problem.

One may also derive these expressions from the electron operators in the kinetic energy band basis, $\gamma_{\mathbf{k},m}$. In this basis, projection simply involves restricting the bands to $m \in M$, where M labels the low-energy flat bands. The projected density reads

$$\bar{n}_{\mathbf{k},\alpha} = \sum_{m,n} U(\mathbf{k})_{\alpha,m}^* U(\mathbf{k})_{\alpha,n} \gamma_{\mathbf{k},m}^\dagger \gamma_{\mathbf{k},n} \quad (\text{A13})$$

$$\begin{aligned} \bar{n}_{\mathbf{k},\alpha}^2 &= \sum_{m,n} U(\mathbf{k})_{\alpha,m}^* U(\mathbf{k})_{\alpha,n} \gamma_{\mathbf{k},m}^\dagger \gamma_{\mathbf{k},n} \sum_{m',n'} U(\mathbf{k})_{\alpha,m'}^* U(\mathbf{k})_{\alpha,n'} \gamma_{\mathbf{k},m'}^\dagger \gamma_{\mathbf{k},n'} \\ &= \sum_{m,n} U(\mathbf{k})_{\alpha,m}^* U(\mathbf{k})_{\alpha,n} \sum_{m',n'} U(\mathbf{k})_{\alpha,m'}^* U(\mathbf{k})_{\alpha,n'} \gamma_{\mathbf{k},m}^\dagger [\{\gamma_{\mathbf{k},n}, \gamma_{\mathbf{k},m'}^\dagger\} - \gamma_{\mathbf{k},m'}^\dagger \gamma_{\mathbf{k},n}] \gamma_{\mathbf{k},n'} \\ &= \sum_{m,n} U(\mathbf{k})_{\alpha,m}^* U(\mathbf{k})_{\alpha,n} \sum_{m',n'} U(\mathbf{k})_{\alpha,m'}^* U(\mathbf{k})_{\alpha,n'} \gamma_{\mathbf{k},m}^\dagger [\delta_{n,m'} - 0] \gamma_{\mathbf{k},n'} \\ &= P_{\alpha\alpha}(\mathbf{k}) \bar{n}_{\mathbf{k},\alpha}. \end{aligned} \quad (\text{A14})$$

The zero in the second to last line arises from the antisymmetry upon interchange of the m, m' indices.

2. Uniform Pairing Condition from the Space group

As Tovmasyan, Peotta, Törmä, and Huber identified in Ref. [18], the solvability of the Hubbard model groundstates and excitations hinges on enforcing a simple criterion called the *uniform pairing condition* (UPC): $\sum_{\mathbf{R},\alpha} \bar{n}_{\mathbf{R},\alpha}^2 \propto$

$\sum_{\mathbf{R}\alpha} \bar{n}_{\mathbf{R},\alpha} + \bar{N}$ where \bar{N} is the total (projected) number operator. The UPC was originally proposed to ensure equal mean-field pairing strength on all the orbital sites, but the UPC is simply a property of the single-particle wavefunctions as we will show. Using Eq. (A12), we expand $\bar{n}_{\mathbf{R},\alpha}^2$ to find

$$\sum_{\mathbf{R}\alpha} \bar{n}_{\mathbf{R},\alpha}^2 = \sum_{\mathbf{R}\alpha} p_{\alpha\alpha}(0) \bar{n}_{\mathbf{R},\alpha} \quad (\text{A15})$$

To enforce Eq. (A15), we must have

$$p_{\alpha\alpha}(0) = \frac{1}{N_f} \sum_{\mathbf{k}} P_{\alpha\alpha}(\mathbf{k}) = \epsilon \text{ if } \bar{n}_{\mathbf{R},\alpha} \neq 0, \quad \forall \alpha \quad (\text{A16})$$

where the constant ϵ is independent of α and is fixed by $\text{Tr } p(0) = \sum_{\alpha} p_{\alpha\alpha}(0) = N_f$. We will derive the UPC (Eq. (A15)) from the appearance of the eta-pairing symmetry in the following section App. B.

The case of $\bar{n}_{\mathbf{R},\alpha} = 0$ can occur for a given α at all \mathbf{R} if the wavefunction of the flat bands is exactly zero on the orbital α (see Eq. (A4)). We will see that this is the case in the bipartite crystalline lattices we consider shortly[34].

We now show that space group symmetries can enforce the uniform pairing condition *generically*: arbitrary hoppings (preserving G) can be chosen as long as the underlying orbitals obey simple symmetry conditions which we make precise shortly. We consider unitary space group symmetries $g \in G$, $g = T_{\delta} g_s$ consisting of a symmorphic part g_s (a rotation or reflection) and non-symmorphic part T_{δ} (a translation by a fraction of a lattice vector). The vector representation of g on real-space vectors \mathbf{r} is defined to be $g\mathbf{r} = g_s\mathbf{r} + \delta$ [109]. The representations in momentum space take the form $D[g] = e^{ig_s\mathbf{k}\cdot\delta} D[g_s]$ where $D[g_s]$ is the $N_{orb} \times N_{orb}$ representation on the orbitals. On the single-particle Hamiltonian, g enforces

$$e^{ig_s\mathbf{k}\cdot\delta} D[g_s] \tilde{h}(\mathbf{k}) \left(e^{ig_s\mathbf{k}\cdot\delta} D[g_s] \right)^{\dagger} = D[g_s] \tilde{h}(\mathbf{k}) D^{\dagger}[g_s] = \tilde{h}(g_s\mathbf{k}), \quad (\text{A17})$$

canceling the non-symmorphic phases. From Eq. (A17), $D[g_s] P(\mathbf{k}) D^{\dagger}[g_s] = P(g_s\mathbf{k})$ [19, 109]. It is understood that the representation matrix $D[g]$ only depends on the symmorphic part of g , and henceforth we drop the s subscript.

We also need some simple notions from topological quantum chemistry. In a lattice with space group G , a Wyckoff position [27, 28] x of multiplicity n consists of the points $\mathbf{x}_1, \dots, \mathbf{x}_n$ in the unit cell which form an orbit of G : there exists $g \in G$ such that $\mathbf{x}_i = g\mathbf{x}_j$ for each $\mathbf{x}_i, \mathbf{x}_j \in x$. The site symmetry group of a point \mathbf{x} is defined by $G_{\mathbf{x}} = \{g \in G | g\mathbf{x} = \mathbf{x}\} \in G$, and all $G_{\mathbf{x}}$ for $\mathbf{x} \in x$ are isomorphic. Hence in any lattice with G , we can organize the orbitals into irreps of G_x at some Wyckoff position x . All such irreps are tabulated on the Bilbao Crystallographic Server [29, 30]. For instance in $G = p2$ generated by C_2 rotation and translations, the $1a$ position (of multiplicity 1) is the origin of the unit cell and $G_{1a} = \{1, C_2\}$ with two 1D irreps (even and odd under C_2). The $2e$ position (of multiplicity 2) is the generic nonmaximal position consisting of a pair of C_2 -related points, so G_{2e} is the trivial group $\{1\}$ (see Fig. 2).

We can now state our claim.

Lemma. Let x be a Wyckoff position (not necessarily maximal) with site-symmetry group G_x and irreps χ . The uniform pairing condition holds between all orbitals forming an irrep χ induced from the Wyckoff position x .

Proof. We define \tilde{G} as the group of symmetries of the unit cell, i.e. the space group mod lattice translations. We define the site-symmetry group $H = G_{\mathbf{x}_1} \cong G_x$ where for concreteness $G_{\mathbf{x}_1}$ is the point group of the site $\mathbf{x}_1 \in x$. For a Wyckoff position of multiplicity n and an irrep χ of G_x with dimension $|\chi|$ and (irreducible) representations $D^{\chi}[h]$ for $h \in H$, the Wyckoff position contains $n|\chi|$ orbitals per unit cell. We index the orbitals in a tensor product basis $\alpha = i, a$ where $i = 1, \dots, n$ and $a = 1, \dots, |\chi|$. It is useful to note that in this basis, the embedding matrices are block diagonal, $V_{ia,jb}[\mathbf{G}] = e^{-i\mathbf{r}_i \cdot \mathbf{G}} \delta_{ij} \delta_{ab}$. It is natural to employ a coset decomposition separating the onsite symmetries of H and the symmetries that connect different points in the Wyckoff position. The formal expression is $\tilde{G} = \tilde{g}_1 H + \dots + \tilde{g}_n H$, $n = \frac{|\tilde{G}|}{|H|}$ such that irreps of H form an induced representation in \tilde{G} [56]. Hence the representation matrices of G can be chosen as

$$\begin{aligned} D[h] &= \mathbb{1}_n \otimes D^{\chi}[h], \quad h \in H \\ D[\tilde{g}_i] &= P_{\tilde{g}_i} \otimes \mathbb{1}_{|\chi|}, \quad \tilde{g}_i \in \{\tilde{g}_1, \dots, \tilde{g}_n\} \end{aligned} \quad (\text{A18})$$

where $[P_{\tilde{g}}]_{ij} = \delta_{\tilde{g}\mathbf{x}_i, \mathbf{x}_j}$ is a permutation matrix[56] on the n sites of the Wyckoff position, and the Kronecker delta is understood mod lattice vectors. First we prove uniform pairing holds within the $|\chi|$ orbitals at a given \mathbf{x}_i . Choose an arbitrary diagonal block of $P(\mathbf{k})$ denoted $[P_i(\mathbf{k})]_{ab} = P_{ia,ib}(\mathbf{k})$. We have denoted $\alpha = ia$ and $\beta = ib$. Note that $P_i(\mathbf{k}) = P_i(\mathbf{k} + \mathbf{G})$ because the embedding matrix acts as $V_{ia,ib}[\mathbf{G}] = e^{-i\mathbf{x}_i \cdot \mathbf{G}} \delta_{ab}$, proportional to the identity. Then

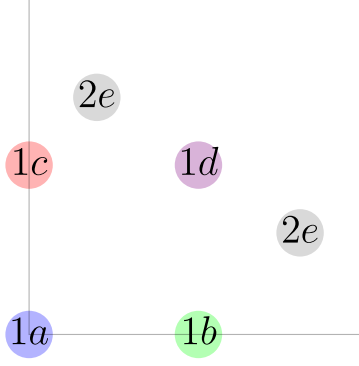


FIG. 2. Unit cell of the wallpaper group $p2$ generated by C_2 and translations (we take $\mathbf{a}_1 = (1, 0)$, $\mathbf{a}_2 = (0, 1)$ for ease). There are four maximal Wyckoff positions $1a = (0, 0)$, $1b = (0, 1/2)$, $1c = (0, 1/2)$, $1d = (1/2, 1/2)$ which all have multiplicity 1 and site symmetry group $G_x = 2$. At $1a$ for instance, the site symmetry group is $\{1, C_2\}$. The non-maximal Wyckoff position $2e = \{(x, y), (1 - x, 1 - y)\}$ has multiplicity 2 and consists of two general inversion-related points in the unit cell. Since C_2 exchanges the two points in $2e$, it is not part of the site symmetry group and thus $G_{2e} = 1$ containing only the identity.

because the BZ is symmetric under H , we have

$$\frac{1}{\mathcal{N}} \sum_{\mathbf{k}} P_i(\mathbf{k}) = \frac{1}{\mathcal{N}} \sum_{\mathbf{k}} P_i(h\mathbf{k}) = D^\chi[h] \left(\frac{1}{\mathcal{N}} \sum_{\mathbf{k}} P_i(\mathbf{k}) \right) D^\chi[h]^\dagger \quad (\text{A19})$$

but because $D^\chi[h]$ is irreducible, by Schur's lemma we find $\frac{1}{\mathcal{N}} \sum_{\mathbf{k}} P_i(\mathbf{k}) = \epsilon_i \mathbb{1}_{|\chi|}$ where ϵ_i is an arbitrary constant. That is, the only matrix invariant under an irreducible representation is proportional to the identity. If there were another invariant matrix, call it M , that matrix M would commute with all symmetries and thus will block-diagonalize the representation matrices, implying the representation was reducible.

To prove that $\epsilon_i = \epsilon_j$, relating different blocks, we use the fact that there exists $\tilde{g} \notin H$ such that $\tilde{g}\mathbf{x}_i = \mathbf{x}_j$. Then because $D[\tilde{g}]P(\mathbf{k})D^\dagger[\tilde{g}] = P(\tilde{g}\mathbf{k})$, we find that

$$\frac{1}{\mathcal{N}} \sum_{\mathbf{k}} P_i(\mathbf{k}) = \frac{1}{\mathcal{N}} \sum_{\mathbf{k}} P_i(g\mathbf{k}) = \frac{1}{\mathcal{N}} \sum_{\mathbf{k}} P_j(\mathbf{k}) \quad (\text{A20})$$

such that $\epsilon_i = \epsilon_j$. Thus $\frac{1}{\mathcal{N}} \sum_{\mathbf{k}} P_{\alpha\alpha}(\mathbf{k}) = \epsilon$ for all α in the irrep χ of the Wyckoff position x . Because $\text{Tr } P(\mathbf{k}) = N_f$, the number of projected bands, we have

$$\frac{1}{\mathcal{N}} \sum_{\mathbf{k}} P_{\alpha\alpha}(\mathbf{k}) = \frac{1}{\mathcal{N}} \sum_{\mathbf{k}} \frac{1}{n|\chi|} \text{Tr } P(\mathbf{k}) = \frac{N_f}{n|\chi|} \equiv \epsilon \leq 1. \quad (\text{A21})$$

The value of ϵ has physical meaning. From Eq. (A8), we see that $\epsilon = p_{\alpha\alpha}(0)$, which is the diagonal of the onsite correlation function. Although we have discussed only unitary symmetry groups in this proof, anti-unitary spatial symmetries, which do not act on spin, also enforce uniform pairing. This is easily seen because $P(\mathbf{k})$ is Hermitian and its diagonal elements must be real, so complex conjugation acts trivially. In App. F, we use the spinless symmetry $C_{6z}T$ to enforce uniform pairing between 6 orbitals.

We now extend this result to the case of a bipartite crystalline lattice consisting of the sublattices L and \tilde{L} . The integers N_L and $N_{\tilde{L}}$ denote the number of orbitals on each sublattice, so $N_{orb} = N_L + N_{\tilde{L}}$. Without loss of generality we take $N_L > N_{\tilde{L}}$. We consider single-particle Hamiltonians of the form

$$\tilde{h}(\mathbf{k}) = \begin{pmatrix} 0 & S_{\mathbf{k}} \\ S_{\mathbf{k}}^\dagger & B_{\mathbf{k}} \end{pmatrix} \quad (\text{A22})$$

where $S_{\mathbf{k}}$ is a $N_L \times N_{\tilde{L}}$ rectangular matrix and $B_{\mathbf{k}}$ is an $N_{\tilde{L}} \times N_{\tilde{L}}$ Hermitian matrix. The number of flat bands is $N_f = N_L - N_{\tilde{L}} > 0$ and their wavefunctions obey [34]

$$\begin{pmatrix} 0 & S_{\mathbf{k}} \\ S_{\mathbf{k}}^\dagger & B_{\mathbf{k}} \end{pmatrix} \begin{pmatrix} \psi_{\mathbf{k}} \\ 0 \end{pmatrix} = \begin{pmatrix} 0 \\ S_{\mathbf{k}}^\dagger \psi_{\mathbf{k}} \end{pmatrix} = 0 \quad (\text{A23})$$

where the existence of $N_f = N_L - N_{\tilde{L}}$ wavefunctions $\psi_{\mathbf{k},n}$, $n = 1, \dots, N_f$ in the nullspace of $S_{\mathbf{k}}^\dagger$ is guaranteed by rank deficiency. Thus the flat band projector

$$P(\mathbf{k}) = \sum_{n=1}^{N_f} \begin{pmatrix} \psi_{\mathbf{k},n} \\ 0 \end{pmatrix} \begin{pmatrix} \psi_{\mathbf{k},n}^\dagger & 0 \end{pmatrix} = \sum_{n=1}^{N_f} \begin{pmatrix} \psi_{\mathbf{k},n} \psi_{\mathbf{k},n}^\dagger & 0 \\ 0 & 0 \end{pmatrix} \quad (\text{A24})$$

has nonzero entries only in the L sublattice. As such, the projected operators $\bar{c}_{\mathbf{k},\alpha} = P_{\alpha\beta}(\mathbf{k})c_{\mathbf{k},\beta}$ are only nonzero when α is an orbital in the L sublattice, and so $\bar{n}_{\mathbf{R},\alpha \in \tilde{L}} = 0$. Hence for Eq. (A15) to hold, we only require $p_{\alpha\alpha}(0)$ to be independent of α within the L sublattice. As proven in the Lemma above, this is accomplished by requiring the L sublattice to consist of orbitals within a single irrep. More than one irrep would no longer guarantee the uniform pairing condition. Again because $\text{Tr } p(0) = N_f = N_L - N_{\tilde{L}}$, we have

$$p_{\alpha\alpha}(0) = \frac{N_f}{N_L} \equiv \epsilon < 1. \quad (\text{A25})$$

For simplicity of notation, we will not distinguish between sums over $\alpha \in L \oplus \tilde{L}$ and $\alpha \in L$. This is because the flat band wavefunctions have no weight in the \tilde{L} sublattice, and so the sums are interchangeable (any additional terms belonging to \tilde{L} are 0).

The notable feature of our construction is the total freedom to choose the hopping elements once the space group and orbitals are fixed. Using the bipartite crystalline lattice construction, we obtain perfectly flat bands obeying the uniform pairing condition in all space groups. The topology of the flat bands can be determined directly as the formal subtraction of the band representations of the two sublattices, and in many cases is fragile topological or obstructed atomic[34]. If the formal subtraction results in a “negative” irrep at high symmetry momentum \mathbf{K} , then the flat bands are gapless with the dispersive bands at \mathbf{K} . In this case, projection into the flat bands is not justified, but this case can be analyzed very generally in mean field theory [61].

Ref. [34] also constructs auxiliary models from the bipartite Hamiltonian in Eq. (A22). By integrating out the \tilde{L} sublattice, one obtains the positive semi-definite $N_L \times N_L$ Hamiltonian $\tilde{h}_L(\mathbf{k}) = S_{\mathbf{k}} S_{\mathbf{k}}^\dagger$ which retains the $N_L - N_{\tilde{L}}$ zero-energy flat bands with wavefunctions $\psi_{\mathbf{k},n}$, as well as $N_{\tilde{L}}$ dispersive bands. These models $\tilde{h}_L(\mathbf{k})$ also possess the uniform pairing condition.

a. Spin

To add spin, we impose S_z conservation and spinful time-reversal symmetry \mathcal{T} . Together, S_z and \mathcal{T} ensure the existence of an eta-pairing operator as we show in App. B. Enforcing these symmetries, the single-particle Hamiltonian takes the form

$$\tilde{h}_s(\mathbf{k}) = \begin{pmatrix} \tilde{h}_\uparrow(\mathbf{k}) & \\ & \tilde{h}_\downarrow(\mathbf{k}) \end{pmatrix} = \begin{pmatrix} \tilde{h}(\mathbf{k}) & \\ & \tilde{h}^*(-\mathbf{k}) \end{pmatrix} \quad (\text{A26})$$

where we used $D[\mathcal{T}] = i\sigma_y K$, so in particular \mathcal{T} acts diagonally on the orbital index α, β . Here σ_y acts on the spin indices and K is complex conjugation. Because of the global symmetry S_z , we can fix the gauge of \mathcal{T} on the eigenstates so that $U^\downarrow(\mathbf{k}) = U^\uparrow(-\mathbf{k})^*$ and $P^\downarrow(\mathbf{k}) = P^\uparrow(-\mathbf{k})^*$. As such we have

$$p_{\alpha\beta}^\downarrow(\mathbf{R} - \mathbf{R}') = \frac{1}{\mathcal{N}} \sum_{\mathbf{k}} e^{-i\mathbf{k} \cdot (\mathbf{R} + \mathbf{r}_\alpha - \mathbf{R}' - \mathbf{r}_\beta)} P_{\alpha\beta}^\uparrow(-\mathbf{k})^* = \left(\frac{1}{\mathcal{N}} \sum_{\mathbf{k}} e^{-i\mathbf{k} \cdot (\mathbf{R} + \mathbf{r}_\alpha - \mathbf{R}' - \mathbf{r}_\beta)} P_{\alpha\beta}^\uparrow(\mathbf{k}) \right)^* = p_{\alpha\beta}^\uparrow(\mathbf{R} - \mathbf{R}')^* \quad (\text{A27})$$

which is just the statement that \mathcal{T} acts locally in real space. If the uniform pairing condition is obeyed by $p^\downarrow(0)$, it is also by $p^\uparrow(0)$ using \mathcal{T} and S_z .

Appendix B: Hubbard Model and Eta-pairing Symmetry

In this section, we construct a class of positive semi-definite attractive Hubbard models using the uniform pairing condition generalizing the model of Ref. [18] (App. B1). The existence of an eta-pairing symmetry in the models we consider is protected by S_z and \mathcal{T} . We derive the form of the eta-pairing symmetry (App. B2) and show that it expands the $U(1) \times U(1)$ charge-spin symmetry group to a non-abelian $SU(2)$ symmetry group (App. B3).

1. Attractive Hubbard Models

We now add a Hubbard term H to the non-interacting Hamiltonian \tilde{H} in Eq. (A2). The form of the Hubbard term was discovered in Ref. [18] and yields an eta-pairing symmetry, $[H, \eta] = 0$. The first step is to define a projected Hermitian spin operator

$$\bar{S}_{\mathbf{R},\alpha}^z = \bar{c}_{\mathbf{R},\alpha,\uparrow}^\dagger \bar{c}_{\mathbf{R},\alpha,\uparrow} - \bar{c}_{\mathbf{R},\alpha,\downarrow}^\dagger \bar{c}_{\mathbf{R},\alpha,\downarrow} = \bar{n}_{\mathbf{R},\alpha,\uparrow} - \bar{n}_{\mathbf{R},\alpha,\downarrow}. \quad (\text{B1})$$

With the uniform pairing condition Eq. (A16), the form of this operator naturally gives an attractive Hubbard model. We define

$$H = \frac{1}{2}|U| \sum_{\mathbf{R},\alpha} (\bar{S}_{\mathbf{R},\alpha}^z)^2. \quad (\text{B2})$$

The crucial feature of H is that it is the sum of squares and thus is positive semi-definite. Hence a state $|\psi\rangle$ obeying $H|\psi\rangle = 0$ must be a ground state. Now we show that H is an attractive Hubbard model. Using Eq. (A12), we compute

$$\begin{aligned} H &= \frac{1}{2}|U| \sum_{\mathbf{R},\alpha} (\bar{n}_{\mathbf{R},\alpha,\uparrow} - \bar{n}_{\mathbf{R},\alpha,\downarrow})^2 \\ &= \frac{1}{2}|U| \sum_{\mathbf{R},\alpha} -2\bar{n}_{\mathbf{R},\alpha,\uparrow}\bar{n}_{\mathbf{R},\alpha,\downarrow} + p_{\alpha\alpha}^\uparrow(0)\bar{n}_{\mathbf{R},\alpha,\uparrow} + p_{\alpha\alpha}^\downarrow(0)\bar{n}_{\mathbf{R},\alpha,\downarrow} \\ &= -|U| \sum_{\mathbf{R},\alpha} \bar{n}_{\mathbf{R},\alpha,\uparrow}\bar{n}_{\mathbf{R},\alpha,\downarrow} + \frac{\epsilon|U|}{2} \sum_{\mathbf{R},\alpha} \bar{n}_{\mathbf{R},\alpha,\uparrow} + \bar{n}_{\mathbf{R},\alpha,\downarrow} \\ &= -|U| \sum_{\mathbf{R},\alpha} \bar{n}_{\mathbf{R},\alpha,\uparrow}\bar{n}_{\mathbf{R},\alpha,\downarrow} + \frac{\epsilon|U|}{2} \bar{N} \end{aligned} \quad (\text{B3})$$

which is a Hubbard interaction with strength $|U|$ and a chemical potential term $\frac{\epsilon|U|}{2}\bar{N}$. To get from line 2 to line 3, we have employed the uniform pairing condition $p_{\alpha\alpha}^\uparrow(0) = p_{\alpha\alpha}^\downarrow(0) = \frac{\epsilon|U|}{2}$. We have also used the fact that

$$\sum_{\mathbf{R},\alpha,\sigma} \bar{n}_{\mathbf{R},\alpha,\sigma} = \frac{1}{\mathcal{N}} \sum_{\mathbf{k},\mathbf{k}'} \sum_{\mathbf{R},\alpha,\sigma} e^{-i(\mathbf{k}-\mathbf{k}')\cdot(\mathbf{R}+\mathbf{r}_\alpha)} \bar{c}_{\mathbf{k}',\alpha,\sigma}^\dagger \bar{c}_{\mathbf{k},\alpha,\sigma} = \sum_{\mathbf{k},\alpha,\sigma} \bar{c}_{\mathbf{k},\alpha,\sigma}^\dagger \bar{c}_{\mathbf{k},\alpha,\sigma} = \sum_{\mathbf{k},n,\sigma} \gamma_{\mathbf{k},n,\sigma}^\dagger \gamma_{\mathbf{k},n,\sigma} = \bar{N} \quad (\text{B4})$$

where the final sum is over the N_f flat bands. Let us make a brief comment about the form of the attractive Hubbard term. The form of $\sum_{\alpha} \bar{n}_{\mathbf{R},\alpha,\uparrow}\bar{n}_{\mathbf{R},\alpha,\downarrow}$ is somewhat special because each orbital α only couples to itself (but opposite in spin). If there is only one orbital per Wyckoff position (i.e. a 1D irrep of G_x), this is the same type of term that one would get from a purely local Coulomb interaction. However if the irrep χ is multi-dimensional, like a pair of p_x, p_y orbitals per site, then a Coulomb interaction coupling the *total* densities would be $\sum_i (\sum_a \bar{n}_{\mathbf{R},ia,\uparrow})(\sum_a \bar{n}_{\mathbf{R},ia,\downarrow})$ in the tensor product notation of App. A 2 where a indexes the orbitals at a given point $\mathbf{x}_i \in x$. Given that the mechanism of generating attractive Hubbard interactions is typically phonons with a complicated coupling structure, we view Eq. (B3) as a simple model capturing the essential physics. Although we focus here on an attractive interaction, a particle-hole transformation[110] on the \downarrow spins maps all our results to the repulsive case with ferromagnetism.

2. Eta Operators

Generically, the $\bar{S}_{\mathbf{R},\alpha}^z$ operators do not commute among themselves because of the projection (see Eq. (A10)). However, in the trivial atomic limit case where the orbitals are totally decoupled, $\bar{S}_{\mathbf{R},\alpha}^z \rightarrow S_{\mathbf{R},\alpha}$ is commuting for all \mathbf{R}, α , yielding an infinite number of conserved charges. This is the classical limit where the model contains only strictly local density operators. This limit does not have superconductivity because there is no coherence – every site is decoupled. This is an indication that some obstruction to atomic localization, like topology or symmetry protected obstructed states, is necessary for the projected strong-coupling model to have a superconducting phase.

There is still a nontrivial symmetry operator when the projected bands are not atomic, the eta-pairing symmetry [18]. We use the most general two-body, charge +2, spin 0, momentum 0 operator for our ansatz of the η^\dagger operator. It takes the form

$$\eta^\dagger = \sum_{\mathbf{q}} \gamma_{\mathbf{q},m,\uparrow}^\dagger \Omega_{mn}(\mathbf{q}) \gamma_{-\mathbf{q},n,\downarrow}^\dagger \quad (\text{B5})$$

involving the yet undetermined matrix $\Omega_{mn}(\mathbf{q})$. We now must discuss the invariance of η^\dagger under the eigenvector gauge freedom $U^\sigma(\mathbf{k}) \rightarrow U^\sigma(\mathbf{k})\mathcal{W}^\sigma(\mathbf{k})$. Clearly for η^\dagger to be a physical symmetry, it must be invariant under the eigenvector gauge freedom which severely restricts the form of η to a simple ansatz. We will find that with S_z and \mathcal{T} , this ansatz is successful. Since S_z and \mathcal{T} are the symmetries relevant for real materials, we only consider this case explicitly in our work. However, we mention that the combination of particle-hole symmetry \mathcal{P} and $SU(2)$ spin symmetry also protects the existence of an η operator.

The operators $\gamma_{\mathbf{q},n,\sigma}^\dagger$ are not gauge invariant. Under the eigenvector gauge freedom, we have $\gamma_{\mathbf{q},n,\sigma}^\dagger \rightarrow \sum_{n'} \gamma_{\mathbf{q},n',\sigma}^\dagger \mathcal{W}_{n'n}^\sigma(\mathbf{q})$ where $\mathcal{W}^\sigma(\mathbf{q})$ is a unitary matrix. Hence

$$\begin{aligned} \eta^\dagger &\rightarrow \sum_{\mathbf{q},mnm'n'} \gamma_{\mathbf{q},m',\uparrow}^\dagger \mathcal{W}_{m'm}^\dagger(\mathbf{q}) \Omega_{mn}(\mathbf{q}) \gamma_{-\mathbf{q},n',\downarrow}^\dagger \mathcal{W}_{n'n}^\downarrow(-\mathbf{q}) \\ &= \sum_{\mathbf{q},m'n'} \gamma_{\mathbf{q},m',\uparrow}^\dagger [\mathcal{W}^\dagger(\mathbf{q}) \Omega(\mathbf{q}) \mathcal{W}^{\downarrow\dagger}(-\mathbf{q})^*]_{m'n'} \gamma_{-\mathbf{q},n',\downarrow}^\dagger. \end{aligned} \quad (\text{B6})$$

In order for η^\dagger to be invariant, we must have

$$\mathcal{W}^\dagger(\mathbf{q}) \Omega(\mathbf{q}) \mathcal{W}^{\downarrow\dagger}(-\mathbf{q})^* = \Omega(\mathbf{q}). \quad (\text{B7})$$

The natural object Ω transforming in this way is a sewing matrix[111, 112] relating states at \mathbf{q} and $-\mathbf{q}$. Because of the conjugation in Eq. (B7), the sewing matrix must be that of an anti-unitary symmetry, like time-reversal.

Fixing the gauge of the S_z and \mathcal{T} sewing matrices so that $U^\dagger(-\mathbf{q})^* = U^\downarrow(\mathbf{q})$, we can choose eigenstates such that $\mathcal{W}^\dagger(\mathbf{q}) = \mathcal{W}^\downarrow(-\mathbf{q})^*$ and thus $\mathcal{W}^\dagger(\mathbf{q}) \Omega(\mathbf{q}) \mathcal{W}^{\downarrow\dagger}(-\mathbf{q})^* = \mathcal{W}^\dagger(\mathbf{q}) \Omega(\mathbf{q}) \mathcal{W}^\dagger(\mathbf{q})^\dagger$. Thus η^\dagger is invariant under the gauge freedom if $\mathcal{W}^\dagger(\mathbf{q}) \Omega(\mathbf{q}) \mathcal{W}^\dagger(\mathbf{q})^\dagger = \Omega(\mathbf{q})$ which is satisfied for all arbitrary $\mathcal{W}^\dagger(\mathbf{q})$ iff $\Omega_{mn}(\mathbf{q}) \propto \delta_{mn}$. Thus we arrive at the ansatz

$$\eta^\dagger = \sum_{\mathbf{q},m} \gamma_{\mathbf{q},m,\uparrow}^\dagger \gamma_{-\mathbf{q},m,\downarrow}^\dagger \quad (\text{B8})$$

in the gauge-fixed wavefunctions where $U^\dagger(\mathbf{k}) = U^\downarrow(-\mathbf{k})^*$. The η^\dagger operator takes a simpler form in terms of the projected operators (which are gauge invariant). Recalling $\gamma_{\mathbf{q},m,\sigma}^\dagger = \sum_\alpha \bar{c}_{\mathbf{q},\alpha,\sigma}^\dagger U_{\alpha,m}^\sigma(\mathbf{q})$, we have

$$\eta^\dagger = \sum_{\mathbf{q},m\alpha\beta} \bar{c}_{\mathbf{q},\alpha,\uparrow}^\dagger U_{\alpha m}^\dagger(\mathbf{q}) U_{\beta m}^\downarrow(-\mathbf{q}) \bar{c}_{-\mathbf{q},\beta,\downarrow}^\dagger = \sum_{\mathbf{q},\alpha\beta} \bar{c}_{\mathbf{q},\alpha,\uparrow}^\dagger P_{\alpha\beta}^\dagger(\mathbf{q}) \bar{c}_{-\mathbf{q},\beta,\downarrow}^\dagger = \sum_{\mathbf{q}\alpha} \bar{c}_{\mathbf{q},\alpha,\uparrow}^\dagger \bar{c}_{-\mathbf{q},\alpha,\downarrow}^\dagger = \sum_{\mathbf{R}\alpha} \bar{c}_{\mathbf{R},\alpha,\uparrow}^\dagger \bar{c}_{\mathbf{R},\alpha,\downarrow}^\dagger. \quad (\text{B9})$$

In the last equality of Eq. (B9), we Fourier transformed to real space. Physically, η^\dagger can be understood as creating a Cooper pair at zero momentum. Note that the wavefunction of $\bar{c}_{\mathbf{R},\alpha,\uparrow}^\dagger \bar{c}_{\mathbf{R},\alpha,\downarrow}^\dagger$ decays exponentially outside the correlation length of $p(\mathbf{R})$, which describes the “size” of the Cooper pair bound state.

We now proceed to the commutator of η^\dagger and $\bar{S}_{\mathbf{R},\alpha}$:

$$\begin{aligned} [\bar{S}_{\mathbf{R},\alpha}^z, \eta^\dagger] &= \sum_{\mathbf{R}'\beta} [\bar{c}_{\mathbf{R},\alpha,\uparrow}^\dagger \bar{c}_{\mathbf{R},\alpha,\uparrow} - \bar{c}_{\mathbf{R},\alpha,\downarrow}^\dagger \bar{c}_{\mathbf{R},\alpha,\downarrow}, \bar{c}_{\mathbf{R}',\beta,\uparrow}^\dagger \bar{c}_{\mathbf{R}',\beta,\downarrow}^\dagger] \\ &= \sum_{\mathbf{R}'\beta} \bar{c}_{\mathbf{R},\alpha,\uparrow}^\dagger [\bar{c}_{\mathbf{R},\alpha,\uparrow}, \bar{c}_{\mathbf{R}',\beta,\uparrow}^\dagger \bar{c}_{\mathbf{R}',\beta,\downarrow}^\dagger] - \bar{c}_{\mathbf{R},\alpha,\downarrow}^\dagger [\bar{c}_{\mathbf{R},\alpha,\downarrow}, \bar{c}_{\mathbf{R}',\beta,\uparrow}^\dagger \bar{c}_{\mathbf{R}',\beta,\downarrow}^\dagger] \\ &= \sum_{\mathbf{R}'\beta} \bar{c}_{\mathbf{R},\alpha,\uparrow}^\dagger p_{\alpha\beta}^\dagger(\mathbf{R} - \mathbf{R}') \bar{c}_{\mathbf{R}',\beta,\downarrow}^\dagger + \bar{c}_{\mathbf{R},\alpha,\downarrow}^\dagger \bar{c}_{\mathbf{R}',\beta,\uparrow}^\dagger p_{\alpha\beta}^\downarrow(\mathbf{R} - \mathbf{R}') \end{aligned} \quad (\text{B10})$$

where we used the anti-commutator $\{\bar{c}_{\mathbf{k},\alpha,\sigma}, \bar{c}_{\mathbf{k},\beta,\sigma'}^\dagger\} = \delta_{\mathbf{k}\mathbf{k}'} P_{\alpha\beta}(\mathbf{k}) \delta_{\sigma\sigma'}$ (see Eq. (A10)). We expand the $\bar{c}_{\mathbf{R}',\beta,\sigma}^\dagger$ operators using Eq. (A6) to find

$$\begin{aligned} [\bar{S}_{\mathbf{R},\alpha}^z, \eta^\dagger] &= \sum_{\mathbf{R}'\mathbf{R}'',\beta\beta'} \bar{c}_{\mathbf{R},\alpha,\uparrow}^\dagger c_{\mathbf{R}'',\beta',\downarrow}^\dagger p_{\alpha\beta}^\dagger(\mathbf{R} - \mathbf{R}') p_{\beta\beta'}^{\downarrow*}(\mathbf{R}' - \mathbf{R}'') + \bar{c}_{\mathbf{R},\alpha,\downarrow}^\dagger c_{\mathbf{R}'',\beta',\uparrow}^\dagger p_{\beta\beta'}^{\uparrow*}(\mathbf{R}' - \mathbf{R}'') p_{\alpha\beta}^\downarrow(\mathbf{R} - \mathbf{R}') \\ &= \sum_{\mathbf{R}'\mathbf{R}'',\beta\beta'} \bar{c}_{\mathbf{R},\alpha,\uparrow}^\dagger c_{\mathbf{R}'',\beta',\downarrow}^\dagger p_{\alpha\beta}^\dagger(\mathbf{R} - \mathbf{R}') p_{\beta\beta'}^\dagger(\mathbf{R}' - \mathbf{R}'') + \bar{c}_{\mathbf{R},\alpha,\downarrow}^\dagger c_{\mathbf{R}'',\beta',\uparrow}^\dagger p_{\beta\beta'}^\downarrow(\mathbf{R}' - \mathbf{R}'') p_{\alpha\beta}^\downarrow(\mathbf{R} - \mathbf{R}') \\ &= \sum_{\mathbf{R}'\mathbf{R}'',\beta\beta'} \bar{c}_{\mathbf{R},\alpha,\uparrow}^\dagger c_{\mathbf{R}'',\beta',\downarrow}^\dagger [p^\dagger(\mathbf{R} - \mathbf{R}') p^\dagger(\mathbf{R}' - \mathbf{R}'')]_{\alpha\beta'} + \bar{c}_{\mathbf{R},\alpha,\downarrow}^\dagger c_{\mathbf{R}'',\beta',\uparrow}^\dagger [p^\downarrow(\mathbf{R} - \mathbf{R}') p^\downarrow(\mathbf{R}' - \mathbf{R}'')]_{\alpha\beta'} \end{aligned} \quad (\text{B11})$$

where we used $p_{\alpha\beta}^\dagger(\mathbf{R})^* = p_{\alpha\beta}^\dagger(\mathbf{R})$ thanks to \mathcal{T} in App. A 2 a. Finally, the convolution identity of $p(\mathbf{R})$ in Eq. (A9) gives

$$\begin{aligned}
[\bar{S}_{\mathbf{R},\alpha}^z, \eta^\dagger] &= \sum_{\mathbf{R}'', \beta'} \bar{c}_{\mathbf{R},\alpha,\uparrow}^\dagger c_{\mathbf{R}'', \beta', \downarrow}^\dagger p_{\alpha\beta'}^\dagger(\mathbf{R} - \mathbf{R}'') + \bar{c}_{\mathbf{R},\alpha,\downarrow}^\dagger c_{\mathbf{R}'', \beta', \uparrow}^\dagger p_{\alpha\beta'}^\dagger(\mathbf{R} - \mathbf{R}'') \\
&= \sum_{\mathbf{R}'', \beta'} \bar{c}_{\mathbf{R},\alpha,\uparrow}^\dagger c_{\mathbf{R}'', \beta', \downarrow}^\dagger p_{\alpha\beta'}^{\downarrow*}(\mathbf{R} - \mathbf{R}'') + \bar{c}_{\mathbf{R},\alpha,\downarrow}^\dagger c_{\mathbf{R}'', \beta', \uparrow}^\dagger p_{\alpha\beta'}^{\uparrow*}(\mathbf{R} - \mathbf{R}'') \\
&= (\bar{c}_{\mathbf{R},\alpha,\uparrow}^\dagger \bar{c}_{\mathbf{R},\alpha,\downarrow}^\dagger + \bar{c}_{\mathbf{R},\alpha,\downarrow}^\dagger \bar{c}_{\mathbf{R},\alpha,\uparrow}^\dagger) \\
&= 0
\end{aligned} \tag{B12}$$

again using Eq. (A6) to recover the projected operators in the penultimate line. Thus we have proven η^\dagger commutes with $\bar{S}_{\mathbf{R},\alpha}^z$, so it is trivially established that $[H, \eta^\dagger] = 0$. It follows that the eta-pairing states are all eigenstates:

$$H \eta^{\dagger n} |0\rangle = \eta^{\dagger n} H |0\rangle = 0 \tag{B13}$$

and in particular must be groundstates because H is positive semi-definite. Note that because $[\eta^\dagger, \bar{S}_{\mathbf{R},\alpha}^z] = 0$, one could consider much more general (though not necessarily physical) Hamiltonians with an eta-pairing symmetry than the onsite $H = \frac{|U|}{2} \sum_{\mathbf{R},\alpha} \bar{S}_{\mathbf{R},\alpha}^z \bar{S}_{\mathbf{R},\alpha}^z$ Hamiltonian studied in this work.

One may also calculate the commutators using the γ basis. We define the momentum space spin operator

$$\bar{S}_{\mathbf{q},\alpha}^z = \sum_{\mathbf{R}} e^{-i\mathbf{q}\cdot\mathbf{R}} \bar{S}_{\mathbf{R},\alpha}^z \tag{B14}$$

$$= \sum_{\mathbf{R},\alpha,\sigma} (-1)^\sigma e^{-i\mathbf{q}\cdot\mathbf{R}} \bar{n}_{\mathbf{R},\alpha,\sigma} \tag{B15}$$

$$= \sum_{\mathbf{k},\alpha,\sigma} (-1)^\sigma \bar{c}_{\mathbf{k}-\mathbf{q},\alpha,\sigma}^\dagger \bar{c}_{\mathbf{k},\alpha,\sigma} \tag{B16}$$

$$= \sum_{\mathbf{k},\alpha,\sigma} (-1)^\sigma [U^*(\mathbf{k} - \mathbf{q})]_{\alpha,m,\sigma} [U(\mathbf{k})]_{\alpha,n,\sigma} \gamma_{\mathbf{k}-\mathbf{q},m,\sigma}^\dagger \gamma_{\mathbf{k},n,\sigma} \tag{B17}$$

The commutator becomes

$$[\bar{S}_{\mathbf{p},\alpha}^z, \eta^\dagger] = \sum_{\mathbf{k},m,n,\sigma} \sum_{\mathbf{q},l} [(-1)^\sigma [U^*(\mathbf{k} - \mathbf{p})]_{\alpha,m,\sigma} [U(\mathbf{k})]_{\alpha,n,\sigma} \gamma_{\mathbf{k}-\mathbf{p},m,\sigma}^\dagger \gamma_{\mathbf{k},n,\sigma} \gamma_{\mathbf{q},l,\uparrow}^\dagger \gamma_{-\mathbf{q},l,\downarrow}^\dagger] \tag{B18}$$

$$= \sum_{\mathbf{k},m,n,\sigma} \sum_{\mathbf{q},l} [U^*(\mathbf{k} - \mathbf{p})]_{\alpha,m,\sigma} [U(\mathbf{k})]_{\alpha,n,\sigma} \left(\gamma_{\mathbf{k}-\mathbf{p},m,\uparrow}^\dagger \delta_{\mathbf{k},\mathbf{q}} \delta_{ln} \delta_{\sigma,\uparrow} \gamma_{-\mathbf{q},l,\downarrow}^\dagger - \gamma_{\mathbf{k}-\mathbf{p},m,\downarrow}^\dagger \delta_{\mathbf{k},-\mathbf{q}} \delta_{ln} \delta_{\sigma,\downarrow} \gamma_{\mathbf{q},l,\uparrow}^\dagger \right) \tag{B19}$$

$$= \sum_{\mathbf{k},m,n,\sigma} [U^*(\mathbf{k} - \mathbf{p})]_{\alpha,m,\sigma} [U(\mathbf{k})]_{\alpha,n,\sigma} \left(\delta_{\sigma,\uparrow} \gamma_{\mathbf{k}-\mathbf{p},m,\uparrow}^\dagger \gamma_{-\mathbf{k},n,\downarrow}^\dagger - \delta_{\sigma,\downarrow} \gamma_{\mathbf{k}-\mathbf{p},m,\downarrow}^\dagger \gamma_{-\mathbf{k},n,\uparrow}^\dagger \right) \tag{B20}$$

$$= \sum_{\mathbf{k},m,n,\sigma} ([U^*(\mathbf{k} - \mathbf{p})]_{\uparrow,m,\sigma} [U(\mathbf{k})]_{\uparrow,n,\sigma} - [U^*(-\mathbf{k})]_{\downarrow,n,\sigma} [U(\mathbf{p} - \mathbf{k})]_{\downarrow,m,\sigma}) \gamma_{\mathbf{k}-\mathbf{p},m,\uparrow}^\dagger \gamma_{-\mathbf{k},n,\downarrow}^\dagger = 0. \tag{B21}$$

3. Symmetry Algebra

The eta-pairing states $\eta^{\dagger n} |0\rangle$ are naturally interpreted as zero-momentum states of charge +2 Cooper pairs, with η^\dagger being their creation operator. Because the states $\eta^{\dagger n} |0\rangle$ are zero energy for each n , we can obtain eigenstates of H by taking superpositions with different numbers of particles. This is the simply the Cooper pair condensate that appears in the mean-field description. However, we work at fixed particle number in this work.

We now show that the eta-pairing operators form an $su(2)$ charge algebra which extends the usual $u(1)$ charge

algebra. We compute

$$\begin{aligned}
[\eta, \eta^\dagger] &= \sum_{\mathbf{k}\alpha\beta} [\bar{c}_{-\mathbf{k},\beta,\downarrow} \bar{c}_{\mathbf{k},\beta,\uparrow}^\dagger, \bar{c}_{\mathbf{q},\alpha,\uparrow}^\dagger \bar{c}_{-\mathbf{q},\alpha,\downarrow}^\dagger] \\
&= \sum_{\mathbf{k}\alpha\beta} \delta_{\mathbf{k},\mathbf{q}} \bar{c}_{-\mathbf{k},\beta,\downarrow} P_{\beta\alpha}^\dagger(\mathbf{k}) \bar{c}_{-\mathbf{q},\alpha,\downarrow}^\dagger - \delta_{\mathbf{k},\mathbf{q}} \bar{c}_{\mathbf{q},\alpha,\uparrow}^\dagger P_{\beta\alpha}^\dagger(-\mathbf{k}) \bar{c}_{\mathbf{k},\beta,\uparrow} \\
&= \sum_{\mathbf{k}\alpha\beta} \bar{c}_{\mathbf{k},\beta,\downarrow} P_{\beta\alpha}^\dagger(-\mathbf{k}) \bar{c}_{\mathbf{k},\alpha,\downarrow}^\dagger - \bar{c}_{\mathbf{k},\alpha,\uparrow}^\dagger P_{\beta\alpha}^\dagger(-\mathbf{k}) \bar{c}_{\mathbf{k},\beta,\uparrow} \\
&= \sum_{\mathbf{k}\alpha\beta} P_{\beta\alpha}^\dagger(-\mathbf{k}) P_{\beta\alpha}^\dagger(\mathbf{k}) - \bar{c}_{\mathbf{k},\alpha,\downarrow}^\dagger P_{\alpha\beta}^\dagger(\mathbf{k}) \bar{c}_{\mathbf{k},\beta,\downarrow} - \bar{c}_{\mathbf{k},\alpha,\uparrow}^\dagger P_{\alpha\beta}^\dagger(\mathbf{k}) \bar{c}_{\mathbf{k},\beta,\uparrow} \\
&= \sum_{\mathbf{k}\alpha\beta} P_{\beta\alpha}^\dagger(-\mathbf{k}) P_{\alpha\beta}^\dagger(-\mathbf{k}) - \bar{c}_{\mathbf{k},\alpha,\downarrow}^\dagger P_{\alpha\beta}^\dagger(\mathbf{k}) \bar{c}_{\mathbf{k},\beta,\downarrow} - \bar{c}_{\mathbf{k},\alpha,\uparrow}^\dagger P_{\alpha\beta}^\dagger(\mathbf{k}) \bar{c}_{\mathbf{k},\beta,\uparrow} \\
&= \sum_{\mathbf{k}} \text{Tr } P^\dagger(-\mathbf{k}) - \bar{N} \\
&= \mathcal{N}N_f - \bar{N}
\end{aligned} \tag{B22}$$

where we used that $P_{\beta\alpha}^\dagger(\mathbf{k}) = P_{\alpha\beta}^\dagger(-\mathbf{k})$ and $\sum_{\beta} P_{\alpha\beta}(\mathbf{k}) \bar{c}_{\mathbf{k},\beta} = \bar{c}_{\mathbf{k},\alpha}$. \bar{N} is the total number operator so

$$[\bar{N}, \eta^\dagger] = 2\eta^\dagger, \quad [\bar{N}, \eta] = -2\eta. \tag{B23}$$

Alternatively, in the γ band basis,

$$[\eta, \eta^\dagger] = \sum_{\mathbf{q},m} \sum_{\mathbf{q}',m'} [\gamma_{-\mathbf{q}',m',\downarrow} \gamma_{\mathbf{q}',m',\uparrow}^\dagger, \gamma_{\mathbf{q},m,\uparrow}^\dagger \gamma_{-\mathbf{q},m,\downarrow}^\dagger] \tag{B24}$$

$$= \sum_{\mathbf{q},m} \sum_{\mathbf{q}',m'} \gamma_{-\mathbf{q}',m',\downarrow} \{ \gamma_{\mathbf{q}',m',\uparrow}^\dagger, \gamma_{\mathbf{q},m,\uparrow}^\dagger \} \gamma_{-\mathbf{q},m,\downarrow}^\dagger - \gamma_{\mathbf{q},m,\uparrow}^\dagger \gamma_{\mathbf{q}',m',\uparrow}^\dagger \{ \gamma_{-\mathbf{q},m,\downarrow}^\dagger, \gamma_{-\mathbf{q}',m',\downarrow} \} \tag{B25}$$

$$= \sum_{\mathbf{q},m} \sum_{\mathbf{q}',m'} \gamma_{-\mathbf{q}',m',\downarrow} \delta_{mm'} \delta_{\mathbf{q}\mathbf{q}'} \gamma_{-\mathbf{q},m,\downarrow}^\dagger - \gamma_{\mathbf{q},m,\uparrow}^\dagger \gamma_{\mathbf{q}',m',\uparrow}^\dagger \delta_{mm'} \delta_{\mathbf{q}\mathbf{q}'} \tag{B26}$$

$$= \sum_{\mathbf{q},m} \gamma_{-\mathbf{q},m,\downarrow} \gamma_{-\mathbf{q},m,\downarrow}^\dagger - \gamma_{\mathbf{q},m,\uparrow}^\dagger \gamma_{\mathbf{q},m,\uparrow} = \mathcal{N}N_f - \bar{N}. \tag{B27}$$

To make the $su(2)$ Lie algebra explicit, the correct normalizations are

$$[\eta^a, \eta^b] = i\epsilon_{abc} \eta^c, \quad \eta^x = (\eta + \eta^\dagger)/2, \quad \eta^y = i(\eta - \eta^\dagger)/2, \quad \eta^z = (\bar{N} - \mathcal{N}N_f)/2. \tag{B28}$$

Thus we have shown that the η operators form a representation of $SU(2)$. It is simple to find the dimension of the representation. For a dimension d irrep of $SU(2)$, $\eta^{\dagger d} = 0$. Indeed, we know that $\eta^{\dagger(\mathcal{N}N_f+1)} = 0$ because the projected Hilbert space only contains $2\mathcal{N}N_f$ electrons, and η^\dagger adds two electrons to the state. It is possible to use the explicit representations of $SU(2)$ to obtain normalized states $|n\rangle \propto \eta^{\dagger n} |0\rangle$, but we will use a more direct method involving a generating function in the next section.

We now briefly address the spin symmetries. In the case of S_z and \mathcal{T} , the many-body S_z operator

$$\bar{S}_z = \sum_{\mathbf{k},n} \gamma_{\mathbf{k},n,\uparrow}^\dagger \gamma_{\mathbf{k},n,\uparrow} - \gamma_{\mathbf{k},n,\downarrow}^\dagger \gamma_{\mathbf{k},n,\downarrow} \tag{B29}$$

commutes with H . To see this, we use $[\bar{S}_z, \gamma_{\mathbf{k},n,\sigma}^\dagger] = s_\sigma^z \gamma_{\mathbf{k},n,\sigma}^\dagger$ (where $s_\sigma^z = \pm 1$ for $\sigma = \uparrow / \downarrow$) to check that $[\bar{S}_z, \bar{c}_{\mathbf{R},\alpha,\sigma}^\dagger] = s_\sigma^z \bar{c}_{\mathbf{R},\alpha,\sigma}^\dagger$. Thus $[\bar{S}_z, \bar{S}_{\mathbf{R},\alpha}^\dagger] = 0$ (so $[\bar{S}_z, H] = 0$) and also $[\bar{S}_z, \eta^\dagger] = 0$. Thus we have a $U(1) \times SU(2)$ symmetry group. We emphasize that H breaks spin $SU(2)$, having only $U(1)$ from conservation of S_z . One sign of this, which we will see later, is that the spin ± 1 excitations are gapped.

Appendix C: Off-diagonal Long Range Order in the Ground State and Generating Functions

In this section, we show that the eta-pairing ground states have ODLRO and thus display superconductivity at zero temperature. This calculation is tractable using a generating function of the BCS form (App. C1). In an effort to

be self-contained, we then show that Wick's theorem holds in the ground state (App. C 2) using a similar generating function with Grassman variables. Our calculations resemble previous calculations involving eta-pairing, for example Refs. [41, 113].

1. ODLRO

To assess the superconducting properties of the groundstate, we will compute the off-diagonals of the two-body density matrix:

$$\lim_{|\mathbf{R}-\mathbf{R}'|\rightarrow\infty} \langle GS | w_{\mathbf{R}'m\downarrow}^\dagger w_{\mathbf{R}m\uparrow}^\dagger w_{\mathbf{R}n\uparrow} w_{\mathbf{R}n\downarrow} | GS \rangle \quad (\text{C1})$$

in an eta-pairing groundstate $|GS\rangle$. Here $w_{\mathbf{R},n,\sigma}^\dagger$ is the Wannier function obtained from the canonical electron operators

$$w_{\mathbf{R},n,\sigma}^\dagger = \frac{1}{\sqrt{\mathcal{N}}} \sum_{\mathbf{k}} e^{i\mathbf{R}\cdot\mathbf{k}} \gamma_{\mathbf{k},n,\sigma}^\dagger. \quad (\text{C2})$$

Such operators can be chosen to be exponentially decaying in obstructed atomic limit bands, and also in fragile bands if we allow their symmetries to not be represented locally [53]. This is because the only obstruction to exponential localization is Chern number [49]. In the Wannier basis (choosing a time-reversal symmetric gauge for the γ operators where $U^\dagger(\mathbf{k}) = U^\dagger(-\mathbf{k})^*$), the η operator reads

$$\eta^\dagger = \sum_{\mathbf{q}n} \gamma_{\mathbf{q},m,\uparrow}^\dagger \gamma_{-\mathbf{q},m,\downarrow}^\dagger = \sum_{\mathbf{R},\mathbf{R}',m} w_{\mathbf{R},m,\uparrow}^\dagger w_{\mathbf{R}',m,\downarrow}^\dagger \frac{1}{\mathcal{N}} \sum_{\mathbf{q}} e^{-i(\mathbf{R}-\mathbf{R}')\cdot\mathbf{q}} = \sum_{\mathbf{R}} w_{\mathbf{R},m,\uparrow}^\dagger w_{\mathbf{R},m,\downarrow}^\dagger. \quad (\text{C3})$$

To calculate the correlator in Eq. (C1), we will employ a BCS-type ground state as a generating function:

$$|\{z\}\rangle = \exp \left(\sum_{\mathbf{R},m} z_{\mathbf{R},m} w_{\mathbf{R},m,\uparrow}^\dagger w_{\mathbf{R},m,\downarrow}^\dagger \right) |0\rangle \quad (\text{C4})$$

with free parameters $z_{\mathbf{R},m}$. First we observe that setting $z_{\mathbf{R},m} = z$ gives

$$\langle \{z\} = z | \{z\} = z \rangle = \langle 0 | e^{\bar{z}\eta} e^{z\eta^\dagger} | 0 \rangle = \sum_n \frac{|z|^{2n}}{n!^2} \langle 0 | \eta^n \eta^{\dagger n} | 0 \rangle \quad (\text{C5})$$

which we will use to determine the norms of the eta-pairing states. Second, we note the ODLRO correlators appear when taking derivatives:

$$\begin{aligned} \left. \frac{\partial}{\partial \bar{z}_{\mathbf{R},n}} \frac{\partial}{\partial z_{\mathbf{R}',m}} \langle \{z\} | \{z\} \rangle \right|_{z_{\mathbf{R},m}=z} &= \langle 0 | e^{\bar{z}\eta} w_{\mathbf{R},n,\downarrow} w_{\mathbf{R},n,\uparrow} w_{\mathbf{R}',m,\uparrow}^\dagger w_{\mathbf{R}',m,\downarrow}^\dagger e^{z\eta^\dagger} | 0 \rangle \\ &= \sum_n \frac{|z|^{2n}}{n!^2} \langle 0 | \eta^n w_{\mathbf{R},n,\downarrow} w_{\mathbf{R},n,\uparrow} w_{\mathbf{R}',m,\uparrow}^\dagger w_{\mathbf{R}',m,\downarrow}^\dagger \eta^{\dagger n} | 0 \rangle. \end{aligned} \quad (\text{C6})$$

We now must compute $\langle \{z\} | \{z\} \rangle$. We use the orthogonality of the Wannier basis, $\{w_{\mathbf{R},m,\sigma}, w_{\mathbf{R}',n,\sigma'}^\dagger\} = \delta_{\mathbf{R}\mathbf{R}'} \delta_{mn} \delta_{\sigma,\sigma'}$ to factor Eq. (C4) into commuting terms

$$\begin{aligned} \langle \{z\} | \{z\} \rangle &= \langle 0 | \prod_{\mathbf{R}m} e^{\bar{z}_{\mathbf{R},m} w_{\mathbf{R},m,\downarrow} w_{\mathbf{R},m,\uparrow}} \prod_{\mathbf{R}'n} e^{z_{\mathbf{R}',n} w_{\mathbf{R}',n,\uparrow}^\dagger w_{\mathbf{R}',n,\downarrow}^\dagger} | 0 \rangle \\ &= \langle 0 | \prod_{\mathbf{R}m} (1 + \bar{z}_{\mathbf{R},m} w_{\mathbf{R},m,\downarrow} w_{\mathbf{R},m,\uparrow}) \prod_{\mathbf{R}'n} (1 + z_{\mathbf{R}',n} w_{\mathbf{R}',n,\uparrow}^\dagger w_{\mathbf{R}',n,\downarrow}^\dagger) | 0 \rangle \end{aligned} \quad (\text{C7})$$

where we used that fact that $(w_{\mathbf{R}',n,\uparrow}^\dagger w_{\mathbf{R}',n,\downarrow}^\dagger)^2 = 0$. Commuting through the different factors and recalling $w_{\mathbf{R},m}^\dagger$ obey canonical commutation relations, we see that

$$\begin{aligned} \langle \{z\} | \{z\} \rangle &= \langle 0 | \prod_{\mathbf{R}m} (1 + \bar{z}_{\mathbf{R},m} w_{\mathbf{R},m,\downarrow} w_{\mathbf{R},m,\uparrow}) (1 + z_{\mathbf{R},m} w_{\mathbf{R},m,\uparrow}^\dagger w_{\mathbf{R},m,\downarrow}^\dagger) | 0 \rangle \\ &= \prod_{\mathbf{R}m} (1 + |z_{\mathbf{R},m}|^2). \end{aligned} \quad (\text{C8})$$

Comparing to Eq. (C5) and using the binomial theorem, using Eq. (C5) we obtain

$$\begin{aligned} \langle \{z\} | \{z\} \rangle |_{\{z\}=z} &= (1 + |z|^2)^{N_f \mathcal{N}} = \prod_{\mathbf{R}m} (1 + |z|^2) = (1 + |z|^2)^{N_f \mathcal{N}} \\ \sum_n \frac{|z|^{2n}}{n!^2} \langle 0 | \eta^n \eta^{\dagger n} | 0 \rangle &= \sum_n \binom{N_f \mathcal{N}}{n} |z|^{2n} \end{aligned} \quad (\text{C9})$$

so equating coefficients, the normed eta-pairing states are

$$|n\rangle = \frac{1}{n!} \binom{N_f \mathcal{N}}{n}^{-\frac{1}{2}} \eta^{\dagger n} |0\rangle. \quad (\text{C10})$$

Then to obtain the ODLRO correlators, we observe that

$$\frac{\partial}{\partial \bar{z}_{\mathbf{R},n}} \frac{\partial}{\partial z_{\mathbf{R}',m}} \langle \{z\} | \{z\} \rangle \Big|_{\{z\}=z} = |z|^2 (1 + |z|^2)^{N_f \mathcal{N} - 2} = \sum_n \binom{N_f \mathcal{N} - 2}{n} |z|^{2n+2}, \quad \mathbf{R}, n \neq \mathbf{R}', m. \quad (\text{C11})$$

Comparing to Eq. (C6) and using, we obtain

$$\binom{N_f \mathcal{N}}{n} \langle 0 | \eta^n w_{\mathbf{R},n,\downarrow} w_{\mathbf{R},n,\uparrow} w_{\mathbf{R}',m,\uparrow}^\dagger w_{\mathbf{R}',m,\downarrow}^\dagger \eta^{\dagger n} | 0 \rangle = \binom{N_f \mathcal{N} - 2}{n-1}. \quad (\text{C12})$$

For $\mathbf{R}, n \neq \mathbf{R}', m$, we commute $w_{\mathbf{R},n,\downarrow} w_{\mathbf{R},n,\uparrow}$ through $w_{\mathbf{R}',m,\uparrow}^\dagger w_{\mathbf{R}',m,\downarrow}^\dagger$ and obtain

$$\begin{aligned} \langle n | w_{\mathbf{R}m\downarrow}^\dagger w_{\mathbf{R}m\uparrow}^\dagger w_{\mathbf{R}'n\uparrow} w_{\mathbf{R}'n\downarrow} | n \rangle &= \frac{(N_f \mathcal{N} - 2)!}{(N_f \mathcal{N} - n - 1)!(n-1)!} \frac{(N_f \mathcal{N} - n)!n!}{(N_f \mathcal{N})!} \\ &= \frac{n(N_f \mathcal{N} - n)}{N_f \mathcal{N}(N_f \mathcal{N} - 1)} \\ &= \nu(1 - \nu) + O(1/\mathcal{N}) \end{aligned} \quad (\text{C13})$$

where we defined the filling $\nu = n/N_f \mathcal{N} \in (0, 1)$. The other notable feature of this calculation is that for $\mathbf{R} \neq \mathbf{R}'$, there is no dependence on $|\mathbf{R} - \mathbf{R}'|$ in the correlator. This is reminiscent of the ODLRO in a $T = 0$ Bose-Einstein condensate, which also has no $|\mathbf{R} - \mathbf{R}'|$ dependence and is equal to the boson density. Indeed, comparing to mean field calculations of the superfluid weight[61], $\nu(1 - \nu)$ is also obtained as the Cooper pair density.

For exponentially decaying Wannier states, Eq. (C13) is a good local measure of off-diagonal long range order. The ODLRO has the interpretation of correlators between two particles at position \mathbf{R} and another two at position \mathbf{R}' : should the Wannier states fail to be localized Eq. (C1) loses this interpretation. We thus must address the question: are the w degrees of freedom employed in the ODLRO correlation exponentially localized? In the uniform pairing, where bands are constructed from the S -matrix method, the bands are fragile or obstructed atomic and thus exponentially localized Wannier states can be found [49], but the symmetries cannot be represented locally on them if there is fragile topology. We remark that it is possible to obtain perfectly flat bands with a nonzero Chern number C_σ with uniform pairing from a single Wyckoff position sublattice, but this requires exponentially decaying (infinite range) hoppings. The total Chern number $C_\uparrow + C_\downarrow$ will vanish due to spin-ful time reversal symmetry, and thus it is possible to find exponentially localized Wannier states by mixing the bands of different spin. However, the calculation in this section relies on the spin-polarized Wannier states Eq. (C2), and thus the optimal decay of the Wannier states, for nonzero C_σ , is a power law [52]. An adaptation of Eq. (C13) in terms of exponentially localized states when $C_\sigma \neq 0$ is left for future work.

2. Wick's theorem

We now extend the generating function method of App. C 1 to show that a version of Wick's theorem holds in the eta-pairing states. In this section we work in the momentum basis using the $\gamma_{\mathbf{k},m,\sigma}^\dagger$ operators. Wick's theorem shows that arbitrary correlators can be determined by enumerating the contractions, which allows us to compute expressions for the norms of the excitations in App. D and calculate expectation values.

The generating function we introduce is the norm $N(z, \xi)$ of the following state:

$$|\xi, z\rangle = \exp \left(\sum_{\mathbf{k}n\sigma} \xi_{\mathbf{k},n,\sigma} \gamma_{\mathbf{k},n,\sigma}^\dagger \right) e^{z\eta^\dagger} |0\rangle, \quad N(z, \xi) = \langle \xi, z | \xi, z \rangle \quad (\text{C14})$$

where $\xi_{\mathbf{k},n,\sigma}$ are anti-commuting (fermionic) Grassman variables, and bar denotes the complex conjugate $\bar{\xi} = \xi^\dagger$. Taking ξ derivatives of $N(\xi, z)$ and then setting $\xi = 0$ pulls down γ^\dagger operators which build the correlation function. We observe that

$$\begin{aligned} \gamma_{\mathbf{k},n,\sigma}^\dagger |\xi, z\rangle &= \partial_{\xi_{\mathbf{k},n,\sigma}} \exp\left(\sum_{\mathbf{k}'n'\sigma'} \xi_{\mathbf{k}',n',\sigma'} \gamma_{\mathbf{k}',n',\sigma'}^\dagger\right) e^{z\eta^\dagger} |0\rangle = \partial_{\xi_{\mathbf{k},n,\sigma}} |\xi, z\rangle \\ \langle \xi, z | \gamma_{\mathbf{k},n,\sigma} &= -\partial_{\bar{\xi}_{\mathbf{k},n,\sigma}} \langle 0 | e^{\bar{z}\eta} \exp\left(\sum_{\mathbf{k}'n'\sigma'} \gamma_{\mathbf{k}',n',\sigma'} \bar{\xi}_{\mathbf{k}',n',\sigma'}\right) = -\partial_{\bar{\xi}_{\mathbf{k},n,\sigma}} \langle \xi, z | . \end{aligned} \quad (\text{C15})$$

We see for instance that

$$\begin{aligned} \langle \xi, z | \gamma_{\mathbf{k}',n',\sigma'}^\dagger \gamma_{\mathbf{k},n,\sigma}^\dagger |\xi, z\rangle &= -\partial_{\bar{\xi}_{\mathbf{k}',n',\sigma'}} \langle \xi, z | \partial_{\xi_{\mathbf{k},n,\sigma}} |\xi, z\rangle = \partial_{\xi_{\mathbf{k},n,\sigma}} \partial_{\bar{\xi}_{\mathbf{k}',n',\sigma'}} N(z, \xi) \\ \langle z | \gamma_{\mathbf{k}',n',\sigma'}^\dagger \gamma_{\mathbf{k},n,\sigma}^\dagger |z\rangle &= \partial_{\xi_{\mathbf{k},n,\sigma}} \partial_{\bar{\xi}_{\mathbf{k}',n',\sigma'}} N(z, \xi) \Big|_{\xi=0} \end{aligned} \quad (\text{C16})$$

and thus by matching powers of $|z|^2$ in $\partial_{\xi_{\mathbf{k},m,\sigma}} \partial_{\bar{\xi}_{\mathbf{k},m,\sigma}} N(z, \xi)$ and $\langle z | \gamma_{\mathbf{k},m,\sigma} \gamma_{\mathbf{k},m,\sigma}^\dagger |z\rangle$, the correlators $\langle n | \gamma_{\mathbf{k},m,\sigma} \gamma_{\mathbf{k},m,\sigma}^\dagger |n\rangle$ can be determined. Generally, any correlator with creation operators to the right and annihilation operators to the left can be reduced by repeated application of Eq. (C15) to derivatives of $\langle \xi, z | \xi, z\rangle = N(\xi, z)$ (and then setting $\xi \rightarrow 0$). This defines a normal ordering.

We can compute $N(z, \xi)$ directly. Because ξ and γ^\dagger are all anti-commuting, we have

$$\begin{aligned} |\xi, z\rangle &= \exp\left(\sum_{\mathbf{k}n\sigma} \xi_{\mathbf{k},n,\sigma} \gamma_{\mathbf{k},n,\sigma}^\dagger\right) e^{z\eta^\dagger} |0\rangle \\ &= \exp\left(\sum_{\mathbf{k}n} \xi_{\mathbf{k},n,\uparrow} \gamma_{\mathbf{k},n,\uparrow}^\dagger + \xi_{-\mathbf{k},n,\downarrow} \gamma_{-\mathbf{k},n,\downarrow}^\dagger + z \gamma_{\mathbf{k},n,\uparrow}^\dagger \gamma_{-\mathbf{k},n,\downarrow}^\dagger\right) |0\rangle \\ &= \prod_{\mathbf{k},n} \exp\left(\xi_{\mathbf{k},n,\uparrow} \gamma_{\mathbf{k},n,\uparrow}^\dagger + \xi_{-\mathbf{k},n,\downarrow} \gamma_{-\mathbf{k},n,\downarrow}^\dagger + z \gamma_{\mathbf{k},n,\uparrow}^\dagger \gamma_{-\mathbf{k},n,\downarrow}^\dagger\right) |0\rangle \\ &= \prod_{\mathbf{k},n} (1 + \xi_{\mathbf{k},n,\uparrow} \gamma_{\mathbf{k},n,\uparrow}^\dagger + \xi_{-\mathbf{k},n,\downarrow} \gamma_{-\mathbf{k},n,\downarrow}^\dagger + (z + \xi_{-\mathbf{k},n,\downarrow} \xi_{\mathbf{k},n,\uparrow}) \gamma_{\mathbf{k},n,\uparrow}^\dagger \gamma_{-\mathbf{k},n,\downarrow}^\dagger) |0\rangle \end{aligned} \quad (\text{C17})$$

using $\xi^2 = \gamma^{\dagger 2} = 0$ and $[\xi \gamma^\dagger, \eta^\dagger] = 0$. The ξ operators must be Grassmanns, else $[\xi_{\mathbf{k},n,\uparrow} \gamma_{\mathbf{k},n,\uparrow}^\dagger, \xi_{\mathbf{k}',n',\uparrow} \gamma_{\mathbf{k}',n',\uparrow}^\dagger] \neq 0$. The only term at second order is the cross term from $\frac{1}{2!}(\xi_{-\mathbf{k},n,\downarrow} \gamma_{-\mathbf{k},n,\downarrow}^\dagger + \gamma_{\mathbf{k},n,\uparrow}^\dagger \xi_{\mathbf{k},n,\uparrow})^2$. Hence we find

$$N(z, \xi) = \langle \xi, z | \xi, z\rangle = \prod_{\mathbf{k},n} (1 + \bar{\xi}_{\mathbf{k},n,\uparrow} \xi_{\mathbf{k},n,\uparrow} + \bar{\xi}_{-\mathbf{k},n,\downarrow} \xi_{-\mathbf{k},n,\downarrow} + (\bar{z} + \bar{\xi}_{\mathbf{k},n,\uparrow} \bar{\xi}_{-\mathbf{k},n,\downarrow})(z + \xi_{-\mathbf{k},n,\downarrow} \xi_{\mathbf{k},n,\uparrow})) \quad (\text{C18})$$

which importantly is decoupled in \mathbf{k} and n . Let us expand out a single factor of Eq. (C18):

$$1 + |z|^2 + \bar{\xi}_{\mathbf{k},n,\uparrow} \xi_{\mathbf{k},n,\uparrow} + \bar{\xi}_{-\mathbf{k},n,\downarrow} \xi_{-\mathbf{k},n,\downarrow} + z \bar{\xi}_{\mathbf{k},n,\uparrow} \bar{\xi}_{-\mathbf{k},n,\downarrow} + \bar{z} \xi_{-\mathbf{k},n,\downarrow} \xi_{\mathbf{k},n,\uparrow} + \bar{\xi}_{\mathbf{k},n,\uparrow} \bar{\xi}_{-\mathbf{k},n,\downarrow} \xi_{-\mathbf{k},n,\downarrow} \xi_{\mathbf{k},n,\uparrow} \quad (\text{C19})$$

which contains only quadratic and quartic terms in ξ . Because we take ξ derivatives and then set $\xi \rightarrow 0$, we see that only two- and four- term derivatives (for each \mathbf{k}, m) are nonzero. From Eq. (C15), we compute

$$\begin{aligned} \langle z | \gamma_{\mathbf{k}m\downarrow} \gamma_{\mathbf{k}'m'\uparrow}^\dagger |z\rangle &= \partial_{\xi_{\mathbf{k},m,\downarrow}} \partial_{\bar{\xi}_{\mathbf{k}',m',\uparrow}} N|_{\xi=0} = \frac{\delta_{\mathbf{k}\mathbf{k}'} \delta_{mm'} \delta_{\sigma\sigma'}}{1 + |z|^2} \langle z | z\rangle \\ \langle z | \gamma_{\mathbf{k}m\downarrow} \gamma_{\mathbf{k}'m'\uparrow}^\dagger |z\rangle &= \partial_{\bar{\xi}_{\mathbf{k},m,\downarrow}} \partial_{\xi_{\mathbf{k}',m',\uparrow}} N|_{\xi=0} = \frac{z \delta_{\mathbf{k},-\mathbf{k}'} \delta_{mm'}}{1 + |z|^2} \langle z | z\rangle \\ \langle z | \gamma_{\mathbf{k}m\uparrow}^\dagger \gamma_{\mathbf{k}'m'\downarrow}^\dagger |z\rangle &= \partial_{\xi_{\mathbf{k},m,\uparrow}} \partial_{\xi_{\mathbf{k}',m',\downarrow}} N|_{\xi=0} = \frac{\bar{z} \delta_{\mathbf{k},-\mathbf{k}'} \delta_{mm'}}{1 + |z|^2} \langle z | z\rangle \end{aligned} \quad (\text{C20})$$

with all other two derivative terms being zero, and $\langle z | z\rangle = (1 + |z|^2)^{N_f N}$. We observe in the second and third line a nonzero anomalous BCS-type contraction between $\gamma\gamma$ or $\gamma^\dagger\gamma^\dagger$. The last nonzero term comes from the four-body derivative:

$$\langle z | \gamma_{-\mathbf{k}m\downarrow} \gamma_{\mathbf{k}m\uparrow}^\dagger \gamma_{\mathbf{k}m\uparrow}^\dagger \gamma_{-\mathbf{k}m\downarrow} |z\rangle = \partial_{\xi_{\mathbf{k},m,\uparrow}} \partial_{\xi_{-\mathbf{k},m,\downarrow}} \partial_{\bar{\xi}_{-\mathbf{k},m,\downarrow}} \partial_{\bar{\xi}_{\mathbf{k},m,\uparrow}} N|_{\xi=0} = \frac{1}{1 + |z|^2} \langle z | z\rangle . \quad (\text{C21})$$

So far we have given a recipe to compute all normal ordered correlators. Using the canonical anti-commutation relations of γ , all correlators can be manipulated into normal order and then evaluated. However, it is of practical interest to evaluate correlators directly in any order. We now calculate the one-body contractions, Eqs. (C20) and (C21), in which a $\gamma^\dagger\gamma$ contraction is introduced to be consistent with the fermion anti-commutation relations. This is a standard result (see Ref. [47]) but we include a proof here to set the notation and be self-contained. All many-body contractions will be built from these one-body contractions.

We compute the non-normal ordered correlator

$$\begin{aligned}\langle z|\gamma_{\mathbf{k}\mathbf{m}\sigma}^\dagger\gamma_{\mathbf{k}'\mathbf{m}'\sigma'}|z\rangle &= -\langle z|\gamma_{\mathbf{k}'\mathbf{m}'\sigma'}\gamma_{\mathbf{k}\mathbf{m}\sigma}^\dagger|z\rangle + \delta_{\mathbf{k}\mathbf{k}'}\delta_{mm'}\delta_{\sigma\sigma'}\langle z|z\rangle \\ &= \delta_{\mathbf{k}\mathbf{k}'}\delta_{mm'}\delta_{\sigma\sigma'}\langle z|z\rangle\left(-\frac{1}{1+|z|^2}+1\right) \\ &= \delta_{\mathbf{k}\mathbf{k}'}\delta_{mm'}\delta_{\sigma\sigma'}\frac{|z|^2}{1+|z|^2}\langle z|z\rangle.\end{aligned}\tag{C22}$$

This correlator will define a two-particle contraction to be included in Wick's theorem: correlators are equal to the signed sum of all possible two-particle contractions defined in Eqs. (C20) and (C22). Because only two- and four-particle contractions are nonzero and the two-particle contractions satisfy Wick's theorem automatically, we only need to check that Eq. (C21) is consistent with this Wick's theorem. Consider the only non-zero normal ordered four-particle correlator $\langle z|\gamma_{-\mathbf{k}\mathbf{m}\downarrow}\gamma_{\mathbf{k}\mathbf{m}\uparrow}\gamma_{\mathbf{k}\mathbf{m}\uparrow}^\dagger\gamma_{-\mathbf{k}\mathbf{m}\downarrow}^\dagger|z\rangle$. There are three possible contractions from Wick's theorem (one vanishing):

$$\begin{aligned}\frac{\langle z|\gamma_{-\mathbf{k}\mathbf{m}\downarrow}\gamma_{\mathbf{k}\mathbf{m}\uparrow}\gamma_{\mathbf{k}\mathbf{m}\uparrow}^\dagger\gamma_{-\mathbf{k}\mathbf{m}\downarrow}^\dagger|z\rangle}{\langle z|z\rangle} &= \frac{\langle z|\gamma_{-\mathbf{k}\mathbf{m}\downarrow}\gamma_{\mathbf{k}\mathbf{m}\uparrow}|z\rangle}{\langle z|z\rangle}\frac{\langle z|\gamma_{\mathbf{k}\mathbf{m}\uparrow}^\dagger\gamma_{-\mathbf{k}\mathbf{m}\downarrow}^\dagger|z\rangle}{\langle z|z\rangle} - \frac{\langle z|\gamma_{-\mathbf{k}\mathbf{m}\downarrow}\gamma_{\mathbf{k}\mathbf{m}\uparrow}^\dagger|z\rangle}{\langle z|z\rangle}\frac{\langle z|\gamma_{\mathbf{k}\mathbf{m}\uparrow}\gamma_{-\mathbf{k}\mathbf{m}\downarrow}^\dagger|z\rangle}{\langle z|z\rangle} \\ &\quad + \frac{\langle z|\gamma_{-\mathbf{k}\mathbf{m}\downarrow}\gamma_{-\mathbf{k}\mathbf{m}\downarrow}^\dagger|z\rangle}{\langle z|z\rangle}\frac{\langle z|\gamma_{\mathbf{k}\mathbf{m}\uparrow}\gamma_{\mathbf{k}\mathbf{m}\uparrow}^\dagger|z\rangle}{\langle z|z\rangle} \\ &= \left(\frac{z}{1+|z|^2}\right)\left(\frac{\bar{z}}{1+|z|^2}\right) - (0)(0) + \left(\frac{1}{1+|z|^2}\right)\left(\frac{1}{1+|z|^2}\right) \\ &= \frac{|z|^2+1}{(1+|z|^2)^2} = \frac{1}{1+|z|^2}\end{aligned}$$

matching Eq. (C21).

For clarity, we list the nonzero elementary contractions of Wick's theorem:

$$\begin{aligned}\frac{1}{\langle z|z\rangle}\langle z|\gamma_{\mathbf{k}'\mathbf{m}'\sigma'}\gamma_{\mathbf{k}\mathbf{m}\sigma}^\dagger|z\rangle &= \frac{1}{1+|z|^2}\delta_{\mathbf{k}\mathbf{k}'}\delta_{mm'}\delta_{\sigma\sigma'} \\ \frac{1}{\langle z|z\rangle}\langle z|\gamma_{\mathbf{k}\mathbf{m}\sigma}^\dagger\gamma_{\mathbf{k}'\mathbf{m}'\sigma'}|z\rangle &= \frac{|z|^2}{1+|z|^2}\delta_{\mathbf{k}\mathbf{k}'}\delta_{mm'}\delta_{\sigma\sigma'} \\ \frac{1}{\langle z|z\rangle}\langle z|\gamma_{\mathbf{k}\mathbf{m}\sigma}\gamma_{\mathbf{k}'\mathbf{m}'\sigma'}|z\rangle &= \frac{z}{1+|z|^2}\delta_{\mathbf{k},-\mathbf{k}'}\delta_{mm'}s_z^{\sigma'}\delta_{\sigma,-\sigma'} \\ \frac{1}{\langle z|z\rangle}\langle z|\gamma_{\mathbf{k}\mathbf{m}\sigma}^\dagger\gamma_{\mathbf{k}'\mathbf{m}'\sigma'}^\dagger|z\rangle &= \frac{\bar{z}}{1+|z|^2}\delta_{\mathbf{k},-\mathbf{k}'}\delta_{mm'}s_z^\sigma\delta_{\sigma,-\sigma'}\end{aligned}\tag{C23}$$

and $\langle z|z\rangle = (1+|z|^2)^{N_f\mathcal{N}}$, $s_z^{\uparrow/\downarrow} = \pm 1$. We will use these results in App. D 2 to evaluate Richardson's criterion.

Appendix D: Charge excitations

In this section, we compute the spectrum and eigenstates of excitations above the eta-pairing ground states. We show that the fermionic excitations are gapped and perfectly flat (App. D 1), while the bosonic excitations are gapless and dispersive. We evaluate Richardson's criterion to show that kinetic energy generically favors superconductivity at half filling (App. D 2). We then study the bosonic (charge +2 and 0) excitations and find that the spin-0 Cooper pair spectrum splits into a set of low-lying bands described exactly by a single-particle pairing Hamiltonian and a flat continuum at the two-electron gap (App. D 3). The spin ± 1 Cooper pair spectrum is entirely flat: all states are at the two-electron gap and are effectively unpaired (App. D 3). We provide explicit examples of the pairing Hamiltonian (App. D 4) for obstructed atomic and fragile bands. Finally, we show that the spin-0 density mode (Goldstone mode) has the same spectrum as the spin-0 Cooper pairs. The spin ± 1 density excitations are all energetically above the two-electron gap, but have nontrivial dispersion also described by a single-particle Hamiltonian (App. D 5).

1. Charge +1

Given an eta-pairing pair groundstate $|GS\rangle = |n\rangle$, we can compute the charge +1, spin $\pm\frac{1}{2}$ excitations from the effective Hamiltonian $R(\mathbf{k})$ defined

$$[H, \gamma_{\mathbf{k},n,\sigma}^\dagger] |GS\rangle = \sum_m \gamma_{\mathbf{k},m,\sigma}^\dagger R_{mn}^\sigma(\mathbf{k}) |GS\rangle . \quad (\text{D1})$$

By diagonalizing $R^\sigma(\mathbf{k})$, we obtain exact eigenstates and their energies. Note that σ is not summed over. The excitation matrix is diagonal in spin because of S_z conservation.

It is simplest to perform the excitation calculations in momentum space using the canonical $\gamma_{\mathbf{k},n,\sigma}^\dagger$ operators, which form a complete basis of the projected Hilbert space. First we define momentum space spin operators $\bar{S}_{\mathbf{R},\alpha}^z = \sum_\sigma s_\sigma^z \bar{n}_{\mathbf{R},\alpha,\sigma}$ (recall $s_\sigma^z = \pm 1$ for $\sigma = \uparrow, \downarrow$) according to

$$\bar{S}_{\mathbf{k},\alpha}^z = \frac{1}{\sqrt{\mathcal{N}}} \sum_{\mathbf{R}} e^{-i\mathbf{k}\cdot(\mathbf{R}+\mathbf{r}_\alpha)} \bar{S}_{\mathbf{R},\alpha}^z, \quad \bar{S}_{\mathbf{k},\alpha}^z = (\bar{S}_{-\mathbf{k},\alpha}^z)^\dagger, \quad \bar{S}_{\mathbf{R},\alpha}^z = \frac{1}{\sqrt{\mathcal{N}}} \sum_{\mathbf{k}} e^{i\mathbf{k}\cdot(\mathbf{R}+\mathbf{r}_\alpha)} \bar{S}_{\mathbf{k},\alpha}^z \quad (\text{D2})$$

such that

$$H = \frac{1}{2} |U| \sum_{\mathbf{R},\alpha} (\bar{S}_{\mathbf{R},\alpha}^z)^2 = \frac{1}{2} |U| \sum_{\mathbf{k},\alpha} \bar{S}_{-\mathbf{k},\alpha}^z \bar{S}_{\mathbf{k},\alpha}^z . \quad (\text{D3})$$

H can be written in terms of the γ modes using

$$\begin{aligned} \bar{n}_{\mathbf{R},\alpha,\sigma} &= \bar{c}_{\mathbf{R},\alpha,\sigma}^\dagger \bar{c}_{\mathbf{R},\alpha,\sigma} = \frac{1}{\mathcal{N}} \sum_{\mathbf{k},\mathbf{k}'} e^{-i(\mathbf{k}-\mathbf{k}')\cdot(\mathbf{R}+\mathbf{r}_\alpha)} \bar{c}_{\mathbf{k}',\alpha,\sigma}^\dagger \bar{c}_{\mathbf{k},\alpha,\sigma} \\ &= \frac{1}{\mathcal{N}} \sum_{\mathbf{k},\mathbf{k}',mn} e^{-i(\mathbf{k}-\mathbf{k}')\cdot(\mathbf{R}+\mathbf{r}_\alpha)} \gamma_{\mathbf{k}',m,\sigma}^\dagger [U_{\alpha m}^\sigma(\mathbf{k}')^* U_{\alpha n}^\sigma(\mathbf{k})] \gamma_{\mathbf{k},n,\sigma} \\ &\equiv \frac{1}{\mathcal{N}} \sum_{\mathbf{k},\mathbf{k}',mn} e^{-i(\mathbf{k}-\mathbf{k}')\cdot(\mathbf{R}+\mathbf{r}_\alpha)} \gamma_{\mathbf{k}',m,\sigma}^\dagger M_{\sigma,\alpha}^{mn}(\mathbf{k}, \mathbf{k}' - \mathbf{k}) \gamma_{\mathbf{k},n,\sigma} \end{aligned} \quad (\text{D4})$$

where we defined the sublattice form factor

$$M_{\sigma,\alpha}^{mn}(\mathbf{k}, \mathbf{q}) = U_{\alpha m}^\sigma(\mathbf{k} + \mathbf{q})^* U_{\alpha n}^\sigma(\mathbf{k}) . \quad (\text{D5})$$

Thus the Fourier transform of the spin operator is

$$\begin{aligned} \bar{S}_{\mathbf{q},\alpha}^z &= \frac{1}{\sqrt{\mathcal{N}}} \sum_{\mathbf{R}} e^{-i\mathbf{q}\cdot(\mathbf{R}+\mathbf{r}_\alpha)} \bar{S}_{\mathbf{R},\alpha}^z \\ &= \frac{1}{\sqrt{\mathcal{N}}} \sum_{\mathbf{R}mn} e^{-i\mathbf{q}\cdot(\mathbf{R}+\mathbf{r}_\alpha)} \frac{1}{\mathcal{N}} \sum_{\mathbf{k},\mathbf{k}',\sigma} e^{-i(\mathbf{k}-\mathbf{k}')\cdot(\mathbf{R}+\mathbf{r}_\alpha)} s_\sigma^z \gamma_{\mathbf{k}',m,\sigma}^\dagger M_{\sigma,\alpha}^{mn}(\mathbf{k}, \mathbf{k}' - \mathbf{k}) \gamma_{\mathbf{k},n,\sigma} \\ &= \frac{1}{\sqrt{\mathcal{N}}} \sum_{\mathbf{k},\mathbf{k}',mn,\sigma} \frac{1}{\mathcal{N}} \sum_{\mathbf{R}} e^{-i(\mathbf{k}+\mathbf{q}-\mathbf{k}')\cdot(\mathbf{R}+\mathbf{r}_\alpha)} s_\sigma^z \gamma_{\mathbf{k}',m,\sigma}^\dagger M_{\sigma,\alpha}^{mn}(\mathbf{k}, \mathbf{k}' - \mathbf{k}) \gamma_{\mathbf{k},n,\sigma} \\ &= \frac{1}{\sqrt{\mathcal{N}}} \sum_{\mathbf{k},mn,\sigma} s_\sigma^z \gamma_{\mathbf{q}+\mathbf{k},m,\sigma}^\dagger M_{\sigma,\alpha}^{mn}(\mathbf{k}, \mathbf{q}) \gamma_{\mathbf{k},n,\sigma} \end{aligned} \quad (\text{D6})$$

and hence it follows that

$$[\bar{S}_{\mathbf{q},\alpha}^z, \gamma_{\mathbf{k},n,\sigma}^\dagger] = \frac{1}{\sqrt{\mathcal{N}}} \sum_m s_\sigma^z \gamma_{\mathbf{k}+\mathbf{q},m,\sigma}^\dagger M_{\sigma,\alpha}^{mn}(\mathbf{k}, \mathbf{q}) . \quad (\text{D7})$$

To prepare to compute the excitation spectrum, we observe

$$\begin{aligned} \sum_{\mathbf{q}\alpha} [\bar{S}_{-\mathbf{q},\alpha}^z \bar{S}_{\mathbf{q},\alpha}^z, \gamma_{\mathbf{k},n,\sigma}^\dagger] &= \sum_{\mathbf{q}\alpha} \bar{S}_{-\mathbf{q},\alpha}^z [\bar{S}_{\mathbf{q},\alpha}^z, \gamma_{\mathbf{k},n,\sigma}^\dagger] + [\bar{S}_{-\mathbf{q},\alpha}^z, \gamma_{\mathbf{k},n,\sigma}^\dagger] \bar{S}_{\mathbf{q},\alpha}^z \\ &= \sum_{\mathbf{q}\alpha} \bar{S}_{-\mathbf{q},\alpha}^z [\bar{S}_{\mathbf{q},\alpha}^z, \gamma_{\mathbf{k},n,\sigma}^\dagger] + [\bar{S}_{\mathbf{q},\alpha}^z, \gamma_{\mathbf{k},n,\sigma}^\dagger] \bar{S}_{-\mathbf{q},\alpha}^z \\ &= \sum_{\mathbf{q}\alpha} [\bar{S}_{-\mathbf{q},\alpha}^z, [\bar{S}_{\mathbf{q},\alpha}^z, \gamma_{\mathbf{k},n,\sigma}^\dagger]] + 2[\bar{S}_{\mathbf{q},\alpha}^z, \gamma_{\mathbf{k},n,\sigma}^\dagger] \bar{S}_{-\mathbf{q},\alpha}^z \end{aligned} \quad (\text{D8})$$

Acting on the groundstate where the second term is zero (recall that $S_{\mathbf{q},\alpha}^z$ annihilates $|n\rangle$ because $S_{\mathbf{q},\alpha}^z|0\rangle = 0$ and $[S_{\mathbf{q},\alpha}^z, \eta^\dagger] = 0$) and using Eq. (D7), we derive

$$\begin{aligned} \sum_{\mathbf{q}\alpha} [\bar{S}_{-\mathbf{q},\alpha}^z \bar{S}_{\mathbf{q},\alpha}^z, \gamma_{\mathbf{k},n,\sigma}^\dagger] |GS\rangle &= \frac{1}{\sqrt{\mathcal{N}}} s_\sigma^z \sum_{\mathbf{q}\alpha m'} [\bar{S}_{-\mathbf{q},\alpha}^z, \gamma_{\mathbf{k}+\mathbf{q},m',\sigma}^\dagger] M_{\sigma,\alpha}^{m'n}(\mathbf{k}, \mathbf{q}) |GS\rangle \\ &= \frac{1}{\mathcal{N}} \sum_{\mathbf{q}\alpha m m'} \gamma_{\mathbf{k},m,\sigma}^\dagger M_{\sigma,\alpha}^{mm'}(\mathbf{k} + \mathbf{q}, -\mathbf{q}) M_{\sigma,\alpha}^{m'n}(\mathbf{k}, \mathbf{q}) |GS\rangle \end{aligned} \quad (\text{D9})$$

where we used that $(s_\sigma^z)^2 = 1$. Thus we obtain

$$\begin{aligned} R_{mn}^\sigma(\mathbf{k}) &= \frac{|U|}{2} \frac{1}{\mathcal{N}} \sum_{\mathbf{q}\alpha m'} M_{\sigma,\alpha}^{mm'}(\mathbf{k} + \mathbf{q}, -\mathbf{q}) M_{\sigma,\alpha}^{m'n}(\mathbf{k}, \mathbf{q}) \\ &= \frac{|U|}{2} \frac{1}{\mathcal{N}} \sum_{\mathbf{q}\alpha m'} U_{\alpha m}^\sigma(\mathbf{k})^* U_{\alpha m'}^\sigma(\mathbf{k} + \mathbf{q}) U_{\alpha m'}^\sigma(\mathbf{k} + \mathbf{q})^* U_{\alpha n}^\sigma(\mathbf{k}) \\ &= \frac{|U|}{2} \sum_{\alpha} U_{\alpha m}^\sigma(\mathbf{k})^* \frac{1}{\mathcal{N}} \sum_{\mathbf{q}} P_{\alpha\alpha}^\sigma(\mathbf{k} + \mathbf{q}) U_{\alpha n}^\sigma(\mathbf{k}) \end{aligned} \quad (\text{D10})$$

and using the uniform pairing condition Eq. (A21), $\frac{1}{\mathcal{N}} \sum_{\mathbf{q}} P_{\alpha\alpha}^\sigma(\mathbf{k} + \mathbf{q}) = \epsilon$, we have

$$\begin{aligned} R_{mn}^\sigma(\mathbf{k}) &= \frac{|U|}{2} \sum_{\alpha} U_{\alpha m}^\sigma(\mathbf{k})^* \epsilon U_{\alpha n}^\sigma(\mathbf{k}) \\ &= \frac{\epsilon|U|}{2} [U_\sigma^\dagger(\mathbf{k}) U_\sigma(\mathbf{k})]_{mn} \\ &= \frac{\epsilon|U|}{2} \delta_{mn} \end{aligned} \quad (\text{D11})$$

which is diagonal for all \mathbf{k} and has completely flat bands with an energy gap $\epsilon|U|/2$ above the ground state. Eq. (D1) simply reads

$$H \gamma_{\mathbf{k},n,\sigma}^\dagger |GS\rangle = \frac{\epsilon|U|}{2} \gamma_{\mathbf{k},n,\sigma}^\dagger |GS\rangle \quad (\text{D12})$$

making use of $H|GS\rangle = 0$. We refer to $\epsilon|U|/2$ as the single-electron gap, whose analogue in BCS theory is the Bogoliubov quasi-particle gap.

We can repeat this calculation for the hole excitations, defined by

$$[H, \gamma_{\mathbf{k},n,\sigma}] |GS\rangle = \sum_m \tilde{R}_{nm}^\sigma(\mathbf{k}) \gamma_{\mathbf{k},m,\sigma} |GS\rangle. \quad (\text{D13})$$

Taking the hermitian conjugate of Eq. (D7), we obtain the requisite formula

$$\begin{aligned} [\bar{S}_{\mathbf{q},\alpha}^z, \gamma_{\mathbf{k},n,\sigma}] &= -\frac{1}{\sqrt{\mathcal{N}}} \sum_m s_\sigma^z \gamma_{\mathbf{k}-\mathbf{q},m,\sigma} M_{\sigma,\alpha}^{mn}(\mathbf{k}, \mathbf{q})^* \\ &= -\frac{1}{\sqrt{\mathcal{N}}} \sum_m M_{\sigma,\alpha}^{nm}(\mathbf{k} + \mathbf{q}, -\mathbf{q}) s_\sigma^z \gamma_{\mathbf{k}-\mathbf{q},m,\sigma}. \end{aligned} \quad (\text{D14})$$

All steps in the calculation of $R_{mn}^\sigma(\mathbf{k})$ proceed identically for $\tilde{R}_{nm}^\sigma(\mathbf{k})$ but with the mapping $M_{\sigma,\alpha}^{mn}(\mathbf{k}, \mathbf{q}) \rightarrow M_{\sigma,\alpha}^{nm}(\mathbf{k} + \mathbf{q}, -\mathbf{q})$, so from Eq. (D10) we find

$$\begin{aligned} \tilde{R}_{nm}^\sigma(\mathbf{k}) &= \frac{|U|}{2} \frac{1}{\mathcal{N}} \sum_{\mathbf{q}\alpha m'} M_{\sigma,\alpha}^{m'm}(\mathbf{k}, \mathbf{q}) M_{\sigma,\alpha}^{nm'}(\mathbf{k} + \mathbf{q}, -\mathbf{q}) \\ &= \frac{|U|}{2} \frac{1}{\mathcal{N}} \sum_{\mathbf{q}\alpha m'} M_{\sigma,\alpha}^{nm'}(\mathbf{k} + \mathbf{q}, -\mathbf{q}) M_{\sigma,\alpha}^{m'm}(\mathbf{k}, \mathbf{q}) \\ &= R_{nm}^\sigma(\mathbf{k}) \end{aligned} \quad (\text{D15})$$

and hence single particle and hole excitations have the same energies. This is not true for systems that do not satisfy the uniform pairing condition. For example, the flat band systems in magic angle twisted bilayer graphene have different particle and hole excitations [57].

2. Richardson Criterion

The Richardson criterion[65, 66] is an approximation of the optimal binding energy of the Cooper pair, defined by $E_\Delta(N) = E(N+2) - E(N) - 2(E(N+1) - E(N))$ where $E(N)$ is the groundstate energy at particle number N . In the flat band case, $E(2n) = 0 \ \forall n$ due to the eta-pairing symmetry because $|n\rangle$ are zero energy ground states. Thus $E_\Delta(N) = -\epsilon|U| < 0$ demonstrating perfect pairing at all densities. Indeed, we will see in App. E that $\epsilon|U|$ is the maximum binding energy computed from the charge +2 Cooper pair excitations.

When weak dispersion (kinetic energy) is added to the model, we will determine which density shows the strongest pairing: that is, the most negative binding energy $E_\Delta(N)$. To evaluate $E(N), E(N+2)$ at $N = 2n$ in the eta-pairing groundstates, we need the expectation value of the kinetic energy in the states $|n\rangle$, and for $E(N+1)$ we need to compute the expectation value in the charge +1 states atop the $N = 2n$ ground state, which is a four operator correlator and can be computed with Wick's theorem.

We consider a more general perturbation than discussed in the Main Text. We consider a perturbation to the kinetic energy defined in Eq. (A2), namely

$$\tilde{H} + \tilde{H}' = \sum_{\mathbf{k}, \alpha\beta, \sigma} c_{\mathbf{k}, \alpha, \sigma}^\dagger \tilde{h}_{\alpha\beta}^\sigma(\mathbf{k}) c_{\mathbf{k}, \beta, \sigma} + \sum_{\mathbf{k}, \alpha\beta, \sigma\sigma'} c_{\mathbf{k}, \alpha, \sigma}^\dagger \tilde{h}'_{\alpha\sigma, \beta\sigma'}(\mathbf{k}) c_{\mathbf{k}, \beta, \sigma'} \quad (\text{D16})$$

where $\tilde{h}_{\alpha\beta}(\mathbf{k})$ is the flat band Hamiltonian and we treat $\tilde{h}'_{\alpha\sigma, \beta\sigma'}(\mathbf{k})$ as a small perturbation (additional hoppings, spin-orbit couplings to break \mathcal{T} and S_z , etc). When projected into the flat bands (still requiring that the conduction bands are much higher in energy than the scale of \tilde{h}' and $|U|$), we find

$$\begin{aligned} \tilde{H}' &\rightarrow \sum_{\mathbf{k}, \alpha\beta, \sigma\sigma'} \bar{c}_{\mathbf{k}, \alpha, \sigma}^\dagger \tilde{h}'_{\alpha\sigma, \beta\sigma'}(\mathbf{k}) \bar{c}_{\mathbf{k}, \beta, \sigma'} \\ &= \sum_{\mathbf{k}, \alpha\alpha'\beta\beta', \sigma\sigma'} \bar{c}_{\mathbf{k}, \alpha', \sigma}^\dagger P_{\alpha'\alpha}^\sigma(\mathbf{k}) \tilde{h}'_{\alpha\sigma, \beta\sigma'}(\mathbf{k}) P_{\beta\beta'}^{\sigma'}(\mathbf{k}) \bar{c}_{\mathbf{k}, \beta', \sigma'} \\ &= \sum_{\mathbf{k}, \alpha\beta, \sigma\sigma', mn} \gamma_{\mathbf{k}, m, \sigma}^\dagger U_{\alpha m}^{\sigma*}(\mathbf{k}) \tilde{h}'_{\alpha\sigma, \beta\sigma'}(\mathbf{k}) U_{\beta n}^{\sigma'}(\mathbf{k}) \gamma_{\mathbf{k}, n, \sigma'} \end{aligned} \quad (\text{D17})$$

using Eq. (A3) to write the \bar{c} operators in terms of γ operators. Thus the correction to the flat band kinetic energy Hamiltonian takes the form

$$\tilde{H}' = \sum_{\mathbf{k}mn\sigma\sigma'} \tilde{E}'_{m\sigma, n\sigma'}(\mathbf{k}) \gamma_{\mathbf{k}, m, \sigma}^\dagger \gamma_{\mathbf{k}, n, \sigma'}, \quad \tilde{E}'_{m\sigma, n\sigma'}(\mathbf{k}) = \sum_{\alpha\beta} U_{\alpha m}^{\sigma*}(\mathbf{k}) \tilde{h}'_{\alpha\sigma, \beta\sigma'}(\mathbf{k}) U_{\beta n}^{\sigma'}(\mathbf{k}) \quad (\text{D18})$$

or in matrix form, recalling $U_\sigma(\mathbf{k})$ is an $N_{orb} \times N_f$ rectangular matrix,

$$\tilde{E}'(\mathbf{k}) = \begin{pmatrix} U_\uparrow^\dagger(\mathbf{k}) & \\ & U_\downarrow(\mathbf{k}) \end{pmatrix} \begin{pmatrix} \tilde{h}'_{\uparrow\uparrow}(\mathbf{k}) & \tilde{h}'_{\uparrow\downarrow}(\mathbf{k}) \\ \tilde{h}'_{\downarrow\uparrow}(\mathbf{k}) & \tilde{h}'_{\downarrow\downarrow}(\mathbf{k}) \end{pmatrix} \begin{pmatrix} U_\uparrow(\mathbf{k}) & \\ & U_\downarrow(\mathbf{k}) \end{pmatrix} \quad (\text{D19})$$

in the spin \otimes orbital tensor product basis. We develop an expression for Richardson's criterion in the general case, but it may be helpful to point out the simplest case: dispersion $\tilde{E}'_{m, \sigma}(\mathbf{k})$ can be added to the flat bands by taking $\tilde{E}'_{m\sigma, n\sigma'}(\mathbf{k}) = \delta_{nm} \delta_{\sigma\sigma'} \tilde{E}'_{m, \sigma}(\mathbf{k})$.

We now need to compute expectation values. The ground states at $N = 2n$ and $N + 2 = 2(n+1)$ are $|n\rangle, |n+1\rangle$ at zeroth order in \tilde{E}' . When \tilde{H}' is added, we determine the shift in energy with degenerate perturbation theory; by computing the matrix elements of \tilde{H}' with respect to the unperturbed states:

$$\begin{aligned} \langle z | \tilde{H}' | z \rangle &= \sum_{\mathbf{k}mn\sigma\sigma'} \tilde{E}'_{m\sigma, n\sigma'}(\mathbf{k}) \langle z | \gamma_{\mathbf{k}, m, \sigma}^\dagger \gamma_{\mathbf{k}, n, \sigma'} | z \rangle \\ &= \sum_{\mathbf{k}mn\sigma\sigma'} \tilde{E}'_{m\sigma, n\sigma'}(\mathbf{k}) \delta_{mn} \delta_{\sigma\sigma'} \frac{|z|^2}{1 + |z|^2} \langle z | z \rangle \\ &= |z|^2 (1 + |z|^2)^{N_f \mathcal{N} - 1} 2N_f \mathcal{N} \tilde{E}', \quad 2N_f \mathcal{N} \tilde{E}' = \sum_{\mathbf{k}m\sigma} \tilde{E}'_{m\sigma, m\sigma}(\mathbf{k}) \end{aligned} \quad (\text{D20})$$

using Eq. (C23). We defined $\tilde{E}' = \frac{1}{2N_f \mathcal{N}} \sum_{\mathbf{k}m\sigma} \tilde{E}'_{m\sigma, m\sigma}$ as the average of the entire spectrum, which is finite in the

thermodynamic limit. Expanding both sides in powers of z , we find

$$\begin{aligned} \sum_n |z|^{2n} \binom{N_f \mathcal{N}}{n} \langle n | \tilde{H}' | n \rangle &= \sum_n |z|^{2(n+1)} \binom{N_f \mathcal{N} - 1}{n} (2N_f \mathcal{N} \tilde{E}') \\ \binom{N_f \mathcal{N}}{n} \langle n | \tilde{H} | n \rangle &= \binom{N_f \mathcal{N} - 1}{n-1} (2N_f \mathcal{N} \tilde{E}') \\ \langle n | \tilde{H} | n \rangle &= \frac{n}{N_f \mathcal{N}} (2N_f \mathcal{N} \tilde{E}') = \nu (2N_f \mathcal{N} \tilde{E}') \end{aligned} \quad (\text{D21})$$

recalling $\frac{n}{N_f \mathcal{N}} = \nu$ is the filling. Next we need the expectation value of \tilde{H}' in the electron excitations Eq. (D12), but first we must normalize them. We compute

$$\begin{aligned} \langle z | \gamma_{\mathbf{k},m,\sigma} \gamma_{\mathbf{k},m,\sigma}^\dagger | z \rangle &= \frac{1}{1+|z|^2} \langle z | z \rangle \\ \binom{N_f \mathcal{N}}{n} \langle n | \gamma_{\mathbf{k},m,\sigma} \gamma_{\mathbf{k},m,\sigma}^\dagger | n \rangle &= \binom{N_f \mathcal{N} - 1}{n} \\ \langle n | \gamma_{\mathbf{k},m,\sigma} \gamma_{\mathbf{k},m,\sigma}^\dagger | n \rangle &= 1 - \nu. \end{aligned} \quad (\text{D22})$$

Because all $\gamma_{\mathbf{k},m,\sigma}^\dagger | n \rangle$ excitations are degenerate, we compute their effective Hamiltonian at first order in degenerate perturbation theory:

$$\langle z | \gamma_{\mathbf{k},m',\sigma'} \tilde{H} \gamma_{\mathbf{k},m,\sigma}^\dagger | z \rangle = \sum_{\mathbf{k}' i j s s'} \tilde{E}'_{is,j s'}(\mathbf{k}') \langle z | \gamma_{\mathbf{k},m',\sigma'} \gamma_{\mathbf{k}',i,s}^\dagger \gamma_{\mathbf{k}',j,s'} \gamma_{\mathbf{k},m,\sigma}^\dagger | z \rangle. \quad (\text{D23})$$

There are only three contractions:

$$\begin{aligned} \langle z | \gamma_{\mathbf{k},m',\sigma'} \gamma_{\mathbf{k}',i,s}^\dagger \gamma_{\mathbf{k}',j,s'} \gamma_{\mathbf{k},m,\sigma}^\dagger | z \rangle &= \frac{1}{(1+|z|^2)^2} \left(\delta_{\mathbf{k}\mathbf{k}'} \delta_{im'} \delta_{\sigma's} \delta_{jm} \delta_{\sigma s'} - |z|^2 \delta_{\mathbf{k},-\mathbf{k}'} \delta_{m'j} \delta_{im} s_z^{s'} \delta_{\sigma',-s'} s_z^s \delta_{\sigma,-s} \right. \\ &\quad \left. + |z|^2 \delta_{mm'} \delta_{\sigma\sigma'} \delta_{ij} \delta_{ss'} \right) \langle z | z \rangle. \end{aligned} \quad (\text{D24})$$

Plugging in, we find

$$\langle z | \gamma_{\mathbf{k},m',\sigma'} \tilde{H}' \gamma_{\mathbf{k},m,\sigma}^\dagger | z \rangle = (1+|z|^2)^{N_f \mathcal{N} - 2} \left(\tilde{E}'_{m'\sigma',m\sigma}(\mathbf{k}) - |z|^2 s_z^{\sigma'} s_z^\sigma \tilde{E}'_{m(-\sigma),m'(-\sigma')}(-\mathbf{k}) + |z|^2 \delta_{mm'} \delta_{\sigma\sigma'} 2N_f \mathcal{N} \tilde{E}' \right). \quad (\text{D25})$$

Now expanding in powers of $|z|^2$ and including the normalization Eq. (D22), we find

$$\begin{aligned} \binom{N_f \mathcal{N}}{n} \frac{\langle n | \gamma_{\mathbf{k},m',\sigma'} \tilde{H}' \gamma_{\mathbf{k},m,\sigma}^\dagger | n \rangle}{1-\nu} &= \frac{1}{1-\nu} \left(\binom{N_f \mathcal{N} - 2}{n} \tilde{E}'_{m'\sigma',m\sigma}(\mathbf{k}) - \binom{N_f \mathcal{N} - 2}{n-1} s_z^{\sigma'} s_z^\sigma \tilde{E}'_{m(-\sigma),m'(-\sigma')}(-\mathbf{k}) \right. \\ &\quad \left. + \binom{N_f \mathcal{N} - 2}{n-1} \delta_{mm'} \delta_{\sigma\sigma'} 2N_f \mathcal{N} \tilde{E}' \right). \end{aligned} \quad (\text{D26})$$

Simplifying the binomial coefficients gives

$$\begin{aligned} \frac{\langle n | \gamma_{\mathbf{k},m',\sigma'} \tilde{H}' \gamma_{\mathbf{k},m,\sigma}^\dagger | n \rangle}{1-\nu} &= \frac{1}{1-\nu} \left(\frac{(N_f \mathcal{N} - n - 1)(N_f \mathcal{N} - n)}{N_f \mathcal{N} (N_f \mathcal{N} - 1)} \tilde{E}'_{m'\sigma',m\sigma}(\mathbf{k}) - \frac{n(N_f \mathcal{N} - n)}{N_f \mathcal{N} (N_f \mathcal{N} - 1)} s_z^{\sigma'} s_z^\sigma \tilde{E}'_{m(-\sigma),m'(-\sigma')}(-\mathbf{k}) \right. \\ &\quad \left. + \frac{n(N_f \mathcal{N} - n)}{N_f \mathcal{N} (N_f \mathcal{N} - 1)} \delta_{mm'} \delta_{\sigma\sigma'} 2N_f \mathcal{N} \tilde{E}' \right) \\ &= \left(\frac{N_f \mathcal{N} - n - 1}{N_f \mathcal{N} - 1} \tilde{E}'_{m'\sigma',m\sigma}(\mathbf{k}) - \frac{n}{N_f \mathcal{N} - 1} s_z^{\sigma'} s_z^\sigma \tilde{E}'_{m(-\sigma),m'(-\sigma')}(-\mathbf{k}) + \frac{n}{N_f \mathcal{N} - 1} \delta_{mm'} \delta_{\sigma\sigma'} 2N_f \mathcal{N} \tilde{E}' \right) \end{aligned} \quad (\text{D27})$$

To write the effective Hamiltonian more transparently, we define the matrix notation

$$\begin{aligned} [\tilde{E}'(\mathbf{k})]_{m'\sigma',m\sigma} &= \tilde{E}'_{m'\sigma',m\sigma}(\mathbf{k}) \\ [\sigma_y \tilde{E}'^T(-\mathbf{k}) \sigma_y]_{m'\sigma',m\sigma} &= s_z^{\sigma'} s_z^\sigma \tilde{E}'_{m(-\sigma),m'(-\sigma')}(-\mathbf{k}) \end{aligned} \quad (\text{D28})$$

where σ_y is a Pauli matrix acting only on the spin indices. Because \tilde{H} is Hermitian, $E^T = E^*$. Thus we can write the matrix Eq. (D26) obtained from degenerate perturbation theory as

$$\frac{\langle n | \gamma_{\mathbf{k}, m', \sigma'} \tilde{H}' \gamma_{\mathbf{k}, m, \sigma}^\dagger | n \rangle}{1 - \nu} = \left[\frac{N_f \mathcal{N} - n - 1}{N_f \mathcal{N} - 1} \tilde{E}'(\mathbf{k}) - \frac{n}{N_f \mathcal{N} - 1} \sigma_y \tilde{E}'^*(-\mathbf{k}) \sigma_y + \frac{n}{N_f \mathcal{N} - 1} \mathbb{1} 2N_f \mathcal{N} \tilde{E}' \right]_{m' \sigma', m \sigma}. \quad (\text{D29})$$

The eigen-energies of this matrix split the electron excitations which were degenerate at energy $\epsilon|U|/2$, forming a band structure for the charge +1 excitations. Let $\lambda_{\min}[M(\mathbf{k})]$ denote the smallest eigenvalue of $M(\mathbf{k})$ for all \mathbf{k} . Then the lowest energy state of the one-particle excitations is

$$E(N+1) = \lambda_{\min} \left[\frac{\epsilon|U|}{2} \mathbb{1} + \frac{N_f \mathcal{N} - n - 1}{N_f \mathcal{N} - 1} \tilde{E}'(\mathbf{k}) - \frac{n}{N_f \mathcal{N} - 1} \sigma_y \tilde{E}'^*(-\mathbf{k}) \sigma_y + \frac{n}{N_f \mathcal{N} - 1} \mathbb{1} 2N_f \mathcal{N} \tilde{E}' \right] \quad (\text{D30})$$

corresponding to the lowest energy single-particle excitation in perturbation theory. With Eqs. (D21) and (D30), the Richardson binding energy can be written as

$$\begin{aligned} E_\Delta(N) &= E(N+2) + E(N) - 2E(N+1) \\ &= \frac{n + (n+1)}{N_f \mathcal{N}} (2N_f \mathcal{N} \tilde{E}') \mathbb{1} - 2\lambda_{\min} \left[\frac{\epsilon|U|}{2} \mathbb{1} + \frac{N_f \mathcal{N} - n - 1}{N_f \mathcal{N} - 1} \tilde{E}'(\mathbf{k}) - \frac{n}{N_f \mathcal{N} - 1} \sigma_y \tilde{E}'^*(-\mathbf{k}) \sigma_y + \frac{n}{N_f \mathcal{N} - 1} \mathbb{1} 2N_f \mathcal{N} \tilde{E}' \right] \\ &= \left(\frac{2n+1}{N_f \mathcal{N}} - \frac{2n}{N_f \mathcal{N} - 1} \right) (2N_f \mathcal{N} \tilde{E}') - \epsilon|U| - 2\lambda_{\min} \left[\frac{N_f \mathcal{N} - n - 1}{N_f \mathcal{N} - 1} \tilde{E}'(\mathbf{k}) - \frac{n}{N_f \mathcal{N} - 1} \sigma_y \tilde{E}'^*(-\mathbf{k}) \sigma_y \right] \\ &= -\epsilon|U| + 2(1 - 2\nu) \tilde{E}' - 2\lambda_{\min} \left[(1 - \nu) \tilde{E}'(\mathbf{k}) - \nu \sigma_y \tilde{E}'^*(-\mathbf{k}) \sigma_y \right] + O(1/\mathcal{N}) \end{aligned} \quad (\text{D31})$$

where in the last line we took the thermodynamic limit with $\nu = n/N_f \mathcal{N}$. In going from the second to third lines we have pulled out terms proportional to the identity out of λ_{\min} : $\lambda_{\min}[aI + B] = a + \lambda_{\min}[B]$. To determine at what filling ν the superconductor is strongest (i.e. has the largest gap), we need to determine when $-E_\Delta(N)$ is largest. In general, this would require diagonalizing $(1 - \nu) \tilde{E}'(\mathbf{k}) - \nu \sigma_y \tilde{E}'^*(-\mathbf{k}) \sigma_y$ as a function of ν . This is easily done for a specific model since $\tilde{E}'(\mathbf{k})$ is an effective single-particle Hamiltonian. Generically, Eq. (D31) can reveal material-specific effects on superconductivity due spin-orbit coupling, applied magnetic field, and other small perturbations.

However, we are able to make a general statement when time-reversal symmetry is preserved by \tilde{H}' , ensuring that $\sigma_y \tilde{E}'^*(-\mathbf{k}) \sigma_y = \tilde{E}'(\mathbf{k})$. We first take $\tilde{E}' = 0$ for convenience; we will restore nonzero \tilde{E}' later. Then noting that $\lambda_{\min}[\tilde{E}'(\mathbf{k})] \leq 0, \lambda_{\max}[\tilde{E}'(\mathbf{k})] \geq 0$, we find

$$\begin{aligned} E_\Delta(N) &= -\epsilon|U| - 2\lambda_{\min} \left[(1 - 2\nu) \tilde{E}'(\mathbf{k}) \right] \\ &= -\epsilon|U| - 2 \begin{cases} (1 - 2\nu) \lambda_{\min}[\tilde{E}'(\mathbf{k})], & \nu < 1/2 \\ (1 - 2\nu) \lambda_{\max}[\tilde{E}'(\mathbf{k})], & \nu > 1/2 \end{cases} \\ &= -\epsilon|U| + 2|1 - 2\nu| \begin{cases} |\lambda_{\min}[\tilde{E}'(\mathbf{k})]|, & \nu < 1/2 \\ \lambda_{\max}[\tilde{E}'(\mathbf{k})], & \nu > 1/2 \end{cases} \end{aligned} \quad (\text{D32})$$

so because the second term is non-negative with a minimum at $\nu = 1/2$, we see that $E_\Delta(N)$ is minimized (the binding energy is largest and negative) at $\nu = 1/2$. This holds for arbitrary time-reversal symmetric $\tilde{E}'(\mathbf{k})$ and is independent of the position of the peak in the density of states, which is very different from standard BCS theory.

Restoring nonzero E' gives

$$\begin{aligned} E_\Delta(N) &= -\epsilon|U| + 2(1 - 2\nu) \tilde{E}' - 2 \begin{cases} (1 - 2\nu) \lambda_{\min}[\tilde{E}'(\mathbf{k})], & \nu < 1/2 \\ (1 - 2\nu) \lambda_{\max}[\tilde{E}'(\mathbf{k})], & \nu > 1/2 \end{cases} \\ &= -\epsilon|U| - 2 \begin{cases} (1 - 2\nu) (\lambda_{\min}[\tilde{E}'(\mathbf{k}) - \tilde{E}' I]), & \nu < 1/2 \\ (1 - 2\nu) (\lambda_{\max}[\tilde{E}'(\mathbf{k}) - \tilde{E}' I]), & \nu > 1/2 \end{cases}. \end{aligned} \quad (\text{D33})$$

Because we have subtracted the average \tilde{E}' from the matrix $\tilde{E}'(\mathbf{k})$, $\lambda_{\min}[\tilde{E}'(\mathbf{k}) - \tilde{E}' I] \leq 0$ and $\lambda_{\max}[\tilde{E}'(\mathbf{k}) - \tilde{E}' I] \geq 0$. The energy $E_\Delta(N)$ is still minimized at $\nu = 1/2$.

3. Charge +2 Excitations

We now study the charge +2 excitations. To do so, we will compute the scattering matrix $R_{\mathbf{k}'m'n',\mathbf{k}mn}^{\sigma\sigma'}(\mathbf{p})$ on the complete basis of charge +2 excitations at many-body momentum \mathbf{p} defined by

$$[H, \gamma_{\mathbf{p}+\mathbf{k},m,\sigma}^\dagger \gamma_{-\mathbf{k},n,\sigma'}^\dagger] |GS\rangle = \sum_{\mathbf{k}'} \gamma_{\mathbf{p}+\mathbf{k}',m',\sigma}^\dagger \gamma_{-\mathbf{k}',n',\sigma'}^\dagger |GS\rangle [R^{\sigma\sigma'}(\mathbf{p})]_{\mathbf{k}'m'n',\mathbf{k}mn} . \quad (\text{D34})$$

There are three flavors of Cooper pair. The $\sigma = \sigma' = \pm \frac{1}{2}$ cases lead to spin ± 1 Cooper pairs, while the $\sigma = -\sigma'$ case leads to a spin 0 Cooper pair. We will find that only the spin 0 Cooper pair has low-energy eigenstates below the two-particle continuum. For instance, we know that there must be a zero-energy excitation η^\dagger at $\mathbf{p} = 0$ since η is a symmetry.

This calculation is made simpler by using the results from the charge +1 electron excitation matrix. Using Eqs. (D7) and (D8), the single electron commutator is

$$[H, \gamma_{\mathbf{k},n,\sigma}^\dagger] = \frac{\epsilon|U|}{2} \gamma_{\mathbf{k},n,\sigma}^\dagger + \frac{|U|}{2} \sum_{\mathbf{q}\alpha m} 2 \frac{1}{\sqrt{N}} s_\sigma^z \gamma_{\mathbf{k}+\mathbf{q},m,\sigma}^\dagger M_{\sigma,\alpha}^{mn}(\mathbf{k}, \mathbf{q}) \bar{S}_{-\mathbf{q},\alpha}^z \quad (\text{D35})$$

and the second term annihilates the groundstate. Now it is straightforward to compute

$$\begin{aligned} [H, \gamma_{\mathbf{p}+\mathbf{k},m,\sigma}^\dagger \gamma_{-\mathbf{k},n,\sigma'}^\dagger] |GS\rangle &= \gamma_{\mathbf{p}+\mathbf{k},m,\sigma}^\dagger [H, \gamma_{-\mathbf{k},n,\sigma'}^\dagger] |GS\rangle + [H, \gamma_{\mathbf{p}+\mathbf{k},m,\sigma}^\dagger] \gamma_{-\mathbf{k},n,\sigma'}^\dagger |GS\rangle \\ &= \epsilon|U| \gamma_{\mathbf{p}+\mathbf{k},m,\sigma}^\dagger \gamma_{-\mathbf{k},n,\sigma'}^\dagger |GS\rangle + |U| \frac{1}{\sqrt{N}} \sum_{\mathbf{q}\alpha m'} s_\sigma^z \gamma_{\mathbf{p}+\mathbf{q}+\mathbf{k},\sigma,m'}^\dagger M_{\sigma,\alpha}^{m'm}(\mathbf{k} + \mathbf{p}, \mathbf{q}) [\bar{S}_{-\mathbf{q},\alpha}^z, \gamma_{-\mathbf{k},n,\sigma'}^\dagger] |GS\rangle \\ &= \epsilon|U| \gamma_{\mathbf{p}+\mathbf{k},m,\sigma}^\dagger \gamma_{-\mathbf{k},n,\sigma'}^\dagger |GS\rangle \\ &\quad + |U| \frac{1}{N} s_\sigma^z s_{\sigma'}^z \sum_{\mathbf{q}\alpha m'} \gamma_{\mathbf{p}+\mathbf{q}+\mathbf{k},\sigma,m'}^\dagger \gamma_{-\mathbf{k}-\mathbf{q},\sigma',n'}^\dagger M_{\sigma,\alpha}^{m'm}(\mathbf{k} + \mathbf{p}, \mathbf{q}) M_{\sigma',\alpha}^{n'n}(-\mathbf{k}, -\mathbf{q}) |GS\rangle \end{aligned} \quad (\text{D36})$$

where in the second line we introduced the commutator $[\bar{S}_{-\mathbf{q},\alpha}^z, \gamma_{-\mathbf{k},n,\sigma'}^\dagger]$ since $\bar{S}_{-\mathbf{q},\alpha}^z$ annihilates the vacuum. Resumming gives

$$\begin{aligned} [H, \gamma_{\mathbf{p}+\mathbf{k},m,\sigma}^\dagger \gamma_{-\mathbf{k},n,\sigma'}^\dagger] |GS\rangle &= \epsilon|U| \gamma_{\mathbf{p}+\mathbf{k},m,\sigma}^\dagger \gamma_{-\mathbf{k},n,\sigma'}^\dagger |GS\rangle \\ &\quad + |U| s_\sigma^z s_{\sigma'}^z \frac{1}{N} \sum_{\mathbf{k}'\alpha} \gamma_{\mathbf{p}+\mathbf{k}',\sigma,m'}^\dagger \gamma_{-\mathbf{k}',\sigma',n'}^\dagger |GS\rangle M_{\sigma,\alpha}^{m'm}(\mathbf{k} + \mathbf{p}, \mathbf{k}' - \mathbf{k}) M_{\sigma',\alpha}^{n'n}(-\mathbf{k}, \mathbf{k} - \mathbf{k}') \end{aligned} \quad (\text{D37})$$

and thus we find

$$[R^{\sigma\sigma'}(\mathbf{p})]_{\mathbf{k}'m'n',\mathbf{k}mn} = \epsilon|U| [\delta_{\mathbf{k}\mathbf{k}'} \delta_{mm'} \delta_{nn'} + s_\sigma^z s_{\sigma'}^z |U| \frac{1}{N} \sum_{\alpha} M_{\sigma,\alpha}^{m'm}(\mathbf{k} + \mathbf{p}, \mathbf{k}' - \mathbf{k}) M_{\sigma',\alpha}^{n'n}(-\mathbf{k}, \mathbf{k} - \mathbf{k}')]. \quad (\text{D38})$$

The second term describes the nontrivial scattering processes. We observe that

$$\begin{aligned} \sum_{\alpha} M_{\sigma,\alpha}^{m'm}(\mathbf{k} + \mathbf{p}, \mathbf{k}' - \mathbf{k}) M_{\sigma',\alpha}^{n'n}(-\mathbf{k}, \mathbf{k} - \mathbf{k}') &= \sum_{\alpha} U_{m'\alpha}^{\sigma*}(\mathbf{p} + \mathbf{k}') U_{m\alpha}^{\sigma}(\mathbf{p} + \mathbf{k}) U_{n'\alpha}^{\sigma'*}(-\mathbf{k}') U_{n\alpha}^{\sigma'}(-\mathbf{k}) \\ &= \sum_{\alpha} \mathcal{U}_{\mathbf{k}'m'n',\alpha}^{\sigma\sigma'}(\mathbf{p}) \mathcal{U}_{\mathbf{k}mn,\alpha}^{\sigma\sigma'*}(\mathbf{p}), \quad \mathcal{U}_{\mathbf{k}mn,\alpha}^{\sigma\sigma'}(\mathbf{p}) = U_{m\alpha}^{\sigma*}(\mathbf{p} + \mathbf{k}) U_{n\alpha}^{\sigma'}(-\mathbf{k}). \end{aligned} \quad (\text{D39})$$

Let us consider the case where $\sigma = \sigma'$. Note that if $\sigma = \sigma'$, $\mathcal{U}_{\mathbf{k}'m'n',\alpha}^{\sigma\sigma'}(\mathbf{p})$ is symmetric under $\mathbf{k}' \rightarrow -(\mathbf{p} + \mathbf{k}')$, $m' \leftrightarrow n'$. But the electron operators $\gamma_{\mathbf{p}+\mathbf{k}',m',\sigma}^\dagger \gamma_{-\mathbf{k}',n',\sigma}^\dagger$ which contract against $\mathcal{U}_{\mathbf{k}'m'n',\alpha}^{\sigma\sigma'}(\mathbf{p})$ in Eq. (D34) are anti-symmetric under $\mathbf{k}' \rightarrow -(\mathbf{p} + \mathbf{k}')$, $m' \leftrightarrow n'$. Thus many-body states which are *not* in the kernel of Eq. (D39) all vanish by fermion anti-symmetry when $\sigma = \sigma'$. Hence all the spin ± 1 Cooper pairs all have energy $\epsilon|U|$, which is twice the single-electron gap. This indicates they are effectively unpaired. Going forward, we take $\sigma = \uparrow, \sigma' = \downarrow$.

We can think of $\mathcal{U} \equiv \mathcal{U}^{\uparrow\downarrow}$ as a large rectangular matrix of dimension $\mathcal{N}\mathcal{N}_f^2 \times N_{orb}$. (In the bipartite case, the matrix is $\mathcal{N}\mathcal{N}_f^2 \times N_L$ because $U_{m\alpha}^{\sigma}(\mathbf{k}) = 0$ for $\alpha \notin L$.) In matrix notation, we have

$$R^{\uparrow\downarrow}(\mathbf{p}) = \epsilon|U| \mathbb{1} - |U| \frac{1}{N} \mathcal{U}(\mathbf{p}) \mathcal{U}^\dagger(\mathbf{p}). \quad (\text{D40})$$

Note that $\mathcal{U}(\mathbf{p})\mathcal{U}^\dagger(\mathbf{p})$ is positive semi-definite, so the spin 0 Cooper pair spectrum is below $\epsilon|U|$, indicating attractive pairing. Because \mathcal{U} is rectangular, it has low rank and $\frac{1}{N}\mathcal{U}\mathcal{U}^\dagger$ has many zero eigenvalues. Its nonzero eigenvalues are the same as the eigenvalues of $h(\mathbf{p}) = \frac{1}{N}\mathcal{U}^\dagger(\mathbf{p})\mathcal{U}(\mathbf{p})$ which is a matrix of dimension $N_{orb} \times N_{orb}$. To see this, define the eigenvector u with energy $\epsilon(\mathbf{p})$ by $h(\mathbf{p})u = \epsilon(\mathbf{p})u$. Then $\mathcal{U}u$ is an eigenvector of the scattering matrix: $\frac{1}{N}\mathcal{U}\mathcal{U}^\dagger(\mathcal{U}u) = \mathcal{U}h(\mathbf{p})u = \epsilon(\mathbf{p})\mathcal{U}u$. This gives $\dim h(\mathbf{p}) = N_{orb}$ nontrivial eigenvalues, which are nonnegative because $\mathcal{U}\mathcal{U}^\dagger$ is positive-semi-definite. Note that the rank of $\mathcal{U}\mathcal{U}^\dagger$ is at most N_{orb} , so all other eigenvalues are zero. Hence we are led to study the spectrum of

$$\begin{aligned} h_{\alpha\beta}(\mathbf{p}) &= \frac{1}{N}[\mathcal{U}^\dagger(\mathbf{p})\mathcal{U}(\mathbf{p})]_{\alpha\beta} \\ &= \frac{1}{N} \sum_{\mathbf{k}mn} U_{m\alpha}^\dagger(\mathbf{p}+\mathbf{k})U_{n\alpha}^\dagger(-\mathbf{k})U_{m\beta}^*(\mathbf{p}+\mathbf{k})U_{n\beta}^*(-\mathbf{k}) \\ &= \frac{1}{N} \sum_{\mathbf{k}} P_{\alpha\beta}^\dagger(\mathbf{p}+\mathbf{k})P_{\alpha\beta}^\dagger(-\mathbf{k}) \\ &= \frac{1}{N} \sum_{\mathbf{k}} P_{\alpha\beta}(\mathbf{p}+\mathbf{k})P_{\beta\alpha}(\mathbf{k}) \end{aligned} \quad (\text{D41})$$

where we used $P^\dagger(\mathbf{k}) = P^\dagger(-\mathbf{k})^*$, and set $P^\dagger(\mathbf{k}) = P(\mathbf{k})$.

A number of extremely useful statements will be proven about this effective single-particle Hamiltonian in the next section. For now, we simply remark that the eigenvectors $u_\mu^\beta(\mathbf{p})$ and eigenvalues $\epsilon_\mu(\mathbf{p})$ are defined as

$$\sum_{\beta} h_{\alpha\beta}(\mathbf{p})u_\mu^\beta(\mathbf{p}) = \epsilon_\mu(\mathbf{p})u_\mu^\alpha(\mathbf{p}) . \quad (\text{D42})$$

We normalize the eigenvectors such that $\sum_{\beta} u_\mu^\beta(\mathbf{p})u_\nu^{\beta*}(\mathbf{p}) = \delta_{\mu\nu}$ where $\mu, \nu \in 0, \dots, N_{orb}-1$ label the boson bands. It is convenient to decreasingly order the eigenvalues of $h(\mathbf{p})$ such that $\mu = 0$ corresponds to the largest eigenvalue. The full eigenstates of the scattering matrix Eq. (D38) not in the kernel of $\mathcal{U}\mathcal{U}^\dagger$ are $\sum_{\alpha} \mathcal{U}_{\mathbf{k}mn,\alpha}(\mathbf{p})u_\mu^\alpha(\mathbf{p})$ with eigenvalue

$$R^{\dagger\downarrow}(\mathbf{p})\mathcal{U}u_\mu = |U|(\epsilon - \epsilon_\mu(\mathbf{p}))\mathcal{U}u_\mu \quad (\text{D43})$$

so the many-body energies are $|U|(\epsilon - \epsilon_\mu(\mathbf{p}))$; $\mu = 0$ corresponds to the lowest energy band of many-body states.

The eigenvectors $\mathcal{U}u_\mu$ have norm squared $u_\mu^\dagger(\mathbf{p})\mathcal{U}^\dagger(\mathbf{p})\mathcal{U}(\mathbf{p})u_\mu(\mathbf{p}) = \mathcal{N}u_\mu^\dagger(\mathbf{p})h(\mathbf{p})u_\mu(\mathbf{p}) = \mathcal{N}\epsilon_\mu(\mathbf{p})$. Thus we define the many-body operators

$$\begin{aligned} \eta_{\mathbf{p},\mu}^\dagger &= \frac{1}{\sqrt{\mathcal{N}\epsilon_\mu(\mathbf{p})}} \sum_{\mathbf{k}\alpha mn} \gamma_{\mathbf{p}+\mathbf{k},m,\uparrow}^\dagger \gamma_{-\mathbf{k},n,\downarrow}^\dagger \mathcal{U}_{\mathbf{k}mn,\alpha}(\mathbf{p})u_\mu^\alpha(\mathbf{p}) \\ &= \frac{1}{\sqrt{\mathcal{N}\epsilon_\mu(\mathbf{p})}} \sum_{\mathbf{k}\alpha mn} \gamma_{\mathbf{p}+\mathbf{k},m,\uparrow}^\dagger \gamma_{-\mathbf{k},n,\downarrow}^\dagger U_{m\alpha}^*(\mathbf{p}+\mathbf{k})U_{n\alpha}^*(-\mathbf{k})u_\mu^\alpha(\mathbf{p}) \\ &= \frac{1}{\sqrt{\mathcal{N}}} \sum_{\mathbf{k}\alpha} \frac{u_\mu^\alpha(\mathbf{p})}{\sqrt{\epsilon_\mu(\mathbf{p})}} \bar{c}_{\mathbf{p}+\mathbf{k},\alpha,\uparrow}^\dagger \bar{c}_{-\mathbf{k},\alpha,\downarrow}^\dagger \\ &= \frac{1}{\sqrt{\mathcal{N}}} \sum_{\mathbf{R}\alpha} \frac{u_\mu^\alpha(\mathbf{p})}{\sqrt{\epsilon_\mu(\mathbf{p})}} e^{-i\mathbf{p}\cdot(\mathbf{R}+\mathbf{r}_\alpha)} \bar{c}_{\mathbf{R},\alpha,\uparrow}^\dagger \bar{c}_{\mathbf{R},\alpha,\downarrow}^\dagger \end{aligned} \quad (\text{D44})$$

which obey

$$[H, \eta_{\mathbf{p},\mu}^\dagger] |GS\rangle = |U|(\epsilon - \epsilon_\mu(\mathbf{p}))\eta_{\mathbf{p},\mu}^\dagger |GS\rangle . \quad (\text{D45})$$

Comparing with Eq. (B5), we see that the Cooper pair operators only show onsite pairing in \mathbf{R}, α in the \bar{c} degrees of freedom, indicating closely bound states. We will show that, up to a normalization, $\eta_{\mathbf{p}=0,\mu=0}^\dagger \propto \eta^\dagger$ and that $\epsilon_{\mu=0}(\mathbf{p}=0) = \epsilon$. Thus the Cooper pair operators $\eta_{\mathbf{p},\mu}^\dagger$ are deformations of the commuting η^\dagger symmetry with the same $\bar{c}_{\mathbf{R},\alpha,\uparrow}^\dagger \bar{c}_{\mathbf{R},\alpha,\downarrow}^\dagger$ orbital structure. They are gapless at $\mathbf{p} = 0$ as a consequence of Goldstone's theorem. The spectrum of the $\eta_{\mathbf{p},\mu}^\dagger$ operators contains the low lying Cooper pair (which condenses) as well as higher energy Cooper pair excitations (also known as Leggett modes).

To compute the normalization of the states $\eta_{\mathbf{p},\mu}^\dagger |n\rangle$, we use Wick's theorem. First we need the correlator

$$\begin{aligned} \langle z | \gamma_{-\mathbf{k}',n',\downarrow} \gamma_{\mathbf{q}+\mathbf{k}',m',\uparrow} \gamma_{\mathbf{p}+\mathbf{k},m,\uparrow}^\dagger \gamma_{-\mathbf{k},n,\downarrow}^\dagger | z \rangle &= \frac{1}{(1+|z|^2)^2} (|z|^2 \delta_{\mathbf{q},0} \delta_{n'm'} \delta_{\mathbf{p},0} \delta_{nm} - 0 + \delta_{\mathbf{k}\mathbf{k}'} \delta_{nn'} \delta_{\mathbf{p},\mathbf{q}} \delta_{mm'}) \langle z | z \rangle \\ &= \frac{\delta_{\mathbf{p},\mathbf{q}}}{(1+|z|^2)^2} (|z|^2 \delta_{\mathbf{p},0} \delta_{n'm'} \delta_{nm} + \delta_{\mathbf{k}\mathbf{k}'} \delta_{nn'} \delta_{mm'}) \langle z | z \rangle. \end{aligned} \quad (\text{D46})$$

We will also need the identity (see Eq. (D39))

$$\frac{1}{\mathcal{N}} \sum_{\mathbf{k}m} \mathcal{U}_{\mathbf{k}mm,\alpha}^{\sigma,-\sigma}(0) = \frac{1}{\mathcal{N}} \sum_{\mathbf{k}m} U_{m\alpha}^{\sigma*}(\mathbf{k}) U_{m\alpha}^{-\sigma*}(-\mathbf{k}) = \frac{1}{\mathcal{N}} \sum_{\mathbf{k}m} U_{m\alpha}^{\sigma*}(\mathbf{k}) U_{m\alpha}^{\sigma}(\mathbf{k}) = \frac{1}{\mathcal{N}} \sum_{\mathbf{k}} P_{\alpha\alpha}^{\sigma}(\mathbf{k}) = \epsilon \quad (\text{D47})$$

using the uniform pairing condition. Thus we obtain

$$\begin{aligned} \langle z | \eta_{\mathbf{q},\nu} \eta_{\mathbf{p},\mu}^\dagger | z \rangle &= \delta_{\mathbf{p},\mathbf{q}} \frac{(1+|z|^2)^{N_f \mathcal{N}-2}}{\mathcal{N} \sqrt{\epsilon_\mu(\mathbf{p}) \epsilon_\nu(\mathbf{q})}} \sum_{\mathbf{k}\mathbf{k}',\alpha\beta} \sum_{mn,m'n'} \mathcal{U}_{\mathbf{k}'m'n',\beta}^* (\mathbf{q}) u_\nu^{\beta*}(\mathbf{q}) (|z|^2 \delta_{n'm'} \delta_{\mathbf{p},0} \delta_{nm} + \delta_{\mathbf{k}\mathbf{k}'} \delta_{nn'} \delta_{mm'}) \mathcal{U}_{\mathbf{k}mn,\alpha}(\mathbf{p}) u_\mu^\alpha(\mathbf{p}) \\ &= \delta_{\mathbf{p},\mathbf{q}} \frac{(1+|z|^2)^{N_f \mathcal{N}-2}}{\mathcal{N} \sqrt{\epsilon_\mu(\mathbf{p}) \epsilon_\nu(\mathbf{p})}} \sum_{\alpha\beta} u_\nu^{\beta*}(\mathbf{p}) \left(|z|^2 \delta_{\mathbf{p},0} \sum_{\mathbf{k}'m'} \mathcal{U}_{\mathbf{k}'m'm',\beta}^*(0) \sum_{\mathbf{k}m} \mathcal{U}_{\mathbf{k}mm,\alpha}(0) + [\mathcal{U}^\dagger(\mathbf{p}) \mathcal{U}(\mathbf{p})]_{\beta\alpha} \right) u_\mu^\alpha(\mathbf{p}) \\ &= \delta_{\mathbf{p},\mathbf{q}} \frac{(1+|z|^2)^{N_f \mathcal{N}-2}}{\sqrt{\epsilon_\mu(\mathbf{p}) \epsilon_\nu(\mathbf{p})}} \sum_{\alpha\beta} u_\nu^{\beta*}(\mathbf{p}) (|z|^2 \delta_{\mathbf{p},0} \mathcal{N} \epsilon^2 + h_{\beta\alpha}(\mathbf{p})) u_\mu^\alpha(\mathbf{p}) \\ &= \delta_{\mathbf{p},\mathbf{q}} \frac{(1+|z|^2)^{N_f \mathcal{N}-2}}{\sqrt{\epsilon_\mu(\mathbf{p}) \epsilon_\nu(\mathbf{p})}} \left(|z|^2 \delta_{\mathbf{p},0} \mathcal{N} \epsilon^2 \sum_{\alpha\beta} u_\nu^{\beta*}(0) u_\mu^\alpha(0) + \delta_{\mu\nu} \epsilon_\mu(\mathbf{p}) \right). \end{aligned} \quad (\text{D48})$$

In App. E, we will prove that $\epsilon_0(\mathbf{p}=0) = \epsilon$ and $\sum_\alpha u_\mu^\alpha(0) = \delta_{\mu,0} \sqrt{N_L}$ where N_L is the number of orbitals where $P_{\alpha\beta}(\mathbf{k})$ is nonzero. With this simple result, we obtain

$$\begin{aligned} \langle z | \eta_{\mathbf{q},\nu} \eta_{\mathbf{p},\mu}^\dagger | z \rangle &= \delta_{\mathbf{p},\mathbf{q}} \frac{(1+|z|^2)^{N_f \mathcal{N}-2}}{\sqrt{\epsilon_\mu(\mathbf{p}) \epsilon_\nu(\mathbf{p})}} (|z|^2 \delta_{\mathbf{p},0} \mathcal{N} N_L \epsilon^2 \delta_{\mu,\nu} \delta_{\mu,0} + \delta_{\mu\nu} \epsilon_\mu(\mathbf{p})) \\ &= \delta_{\mathbf{p},\mathbf{q}} \delta_{\mu,\nu} (1+|z|^2)^{N_f \mathcal{N}-2} (|z|^2 \delta_{\mathbf{p},0} \mathcal{N} N_L \epsilon \delta_{\mu,0} + 1) \\ &= \delta_{\mathbf{p},\mathbf{q}} \delta_{\mu,\nu} (1+|z|^2)^{N_f \mathcal{N}-2} (|z|^2 \delta_{\mathbf{p},0} \delta_{\mu,0} N_f \mathcal{N} + 1) \end{aligned} \quad (\text{D49})$$

making use of $\epsilon = N_f/N_L$. We see that there is an anomalous term when $\mathbf{p}=0, \mu=0$. This is because $\eta_{\mathbf{p},0}^\dagger \propto \eta^\dagger$, which produces a zero-energy eta-pairing state. These states are the ground states we have already computed the normalization for in Eq. (C10). Expanding in powers of z and picking $\mathbf{p} \neq 0, \mu \neq 0$, we obtain

$$\begin{aligned} \sum_n |z|^{2n} \binom{N_f \mathcal{N}}{n} \langle n | \eta_{\mathbf{q},\nu} \eta_{\mathbf{p},\mu}^\dagger | n \rangle &= \sum_n |z|^{2n} \delta_{\mathbf{p},\mathbf{q}} \delta_{\mu,\nu} \binom{N_f \mathcal{N}-2}{n}, \quad \mathbf{p} \neq 0, \mu \neq 0 \\ \langle n | \eta_{\mathbf{q},\nu} \eta_{\mathbf{p},\mu}^\dagger | n \rangle &= (1-\nu)^2 \delta_{\mathbf{p},\mathbf{q}} \delta_{\mu,\nu} \end{aligned} \quad (\text{D50})$$

and in the last line we took the thermodynamic limit $\mathcal{N} \rightarrow \infty$.

4. Examples of the Cooper Pair Spectrum

To illustrate the Cooper pair spectrum, we consider three examples: an inversion-protected SSH chain in 1D, an obstructed atomic limit in 2D, and an S -matrix construction of fragile bands in 2D. We use the same notation $\tilde{h}(\mathbf{k})$ for the single-particle electron Hamiltonian, $P(\mathbf{k})$ for the flat band projector, and $h(\mathbf{p})$ for the bosonic pairing Hamiltonian for all the models used in this section. We recall that in general, the projection into the flat bands is valid when $W \ll |U| \ll t$ where W is the bandwidth of the flat band ($W=0$ if the band is perfectly flat), $|U|$ is the interaction strength, and t is the single-particle gap above the flat band.

a. *SSH Chain*

The 1D Hamiltonian we consider was studied in Ref. [56] as a minimal model of a flat band obstructed atomic insulator. We place s and p orbitals at the 1a position (the center of the unit cell) in the 1D space group pm . The electron Hamiltonian is

$$\tilde{h}(k) = \sin k \sigma_2 + \cos k \sigma_3 \quad (\text{D51})$$

with exactly flat bands at energies ± 1 . The eigenstate of the lower band is

$$U(k) = \frac{1}{2} \begin{pmatrix} 1 - e^{-ik} \\ 1 + e^{-ik} \end{pmatrix} \quad (\text{D52})$$

and one can calculate the Berry phase $U^\dagger i \partial_k U = \frac{1}{2}$, indicating an obstruction to the trivial atomic phase where the Wannier functions are onsite. Indeed, $h(k)$ obeys inversion symmetry with $D[\mathcal{I}]h(k)D^\dagger[\mathcal{I}] = h(-k)$ where $D[\mathcal{I}] = \sigma_3$, and real space invariants and/or symmetry eigenvalues diagnose $h(k)$ as being in an obstructed atomic limit [56].

Projecting into the single flat band, we find that the uniform pairing condition is obeyed:

$$\int \frac{dk}{2\pi} P_{\alpha\alpha}(k) = \frac{N_f}{N_{orb}} = \epsilon = \frac{1}{2}, \quad P(k) = U(k)U^\dagger(k) = \begin{pmatrix} \sin^2 \frac{k}{2} & \frac{i}{2} \sin k \\ -\frac{i}{2} \sin k & \cos^2 \frac{k}{2} \end{pmatrix}. \quad (\text{D53})$$

Note that the uniform pairing condition is not enforced by inversion because the s and p orbitals are *different* irreps of the 1a Wyckoff position and hence are not interrelated by crystalline symmetry. In other words, adding \mathcal{I} -preserving hoppings could destroy the uniform pairing condition. However, there may be non-crystallographic symmetries that enforce UPC. In this model, two anti-commuting symmetries: $\mathcal{C} = \sigma_1$ and $\mathcal{Z} = \mathbf{k} \rightarrow \mathbf{k} + \pi$, combine into a commuting unitary symmetry \mathcal{CZ} that enforces UPC:

$$\mathcal{CZ}P(\mathbf{k})\mathcal{CZ} = \sigma_1 \begin{bmatrix} \cos^2 \frac{k+\pi}{2} & -\frac{i}{2} \sin(k+\pi) \\ \frac{i}{2} \sin(k+\pi) & \sin^2 \frac{k+\pi}{2} \end{bmatrix} \sigma_1 = P(\mathbf{k}) \quad (\text{D54})$$

$$P_{\alpha\alpha}(\mathbf{k}) = \sum_{\beta} [\sigma_1]_{\alpha\beta} P_{\beta\beta}(\mathbf{k} + \pi). \quad (\text{D55})$$

The form of the interaction is still density-density, with the spin up s -orbital density multiplying the spin down s -orbital density and the same for the p -orbitals:

$$H_{\text{int}} = -|U| \sum_{\mathbf{R}, \alpha=s,p} \bar{n}_{\mathbf{R}, \alpha, \uparrow} \bar{n}_{\mathbf{R}, \alpha, \downarrow}. \quad (\text{D56})$$

Using the formula for the projector in Eq. (D53), we find the pairing Hamiltonian

$$h_{\alpha\beta}(p) = \int \frac{dk}{2\pi} P_{\alpha\beta}(k+p) P_{\beta\alpha}(k) = \frac{1}{8} \begin{pmatrix} 2 + \cos p & \cos p \\ \cos p & 2 + \cos p \end{pmatrix}_{\alpha\beta} \quad (\text{D57})$$

which has eigenvalues $\epsilon_\mu(p) = \frac{1}{4}(1 + \cos p), \frac{1}{4}$. The many-body energies are $E_\mu(p)/|U| = \epsilon - \epsilon_\mu(p) = \frac{1}{4}(1 - \cos p), \frac{1}{4}$. The unpaired continuum of states appears at $E/|U| = \epsilon = \frac{1}{2}$. The spectrum is depicted in Fig. 3(a).

As a final comment, we note that in this symmetry group pm , one may imagine deforming the s and p orbitals at 1a into symmetric and antisymmetric combinations of orbitals at non-maximal Wyckoff positions of s orbitals at 2b. This deformation involves a unitary transformation that combines s and p orbitals at position \mathbf{R} into symmetric and antisymmetric combinations. While the orbitals now obey the uniform pairing condition, the density-density interactions are not invariant under this transformation. However, the following interaction

$$H = -\frac{|U|}{2} \sum_{\mathbf{R}, \sigma=\uparrow, \downarrow} [\bar{n}_{\mathbf{R}, s, \sigma} + \bar{n}_{\mathbf{R}, p, \sigma}]^2 \quad (\text{D58})$$

is invariant, though we are currently unable to treat this interaction with the eta-pairing operator.

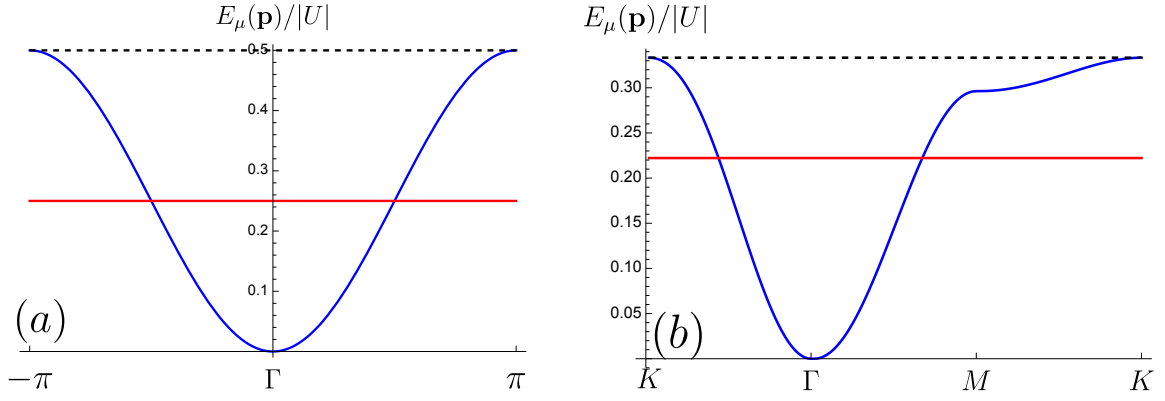


FIG. 3. The many-body Cooper pair/density excitation spectrum $E_\mu(\mathbf{p}) = |U|(\epsilon - \epsilon_\mu(\mathbf{p}))$ is shown for (a) the 1D SSH-like model in App. D 4 a and (b) the 2D compact obstructed atomic limit in App. D 4 b. The blue band is the quadratic gapless mode guaranteed by the $su(2)$ eta-pairing symmetry. The red band is perfectly flat for both models and is singly degenerate at $\frac{E}{|U|} = \frac{1}{4}$ in (a) and doubly degenerate at $\frac{E}{|U|} = \frac{2}{9}$ in (b). The dashed black line shows the macroscopically degenerate continuum of unpaired states at $E = \epsilon|U|$. The flatness of the Leggett modes (in red) is due to the simple, low-harmonic structure of the eigenstates. See the Cooper pair spectrum in the Main Text for nontrivially dispersing Leggett modes.

b. $p3$ Compact Obstructed atomic Insulator

A second compact OAI model with the uniform pairing condition and flat bands was first presented in Ref. [19] in the wallpaper group $p3$. The Hamiltonian is built from s and p_x, p_y orbitals on the 1a position (the unit cell center) which form the C_3 irreps $A, {}^1E, {}^2E$. As constructed in Ref. [19], the single valence band of the Hamiltonian forms a compact obstructed atomic limit, much like the obstructed phase of the SSH chain in App. D 4 a, and is indicated by real space invariants. Thus $\epsilon = \frac{N_f}{N_{orb}} = \frac{1}{3}$. The valence band eigenstate is

$$U(\mathbf{k}) = \frac{1}{3} \begin{pmatrix} 1 \\ 1 \\ 1 \end{pmatrix} + \frac{1}{3} \begin{pmatrix} 1 \\ e^{-\frac{2\pi i}{3}} \\ e^{\frac{2\pi i}{3}} \end{pmatrix} e^{i(k_1+k_2)} + \frac{1}{3} \begin{pmatrix} 1 \\ e^{\frac{2\pi i}{3}} \\ e^{-\frac{2\pi i}{3}} \end{pmatrix} e^{ik_2}. \quad (\text{D59})$$

We can calculate the pairing Hamiltonian analytically from $P(\mathbf{k}) = U(\mathbf{k})U^\dagger(\mathbf{k})$:

$$h_{\alpha\beta}(\mathbf{p}) = \int \frac{dk_1 dk_2}{(2\pi)^2} P_{\alpha\beta}(\mathbf{p} + \mathbf{k}) P_{\beta\alpha}(\mathbf{k}) = \frac{1}{9} \delta_{\alpha\beta} + \frac{2}{81} (\cos(p_1 + p_2) + \cos p_1 + \cos p_2) \quad (\text{D60})$$

$$h(\mathbf{p}) = \frac{2}{81} (\cos(p_1 + p_2) + \cos p_1 + \cos p_2) \begin{pmatrix} 1 & 1 & 1 \\ 1 & 1 & 1 \\ 1 & 1 & 1 \end{pmatrix} + \frac{1}{9} \begin{pmatrix} 1 & & \\ & 1 & \\ & & 1 \end{pmatrix}$$

which has eigenvalues $\epsilon_\mu(\mathbf{p}) = \frac{1}{27}(3 + 2\cos(p_1 + p_2) + 2\cos p_1 + 2\cos p_2), \frac{1}{9}, \frac{1}{9}$. The many-body spectrum $E_\mu(\mathbf{p})/|U| = \frac{1}{3} - \epsilon_\mu(\mathbf{p})$ is shown in Fig. 3(b) along with the un-paired continuum at $E/|U| = \epsilon = \frac{1}{3}$.

c. $p6mm$ Fragile S -matrix Bands

Finally, we construct a perfectly flat fragile band in symmetry group $p6mm$ using the S -matrix method introduced in Ref. [34]. To this end, we choose a 1D irrep (only one to enforce UPC) and place there an s -orbital, as we show in App. E 4 the Cooper pair transforms like an electronic s -orbital under the crystalline symmetries. As the set of bands induced from an atomic position is trivial, to get a fragile set of bands one requires the induced band representation decomposes into two sets, one of them fragile. As shown in Table E 5, the Cooper pair band structure we desire can be induced by placing any 1D irrep (for instance an s orbital) at the 3c (kagome) positions. The uniform pairing condition is guaranteed because the orbitals form an irrep of a single Wyckoff position. To obtain flat bands, we use the S -matrix construction define the two sublattices as $L = A_1^{3c}$ with $N_L = 3$ orbitals per unit cell and

$\tilde{L} = A_1^{1a}$ with $N_{\tilde{L}} = 1$ orbital per unit cell. The A_1 irrep denotes the s orbital representation at the 1a and 3c positions (see the Bilbao Crystallographic Server <https://www.cryst.ehu.es/cgi-bin/cryst/programs/mbandrep.pl>). The momentum space irreps of the two sublattices are

$$\begin{aligned}\mathcal{B}_L &= A_1^{3c} \uparrow 6mm = \Gamma_1 \oplus \Gamma_5 + K_1 \oplus K_3 + M_1 \oplus M_3 \oplus M_4 \\ \mathcal{B}_{\tilde{L}} &= A_1^{1a} \uparrow 6mm = \Gamma_1 + K_1 + M_1.\end{aligned}\quad (\text{D61})$$

In the bipartite S -matrix construction, hoppings are only allowed between the L and \tilde{L} sublattices resulting in $N_f = N_L - N_{\tilde{L}} = 3 - 1 = 2$ flat bands. The momentum space irreps of the flat bands are [34]

$$\mathcal{B}_L \ominus \mathcal{B}_{\tilde{L}} = \Gamma_5 + K_3 + M_3 \oplus M_4 \quad (\text{D62})$$

which is fragile topological [33]. To be concrete, we choose hoppings such that the single-particle electron Hamiltonian is

$$\tilde{h}(\mathbf{k}) = \begin{pmatrix} 0 & S^\dagger(\mathbf{k}) \\ S(\mathbf{k}) & 0_{3 \times 3} \end{pmatrix}, \quad S(\mathbf{k}) = t \begin{pmatrix} \cos \mathbf{k} \cdot \mathbf{a}_1/2 \\ \cos \mathbf{k} \cdot (\mathbf{a}_1 + \mathbf{a}_2)/2 \\ \cos \mathbf{k} \cdot \mathbf{a}_2/2 \end{pmatrix} = t \begin{pmatrix} \cos k_1/2 \\ \cos(k_1 + k_2)/2 \\ \cos k_2/2 \end{pmatrix} \quad (\text{D63})$$

where $\mathbf{a}_1 = (0, 1)$, $\mathbf{a}_2 = C_3 \mathbf{a}_1$ are the lattice vectors and $\mathbf{a}_1/2, (\mathbf{a}_1 + \mathbf{a}_2)/2, \mathbf{a}_2/2$ are the sites of the 2c position. The projector into the flat bands of $\tilde{h}(\mathbf{k})$ is given by

$$P(\mathbf{k}) = \begin{pmatrix} 0 & 0 & 0 & 0 \\ 0 & 2 + \cos k_2 + \cos(k_1 + k_2) & -2 \cos \frac{k_1}{2} \cos \frac{k_1 + k_2}{2} & -\cos \frac{k_1}{2} \cos \frac{k_2}{2} \\ 0 & -2 \cos \frac{k_1}{2} \cos \frac{k_1 + k_2}{2} & 2 + \cos k_1 + \cos k_2 & -2 \cos \frac{k_2}{2} \cos \frac{k_1 + k_2}{2} \\ 0 & -2 \cos \frac{k_1}{2} \cos \frac{k_2}{2} & -2 \cos \frac{k_2}{2} \cos \frac{k_1 + k_2}{2} & 2 + \cos k_1 + \cos k_1 + k_2 \end{pmatrix} / (3 + \cos k_1 + \cos(k_1 + k_2) + \cos k_2) \quad (\text{D64})$$

which is identically zero on the 1a position and obeys

$$\int \frac{dk_1 dk_2}{(2\pi)^2} P_{\alpha\alpha}(\mathbf{k}) = \begin{pmatrix} 0 \\ \frac{2}{3} \\ \frac{2}{3} \\ \frac{2}{3} \end{pmatrix} \quad (\text{D65})$$

which shows that the uniform pairing condition is satisfied on the 3c position, as guaranteed by App. A 2, with $\epsilon = \frac{N_f}{N_L} = \frac{2}{3}$.

We are unable to compute $h_{\alpha\beta}(\mathbf{p})$ analytically from the projectors in Eq. (D64), but it is very simple to compute the spectrum numerically. The lattice model and Cooper pair band structure are depicted in Fig. 4. The irreps of these bands are precisely those irreps induced by s orbitals at 3c:

$$\mathcal{B}_{\text{Cooper}} = A_1^{3c} \uparrow 6mm = \Gamma_1 \oplus \Gamma_5 + K_1 \oplus K_3 + M_1 \oplus M_3 \oplus M_4. \quad (\text{D66})$$

The Cooper pair band structure is decomposable, and as shown in Fig. 4(b), the blue band and red bands carry irreps

$$\begin{aligned}\mathcal{B}_1 &= \Gamma_1 + K_1 + M_1 \\ \mathcal{B}_2 &= \Gamma_5 + K_3 + M_3 \oplus M_4.\end{aligned} \quad (\text{D67})$$

The first band carries the Γ_1 irrep that is the zero-energy Cooper pair, and its global topology is trivial because $\Gamma_1 + K_1 + M_1$ is the band representation of an s orbital at the 1a position. The second set of bands is fragile topological as predicted from topological quantum chemistry, and cannot induced from local orbitals.

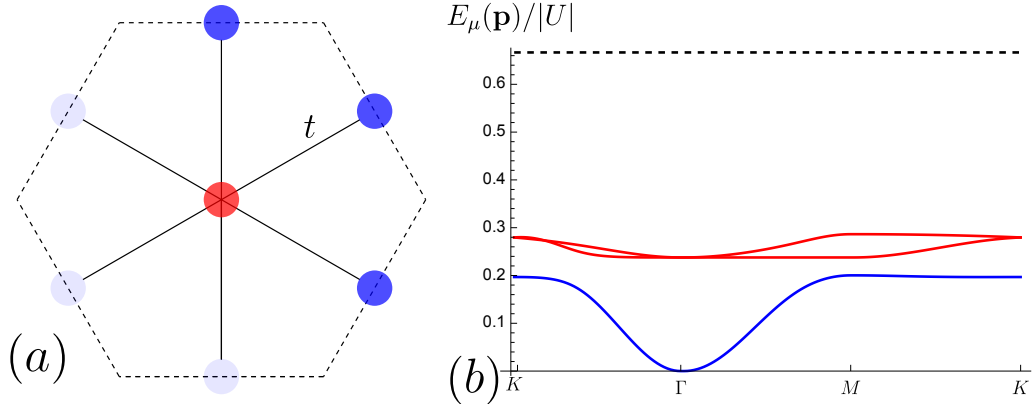


FIG. 4. (a) Bipartite hoppings t of the single-particle electron Hamiltonian Eq. (D63) resulting in two-fold degenerate fragile flat bands. The three s orbitals at the 3c position are blue, and the one s orbital at the 1a position is marked in red. (b) The many-body Cooper pair/Goldstone mode spectrum $E_\mu(\mathbf{p}) = |U|(\epsilon - \epsilon_\mu(\mathbf{p}))$ is shown. The blue band is the quadratic gapless mode guaranteed by the $su(2)$ eta-pairing symmetry. The two red bands are fragile topological (see Eq. D67) and are gapped from the low-energy quadratic band. The dashed black line shows the macroscopically degenerate continuum of unpaired states at $E = \epsilon|U|$.

5. Density Excitations

We now study the (spin) density modes which are in the form

$$[H, \gamma_{\mathbf{p}+\mathbf{k}, m, \sigma}^\dagger \gamma_{\mathbf{k}, n, \sigma'}] |GS\rangle = \sum_{\mathbf{k}'} \gamma_{\mathbf{p}+\mathbf{k}', m', \sigma}^\dagger \gamma_{\mathbf{k}', n', \sigma'} |GS\rangle [\mathcal{R}^{\sigma\sigma'}(\mathbf{p})]_{\mathbf{k}'m'n', \mathbf{k}mn}. \quad (\text{D68})$$

The eigenstates obtained from Eq. (D68) are charge-neutral, so they contribute to the partition function at fixed particle-number.

To compute $\mathcal{R}^{\sigma\sigma'}(\mathbf{p})$, we need the identities from App. D 1:

$$\begin{aligned} [\bar{S}_{\mathbf{q}, \alpha}^z, \gamma_{\mathbf{k}, n, \sigma}] &= -\frac{1}{\sqrt{N}} s_\sigma^z \sum_m M_{\sigma, \alpha}^{nm}(\mathbf{k} - \mathbf{q}, \mathbf{q}) \gamma_{\mathbf{k}-\mathbf{q}, m, \sigma} \\ [H, \gamma_{\mathbf{k}, n, \sigma}] &= \frac{\epsilon|U|}{2} \gamma_{\mathbf{k}, n, \sigma} - \frac{|U|}{2} \sum_{\mathbf{q}\alpha m} 2 \frac{1}{\sqrt{N}} s_\sigma^z M_{\sigma, \alpha}^{nm}(\mathbf{k} - \mathbf{q}, \mathbf{q}) \gamma_{\mathbf{k}-\mathbf{q}, m, \sigma} \bar{S}_{-\mathbf{q}, \alpha}^z \end{aligned} \quad (\text{D69})$$

and as usual, the second term in $[H, \gamma_{\mathbf{k}, n, \sigma}]$ annihilates the groundstate. The scattering matrix \mathcal{R} is obtained from a direct calculation:

$$\begin{aligned} [H, \gamma_{\mathbf{p}+\mathbf{k}, m, \sigma}^\dagger \gamma_{\mathbf{k}, n, \sigma'}] |GS\rangle &= \gamma_{\mathbf{p}+\mathbf{k}, m, \sigma}^\dagger [H, \gamma_{\mathbf{k}, n, \sigma'}] |GS\rangle + [H, \gamma_{\mathbf{p}+\mathbf{k}, m, \sigma}^\dagger] \gamma_{\mathbf{k}, n, \sigma'} |GS\rangle \\ &= \epsilon|U| \gamma_{\mathbf{p}+\mathbf{k}, m, \sigma}^\dagger \gamma_{\mathbf{k}, n, \sigma'} |GS\rangle + |U| \frac{1}{\sqrt{N}} \sum_{\mathbf{q}\alpha m'} s_\sigma^z \gamma_{\mathbf{p}+\mathbf{q}+\mathbf{k}, m', \sigma}^\dagger M_{\sigma, \alpha}^{m'm}(\mathbf{k} + \mathbf{p}, \mathbf{q}) [\bar{S}_{-\mathbf{q}, \alpha}^z, \gamma_{\mathbf{k}, n, \sigma'}] |GS\rangle \\ &= \epsilon|U| \gamma_{\mathbf{p}+\mathbf{k}, m, \sigma}^\dagger \gamma_{\mathbf{k}, n, \sigma'} |GS\rangle \\ &\quad - |U| \frac{1}{N} s_\sigma^z s_{\sigma'}^z \sum_{\mathbf{q}\alpha m' n'} \gamma_{\mathbf{p}+\mathbf{q}+\mathbf{k}, \sigma, m'}^\dagger \gamma_{\mathbf{k}+\mathbf{q}, \sigma', n'} M_{\sigma, \alpha}^{m'm}(\mathbf{k} + \mathbf{p}, \mathbf{q}) M_{\sigma', \alpha}^{nn'}(\mathbf{k} + \mathbf{q}, -\mathbf{q}) |GS\rangle \end{aligned} \quad (\text{D70})$$

from which we identify the scattering matrix

$$\begin{aligned} [\mathcal{R}^{\sigma\sigma'}(\mathbf{p})]_{\mathbf{k}'m'n', \mathbf{k}mn} &= \epsilon|U| \delta_{\mathbf{k}\mathbf{k}'} \delta_{mm'} \delta_{nn'} - s_\sigma^z s_{\sigma'}^z |U| \frac{1}{N} \sum_{\alpha} M_{\sigma, \alpha}^{m'm}(\mathbf{k} + \mathbf{p}, \mathbf{k}' - \mathbf{k}) M_{\sigma', \alpha}^{nn'}(\mathbf{k}', \mathbf{k} - \mathbf{k}') \\ &= \epsilon|U| \delta_{\mathbf{k}\mathbf{k}'} \delta_{mm'} \delta_{nn'} - s_\sigma^z s_{\sigma'}^z |U| \frac{1}{N} \sum_{\alpha} U_{m'\alpha}^{\sigma*}(\mathbf{p} + \mathbf{k}') U_{m\alpha}^{\sigma}(\mathbf{p} + \mathbf{k}) U_{n\alpha}^{\sigma'*}(\mathbf{k}) U_{n'\alpha}^{\sigma'}(\mathbf{k}') \\ &= \epsilon|U| \delta_{\mathbf{k}\mathbf{k}'} \delta_{mm'} \delta_{nn'} - s_\sigma^z s_{\sigma'}^z |U| \frac{1}{N} \sum_{\alpha} U_{m'\alpha}^{\sigma*}(\mathbf{p} + \mathbf{k}') U_{n'\alpha}^{\sigma'}(\mathbf{k}') U_{m\alpha}^{\sigma}(\mathbf{p} + \mathbf{k}) U_{n\alpha}^{\sigma'*}(\mathbf{k}). \end{aligned} \quad (\text{D71})$$

Let us recall the definition from Eq. (D39),

$$\mathcal{U}_{\mathbf{k}mn,\alpha}^{\sigma\sigma'}(\mathbf{p}) = U_{m\alpha}^{\sigma*}(\mathbf{p} + \mathbf{k})U_{n\alpha}^{\sigma'*}(-\mathbf{k}) . \quad (\text{D72})$$

In the Cooper pair case (see discussion after Eq. (D39)), the anti-commutation of the fermions, schematically $\gamma_{i\uparrow}^\dagger \gamma_{j\uparrow}^\dagger + \gamma_{j\uparrow}^\dagger \gamma_{i\uparrow}^\dagger = 0$, prevented nontrivial excitations of nonzero spin. In the density excitation case, $\gamma_{i\uparrow}^\dagger \gamma_{i\downarrow} + \gamma_{j\uparrow}^\dagger \gamma_{j\uparrow} \neq 0$, so nontrivial spin ± 1 excitations are allowed. Enumerating the possible choices of σ, σ' in Eq. (D68) gives the effective Hamiltonians

$$\begin{aligned} \gamma_{\mathbf{p}+\mathbf{k},m,\uparrow}^\dagger \gamma_{\mathbf{k},n,\uparrow} : \quad & \mathcal{R}^{\uparrow\uparrow}(\mathbf{p}) = \epsilon|U|\mathbb{1} - |U|\frac{1}{\mathcal{N}}\mathcal{U}_{\uparrow\downarrow}(\mathbf{p})\mathcal{U}_{\uparrow\downarrow}^\dagger(\mathbf{p}) \\ \gamma_{\mathbf{p}+\mathbf{k},m,\downarrow}^\dagger \gamma_{\mathbf{k},n,\downarrow} : \quad & \mathcal{R}^{\downarrow\downarrow}(\mathbf{p}) = \epsilon|U|\mathbb{1} - |U|\frac{1}{\mathcal{N}}\mathcal{U}_{\downarrow\uparrow}(\mathbf{p})\mathcal{U}_{\downarrow\uparrow}^\dagger(\mathbf{p}) \\ \gamma_{\mathbf{p}+\mathbf{k},m,\uparrow}^\dagger \gamma_{\mathbf{k},n,\downarrow} : \quad & \mathcal{R}^{\uparrow\downarrow}(\mathbf{p}) = \epsilon|U|\mathbb{1} + |U|\frac{1}{\mathcal{N}}\mathcal{U}_{\uparrow\uparrow}(\mathbf{p})\mathcal{U}_{\uparrow\uparrow}^\dagger(\mathbf{p}) \\ \gamma_{\mathbf{p}+\mathbf{k},m,\downarrow}^\dagger \gamma_{\mathbf{k},n,\uparrow} : \quad & \mathcal{R}^{\downarrow\uparrow}(\mathbf{p}) = \epsilon|U|\mathbb{1} + |U|\frac{1}{\mathcal{N}}\mathcal{U}_{\downarrow\downarrow}(\mathbf{p})\mathcal{U}_{\downarrow\downarrow}^\dagger(\mathbf{p}) . \end{aligned} \quad (\text{D73})$$

Note that the first two lines are spin 0 operators and the $\mathcal{U}\mathcal{U}^\dagger$ term comes with an overall minus, while the last two lines are spin ± 1 and the $\mathcal{U}\mathcal{U}^\dagger$ term comes with an overall plus. Because $\mathcal{U}\mathcal{U}^\dagger$ is positive semi-definite, we learn that the spin 0 excitations are always at or below the two-electron gap $\epsilon|U|$, whereas the spin ± 1 excitations are at or above the $\epsilon|U|$. This leads to a simple phenomenological prediction: the spin susceptibility is exponentially suppressed at temperatures below the spin gap $\epsilon|U|$.

By the same argument in Eq. (D40), the nonzero eigenvalues of $\mathcal{U}\mathcal{U}^\dagger$ are determined by the effective single-particle Hamiltonians

$$\begin{aligned} \mathcal{R}^{\uparrow\uparrow} : \quad & h_{\uparrow\uparrow}(\mathbf{p}) = h(\mathbf{p}) \\ \mathcal{R}^{\downarrow\downarrow} : \quad & h_{\downarrow\downarrow}(\mathbf{p}) = \frac{1}{\mathcal{N}} \sum_{\mathbf{k}} P_{\alpha\beta}^\downarrow(\mathbf{p} + \mathbf{k}) P_{\alpha\beta}^\uparrow(-\mathbf{k}) = \frac{1}{\mathcal{N}} \sum_{\mathbf{k}} P_{\alpha\beta}^\uparrow(\mathbf{p} + \mathbf{k}) P_{\alpha\beta}^\downarrow(-\mathbf{k}) \\ & = h(\mathbf{p}) \\ \mathcal{R}^{\uparrow\downarrow} : \quad & h_{\uparrow\downarrow}(\mathbf{p}) = \frac{1}{\mathcal{N}} \sum_{\mathbf{k}mn} U_{m\alpha}^\uparrow(\mathbf{p} + \mathbf{k}) U_{n\alpha}^\uparrow(-\mathbf{k}) U_{m\beta}^{\uparrow*}(\mathbf{p} + \mathbf{k}) U_{n\beta}^{\uparrow*}(-\mathbf{k}) = \frac{1}{\mathcal{N}} \sum_{\mathbf{k}} P_{\alpha\beta}^\uparrow(\mathbf{p} + \mathbf{k}) P_{\beta\alpha}^\downarrow(\mathbf{k}) \\ & = \frac{1}{\mathcal{N}} \sum_{\mathbf{k}} P_{\alpha\beta}(\mathbf{p} + \mathbf{k}) P_{\beta\alpha}(-\mathbf{k})^* \\ \mathcal{R}^{\downarrow\uparrow} : \quad & h_{\downarrow\uparrow}(\mathbf{p}) = \frac{1}{\mathcal{N}} \sum_{\mathbf{k}} P_{\alpha\beta}^\downarrow(\mathbf{p} + \mathbf{k}) P_{\alpha\beta}^\downarrow(-\mathbf{k}) = h_{\uparrow\downarrow}(-\mathbf{p})^* \end{aligned} \quad (\text{D74})$$

so we see that the two branches of spin 0 Goldstone modes have the same spectrum as the spin 0 Cooper pair, $h(\mathbf{p})$ in Eq. (D41). This is evidence of an enlarged symmetry group, which we will explain in forthcoming work. In Eq. (D74), the Hamiltonians $h_{\uparrow\downarrow}(\mathbf{p})$ of the spin ± 1 density excitations are related by \mathcal{T} which flips the spins. If the single-particle bands have $SU(2)$ spin symmetry, then $P(\mathbf{k}) = P(-\mathbf{k})^*$ and $h_{\uparrow\downarrow}(\mathbf{p}) = h(\mathbf{p})$. This symmetry will manifest itself in the excitation spectrum, where there will be particle-hole symmetric excitations about the flat band continuum at $E = \epsilon|U|$. Otherwise, the spectrum of $h_{\uparrow\downarrow}(\mathbf{p})$ is generically different from that of $h(\mathbf{p})$. Because our interest in this work is the low-energy excitations, we postpone a detailed study of $h_{\uparrow\downarrow}(\mathbf{p})$ to future work.

We now write down the spin-0 density operators as in Eq. (D44):

$$\begin{aligned} \rho_{\mathbf{p},\mu,\sigma} &= \frac{1}{\sqrt{\mathcal{N}\epsilon_\mu(\mathbf{p})}} \sum_{\mathbf{k}\alpha mn} \gamma_{\mathbf{p}+\mathbf{k},m,\sigma}^\dagger \gamma_{\mathbf{k},n,\sigma} \mathcal{U}_{\mathbf{k}mn,\alpha}^{\sigma,-\sigma}(\mathbf{p}) u_\mu^\alpha(\mathbf{p}) \\ &= \frac{1}{\sqrt{\mathcal{N}\epsilon_\mu(\mathbf{p})}} \sum_{\mathbf{k}\alpha mn} \gamma_{\mathbf{p}+\mathbf{k},m,\sigma}^\dagger \gamma_{\mathbf{k},n,\sigma} U_{m\alpha}^{\sigma*}(\mathbf{p} + \mathbf{k}) U_{n\alpha}^{-\sigma,*}(-\mathbf{k}) u_\mu^\alpha(\mathbf{p}) \\ &= \frac{1}{\sqrt{\mathcal{N}}} \sum_{\mathbf{k}\alpha} \frac{u_\mu^\alpha(\mathbf{p})}{\sqrt{\epsilon_\mu(\mathbf{p})}} \bar{c}_{\mathbf{p}+\mathbf{k},\alpha,\sigma}^\dagger \bar{c}_{\mathbf{k},\alpha,\sigma} \\ &= \frac{1}{\sqrt{\mathcal{N}}} \sum_{\mathbf{R}\alpha} \frac{u_\mu^\alpha(\mathbf{p})}{\sqrt{\epsilon_\mu(\mathbf{p})}} e^{-i\mathbf{p}\cdot(\mathbf{R}+\mathbf{r}_\alpha)} \bar{n}_{\mathbf{R},\alpha,\sigma} . \end{aligned} \quad (\text{D75})$$

To compute the normalized states, we use Wick's theorem. To start, we require the correlator

$$\langle z | \gamma_{\mathbf{k}', n', \sigma}^\dagger \gamma_{\mathbf{q} + \mathbf{k}', m', \sigma} \gamma_{\mathbf{p} + \mathbf{k}, m, \sigma}^\dagger \gamma_{\mathbf{k}, n, \sigma} | z \rangle = \frac{\delta_{\mathbf{p}\mathbf{q}}}{(1 + |z|^2)^2} (|z|^4 \delta_{\mathbf{p}, 0} \delta_{n' m'} \delta_{nm} - 0 + |z|^2 \delta_{\mathbf{k}, \mathbf{k}'} \delta_{nn'} \delta_{mm'}) \langle z | z \rangle. \quad (\text{D76})$$

The presence of the $\delta_{\mathbf{p}, 0}$ term is similar to Eq. (D46). Following the same steps as in Eq. (D48) and using Eq. (D47), we find

$$\begin{aligned} \langle z | \rho_{\mathbf{q}, \nu}^\dagger \rho_{\mathbf{p}, \mu} | z \rangle &= \delta_{\mathbf{p}, \mathbf{q}} \frac{(1 + |z|^2)^{N_f \mathcal{N} - 2}}{\mathcal{N} \sqrt{\epsilon_\mu(\mathbf{p})} \epsilon_\nu(\mathbf{q})} \sum_{\mathbf{k}\mathbf{k}', \alpha\beta} \mathcal{U}_{\mathbf{k}' m' n', \beta}^{\sigma, -\sigma}(\mathbf{q})^* u_{\nu}^{\beta*}(\mathbf{q}) (|z|^4 \delta_{n' m'} \delta_{\mathbf{p}, 0} \delta_{nm} + |z|^2 \delta_{\mathbf{k}\mathbf{k}'} \delta_{nn'} \delta_{mm'}) \mathcal{U}_{\mathbf{k} m n, \alpha}^{\sigma, -\sigma}(\mathbf{p}) u_\mu^\alpha(\mathbf{p}) \\ &= \delta_{\mathbf{p}, \mathbf{q}} \frac{(1 + |z|^2)^{N_f \mathcal{N} - 2}}{\sqrt{\epsilon_\mu(\mathbf{p})} \epsilon_\nu(\mathbf{p})} \sum_{\alpha\beta} u_\nu^{\beta*}(\mathbf{p}) (|z|^4 \delta_{\mathbf{p}, 0} \mathcal{N} \epsilon^2 + |z|^2 h_{\beta\alpha}(\mathbf{p})) u_\mu^\alpha(\mathbf{p}) \\ &= \delta_{\mathbf{p}, \mathbf{q}} \delta_{\mu, \nu} (1 + |z|^2)^{N_f \mathcal{N} - 2} (|z|^4 \delta_{\mathbf{p}, 0} \delta_{\mu, 0} N_f \mathcal{N} + |z|^2). \end{aligned} \quad (\text{D77})$$

The case of $\mathbf{p} = 0, \mu = 0$ again corresponds to the symmetry \bar{N}_\uparrow and \bar{N}_\downarrow operators at zero energy. Otherwise, we compute

$$\begin{aligned} \sum_n |z|^{2n} \binom{N_f \mathcal{N}}{n} \langle n | \rho_{\mathbf{q}, \nu}^\dagger \rho_{\mathbf{p}, \mu} | n \rangle &= \sum_n |z|^{2n+2} \delta_{\mathbf{p}, \mathbf{q}} \delta_{\mu, \nu} \binom{N_f \mathcal{N} - 2}{n}, \quad \mathbf{p} \neq 0, \mu \neq 0 \\ \langle n | \rho_{\mathbf{q}, \nu}^\dagger \rho_{\mathbf{p}, \mu} | n \rangle &= \nu(1 - \nu) \delta_{\mathbf{p}, \mathbf{q}} \delta_{\mu, \nu} \end{aligned} \quad (\text{D78})$$

which fixes the normalization of the states.

Appendix E: Spectrum and Topology of the Cooper Pairs

In this section, we study the effective single-particle boson Hamiltonian $h(\mathbf{p})$ (Eq. (13) of the Main Text) in detail, first showing clearly the invariance of all many-body observables under the momentum space gauge freedom corresponding to the orbital positions (App. E1). We then prove a number of generic features of the spectrum of $h(\mathbf{p})$ (App. E2), demonstrating a unique low-energy branch corresponding to the s -wave Cooper pairing channel. Its effective mass is determined by the minimal quantum metric (App. E3). We then prove the symmetry properties of $h(\mathbf{p})$ and determine the many-body symmetry transformations of the Cooper pair (App. E4). Finally, we use topological quantum chemistry to enumerate the possible band connectivities and discover fragile topological Cooper pair bands (App. E5).

1. Momentum Space Conventions

Before discussing the spectrum of $h(\mathbf{p})$, we discuss the dependence of $h(\mathbf{p})$ on the choice of momentum space operator convention in Eq. (A1). We start by recalling the single-particle Hamiltonian

$$\tilde{H} = \sum_{\mathbf{R}\mathbf{R}', \alpha\beta, \sigma} c_{\mathbf{R}, \alpha, \sigma}^\dagger t_{\alpha\beta}^\sigma(\mathbf{R} - \mathbf{R}') c_{\mathbf{R}', \beta, \sigma} = \sum_{\mathbf{k}\alpha\beta, \sigma} c_{\mathbf{k}, \alpha, \sigma}^\dagger \tilde{h}_{\alpha\beta}^\sigma(\mathbf{k}) c_{\mathbf{k}, \beta, \sigma} \quad (\text{E1})$$

where the momentum operators are $c_{\mathbf{k}, \alpha, \sigma}^\dagger = \frac{1}{\sqrt{\mathcal{N}}} \sum_{\mathbf{R}} e^{-i\mathbf{k} \cdot (\mathbf{R} + \mathbf{r}_\alpha)} c_{\mathbf{R}, \alpha, \sigma}^\dagger$. The choice of the \mathbf{r}_α term in the momentum space operators is arbitrary but convenient for representations of the space group symmetries [19, 109]. We now show that the spectrum of $h(\mathbf{p})$ and the many-body operators $\eta_{\mathbf{p}, \mu}^\dagger$ are all invariant under $\mathbf{r}_\alpha \rightarrow \mathbf{r}_\alpha + \mathbf{x}_\alpha$. However, under $\mathbf{r}_\alpha \rightarrow \mathbf{r}_\alpha + \mathbf{x}_\alpha$, we see nontrivial transformations

$$\begin{aligned} c_{\mathbf{k}, \alpha, \sigma}^\dagger &\rightarrow e^{-i\mathbf{k} \cdot \mathbf{x}_\alpha} c_{\mathbf{k}, \alpha, \sigma}^\dagger \\ \tilde{h}_{\alpha\beta}^\sigma(\mathbf{k}) &\rightarrow e^{i\mathbf{k} \cdot \mathbf{x}_\alpha} \tilde{h}_{\alpha\beta}^\sigma(\mathbf{k}) e^{-i\mathbf{k} \cdot \mathbf{x}_\beta}. \end{aligned} \quad (\text{E2})$$

If we define the local embedding matrix $[V_{\mathbf{x}}(\mathbf{k})]_{\alpha\beta} = e^{-i\mathbf{k} \cdot \mathbf{x}_\alpha} \delta_{\alpha\beta}$, then the transformation can be written $\tilde{h}(\mathbf{k}) \rightarrow V_{\mathbf{x}}^\dagger(\mathbf{k}) \tilde{h}(\mathbf{k}) V_{\mathbf{x}}(\mathbf{k})$. Thus the electron eigenvectors $U_\sigma(\mathbf{k})$ obey $U_\sigma(\mathbf{k}) \rightarrow V_{\mathbf{x}}^\dagger(\mathbf{k}) U_\sigma(\mathbf{k})$ and the projectors transform like $\tilde{h}: P_\sigma(\mathbf{k}) \rightarrow V_{\mathbf{x}}^\dagger(\mathbf{k}) P_\sigma(\mathbf{k}) V_{\mathbf{x}}(\mathbf{k})$. As such, we have

$$P_{\alpha\beta}^\sigma(\mathbf{k}) \rightarrow e^{i\mathbf{k} \cdot (\mathbf{x}_\alpha - \mathbf{x}_\beta)} P_{\alpha\beta}^\sigma(\mathbf{k}). \quad (\text{E3})$$

We now consider the transformation of the Cooper pair Hamiltonian:

$$\begin{aligned}
h_{\alpha\beta}(\mathbf{p}) &\rightarrow \frac{1}{\mathcal{N}} \sum_{\mathbf{k}} e^{i(\mathbf{p}+\mathbf{k})\cdot(\mathbf{x}_\alpha-\mathbf{x}_\beta)} e^{i\mathbf{k}\cdot(\mathbf{x}_\beta-\mathbf{x}_\alpha)} P_{\alpha\beta}(\mathbf{p}+\mathbf{k}) P_{\beta\alpha}(\mathbf{k}) \\
&= e^{i\mathbf{p}\cdot(\mathbf{x}_\alpha-\mathbf{x}_\beta)} \frac{1}{\mathcal{N}} \sum_{\mathbf{k}} P_{\alpha\beta}(\mathbf{p}+\mathbf{k}) P_{\beta\alpha}(\mathbf{k}) \\
&= [V_{\mathbf{x}}^\dagger(\mathbf{p}) h(\mathbf{p}) V_{\mathbf{x}}(\mathbf{p})]_{\alpha\beta} .
\end{aligned} \tag{E4}$$

Hence the Cooper pair eigenvectors transform just like the electron eigenvectors: $u_\mu(\mathbf{p}) \rightarrow V_{\mathbf{x}}^\dagger(\mathbf{p}) u_\mu(\mathbf{p})$. We see that the Cooper pair operators are invariant under the embedding:

$$\begin{aligned}
\eta_{\mathbf{p},\mu}^\dagger &= \frac{1}{\sqrt{\mathcal{N}}} \sum_{\mathbf{k}\alpha} \frac{u_\mu^\alpha(\mathbf{p})}{\sqrt{\epsilon_\mu(\mathbf{p})}} \bar{c}_{\mathbf{p}+\mathbf{k},\alpha,\uparrow}^\dagger \bar{c}_{-\mathbf{k},\alpha,\downarrow}^\dagger \\
&\rightarrow \frac{1}{\sqrt{\mathcal{N}}} \sum_{\mathbf{k}\alpha} \frac{u_\mu^\alpha(\mathbf{p}) e^{i\mathbf{p}\cdot\mathbf{x}_\alpha}}{\sqrt{\epsilon_\mu(\mathbf{p})}} e^{-i(\mathbf{k}+\mathbf{p})\cdot\mathbf{x}_\alpha} \bar{c}_{\mathbf{p}+\mathbf{k},\alpha,\uparrow}^\dagger e^{i\mathbf{k}\cdot\mathbf{x}_\alpha} \bar{c}_{-\mathbf{k},\alpha,\downarrow}^\dagger \\
&= \eta_{\mathbf{p},\mu}^\dagger
\end{aligned} \tag{E5}$$

It is also obvious that the spectrum of the Cooper pairs, $\epsilon_\mu(\mathbf{p})$, is invariant because the $V_{\mathbf{x}}(\mathbf{k})$ conjugate the Cooper pair Hamiltonian. Hence, as expected, all of the many-body observables are invariant under the arbitrary choice of \mathbf{x}_α .

2. Cooper Pair Hamiltonian and Spectrum

The fact that the Cooper pair and density excitations are determined by an effective single-particle Hamiltonian $h(\mathbf{p})$ is very evocative. It shows that the tightly-bound Cooper pairs behave much like a free boson whose hoppings arise from the quantum geometry, encoded in $P(\mathbf{k})$, of the flat bands. We will study the effective single-particle boson Hamiltonian and prove a number of properties about its spectrum and topology.

Let us restate the effective Hamiltonian derived in Eq. (D41),

$$h_{\alpha\beta}(\mathbf{p}) = \frac{1}{\mathcal{N}} \sum_{\mathbf{k}} P_{\alpha\beta}(\mathbf{p}+\mathbf{k}) P_{\beta\alpha}(\mathbf{k}) \tag{E6}$$

where $P(\mathbf{k}) = U(\mathbf{k})U^\dagger(\mathbf{k})$ is the Hermitian projector into the spin- \uparrow electronic flat bands. The α, β orbital indices range from $1, \dots, N_{orb}$. In the bipartite crystalline lattice construction, $N_{orb} \rightarrow N_L$ is understood to be the number of orbitals in the L sublattice. ($P_{\alpha\beta}(\mathbf{k}) = 0$ for α or $\beta \notin L$.)

First we show $h(\mathbf{p})$ is Hermitian:

$$h_{\beta\alpha}^*(\mathbf{p}) = \frac{1}{\mathcal{N}} \sum_{\mathbf{k}} P_{\beta\alpha}^*(\mathbf{p}+\mathbf{k}) P_{\alpha\beta}^*(\mathbf{k}) = \frac{1}{\mathcal{N}} \sum_{\mathbf{k}} P_{\alpha\beta}(\mathbf{p}+\mathbf{k}) P_{\beta\alpha}(\mathbf{k}) = h_{\alpha\beta}(\mathbf{p}) . \tag{E7}$$

The eigenvalues of $h(\mathbf{p})$ are denoted by $\epsilon_\mu(\mathbf{p})$ where $\mu = 0, \dots, N_{orb} - 1$ will denote the boson band index. We will now show that the spectrum of $h(\mathbf{p})$ is bounded by $0 \leq \epsilon_\mu(\mathbf{p}) \leq \epsilon$. Importantly, the many-body energies (see Eq. (D40)) of the boson excitations are given by $|U|(\epsilon - \epsilon_\mu(\mathbf{p}))$ so the bounds on the eigenvalues of $h(\mathbf{p})$ show that the many-body spectrum of the boson bands is between 0 and $\epsilon|U|$. Note that the largest eigenvalue of $h(\mathbf{p})$ corresponds to the lowest energy in the many-body spectrum. Thus we can think of $|U|\epsilon_\mu(\mathbf{p})$ as the binding energy gained by the pairing relative to the unpaired continuum of states at energy $\epsilon|U|$.

To show $h(\mathbf{p})$ is positive semi-definite, we observe that for an arbitrary vector v ,

$$\begin{aligned}
\sum_{\alpha\beta} v_\alpha^* h_{\alpha\beta}(\mathbf{p}) v_\beta &= \frac{1}{\mathcal{N}} \sum_{\mathbf{k}} \sum_{mn,\alpha\beta} v_\alpha^* U_{\alpha m}(\mathbf{p}+\mathbf{k}) U_{\beta m}^*(\mathbf{p}+\mathbf{k}) U_{\beta n}(\mathbf{k}) U_{\alpha n}^*(\mathbf{k}) v_\beta \\
&= \frac{1}{\mathcal{N}} \sum_{\mathbf{k}} \sum_{mn} [\sum_{\alpha} U_{\alpha m}^*(\mathbf{p}+\mathbf{k}) v_\alpha U_{\alpha n}(\mathbf{k})]^* \sum_{\beta} U_{\beta m}^*(\mathbf{p}+\mathbf{k}) v_\beta U_{\beta n}(\mathbf{k}) \\
&= \frac{1}{\mathcal{N}} \sum_{\mathbf{k}} \sum_{mn} V_{mn}^* V_{mn} \\
&= \frac{1}{\mathcal{N}} \sum_{\mathbf{k}} \|V\|_F^2 \geq 0 .
\end{aligned} \tag{E8}$$

where we defined the $N_f \times N_f$ matrix $V_{mn} = \sum_{\beta} U_{\beta m}^*(\mathbf{p} + \mathbf{k}) v_{\beta} U_{\beta n}(\mathbf{k})$ and used the Frobenius norm $\|V\|_F^2 = \sum_{mn} |V_{mn}|^2$. This establishes $\epsilon_{\mu}(\mathbf{p}) \geq 0$. Alternatively, we observe that $P_{\alpha\beta}(\mathbf{p} + \mathbf{k}) P_{\beta\alpha}(\mathbf{k}) = [P(\mathbf{p} + \mathbf{k}) \circ P^T(\mathbf{k})]_{\alpha\beta}$ is the Hadamard product of two positive semi-definite matrices $P(\mathbf{p} + \mathbf{k})$ and $P^T(\mathbf{k})$. By the Schur product theorem, $P_{\alpha\beta}(\mathbf{p} + \mathbf{k}) P_{\beta\alpha}(\mathbf{k})$ is positive semi-definite, and so $h_{\alpha\beta}(\mathbf{p})$ is the sum of positive semi-definite matrices with positive coefficients, and hence is positive-semi definite itself.

To prove $\epsilon_{\mu}(\mathbf{p}) \leq \epsilon$, we show that $\epsilon \mathbb{1} - h(\mathbf{p})$ is positive semi-definite. Using the uniform pairing condition, note that

$$\begin{aligned} [\epsilon \mathbb{1} - h(\mathbf{p})]_{\alpha\beta} &= \epsilon \delta_{\alpha\beta} - h_{\alpha\beta}(\mathbf{p}) = \frac{1}{\mathcal{N}} \sum_{\mathbf{k}} P_{\alpha\alpha}(\mathbf{k}) \delta_{\beta\alpha} - h_{\alpha\beta}(\mathbf{p}) \\ &= \frac{1}{\mathcal{N}} \sum_{\mathbf{k}} P_{\alpha\beta}(\mathbf{p} + \mathbf{k}) \delta_{\beta\alpha} - h_{\alpha\beta}(\mathbf{p}) \\ &= \frac{1}{\mathcal{N}} \sum_{\mathbf{k}} P_{\alpha\beta}(\mathbf{p} + \mathbf{k}) (\delta_{\beta\alpha} - P_{\beta\alpha}(\mathbf{k})) \\ &= \frac{1}{\mathcal{N}} \sum_{\mathbf{k}} P_{\alpha\beta}(\mathbf{p} + \mathbf{k}) Q_{\beta\alpha}(\mathbf{k}) \end{aligned} \quad (\text{E9})$$

where we defined $Q(\mathbf{k}) = \mathbb{1} - P(\mathbf{k})$. Note that $Q(\mathbf{k})$ is also a positive semi-definite matrix (it is a projector), and so $\epsilon \mathbb{1} - h(\mathbf{p})$ is positive semi-definite by the Schur product theorem.

We have shown that $\epsilon_{\mu}(\mathbf{p}) \leq \epsilon$. We now prove that this bound is tight by exhibiting the corresponding eigenvector at $\mathbf{p} = 0$. Claim: there is an eigenvector $u_0^{\alpha}(\mathbf{p} = 0) = 1/\sqrt{N_{orb}}$ with eigenvalue ϵ . This is simply the normalized uniform eigenvector corresponding to the eta-pairing symmetry η^{\dagger} . The claim is proven using the uniform pairing condition:

$$\begin{aligned} [h(0)u_0]_{\alpha} &= \frac{1}{\mathcal{N}} \sum_{\mathbf{k}} \sum_{\beta} P_{\alpha\beta}(\mathbf{k}) P_{\beta\alpha}(\mathbf{k}) u_0^{\beta}(0) \\ &= \frac{1}{\sqrt{N_{orb}}} \frac{1}{\mathcal{N}} \sum_{\mathbf{k}} \sum_{\beta} P_{\alpha\beta}(\mathbf{k}) P_{\beta\alpha}(\mathbf{k}) \\ &= \frac{1}{\sqrt{N_{orb}}} \frac{1}{\mathcal{N}} \sum_{\mathbf{k}} [P(\mathbf{k})^2]_{\alpha\alpha} \\ &= \frac{1}{\sqrt{N_{orb}}} \frac{1}{\mathcal{N}} \sum_{\mathbf{k}} P_{\alpha\alpha}(\mathbf{k}) \\ &= \epsilon u_0^{\alpha} . \end{aligned} \quad (\text{E10})$$

The existence of this state is tied to the η^{\dagger} symmetry. The $\mathbf{p} = 0$ Cooper pair excitation spectrum includes the η^{\dagger} operator in its Hilbert space, and η^{\dagger} commutes with the Hamiltonian and therefore has zero energy. Because the many-body energy is $|U|(\epsilon - \epsilon_{\mu}(\mathbf{p}))$, there must be a band with $\epsilon_{\mu}(0) = \epsilon$, and as such this excitation is gapless. We refer to this as the $\mu = 0$ band. Indeed, the excitation operator defined in Eq. (D44) yields

$$\eta_{\mathbf{p}=0, \mu=0}^{\dagger} = \frac{1}{\sqrt{\mathcal{N}}} \sum_{\mathbf{k}\alpha} \frac{1/\sqrt{N_{orb}}}{\sqrt{\epsilon}} \bar{c}_{\mathbf{k}, \alpha, \uparrow}^{\dagger} \bar{c}_{-\mathbf{k}, \alpha, \downarrow}^{\dagger} = \frac{1}{\sqrt{N_f \mathcal{N}}} \sum_{\mathbf{k}\alpha} \bar{c}_{\mathbf{k}, \alpha, \uparrow}^{\dagger} \bar{c}_{-\mathbf{k}, \alpha, \downarrow}^{\dagger} = \frac{1}{\sqrt{N_f \mathcal{N}}} \eta^{\dagger} \quad (\text{E11})$$

using $\epsilon = N_f/N_{orb}$. (In the bipartite case, $N_{orb} \rightarrow N_L$.)

We now show that the gapless Cooper pair band is unique, i.e. that there are no other zero-energy excitations for all \mathbf{p} . To do so, we first Fourier transform into real space using Eq. (A8), which reads

$$P_{\alpha\beta}(\mathbf{k}) = \sum_{\mathbf{R}} e^{i\mathbf{k} \cdot (\mathbf{R} + \mathbf{r}_{\alpha} - \mathbf{r}_{\beta})} p_{\alpha\beta}(\mathbf{R}) . \quad (\text{E12})$$

A direct calculation gives

$$\begin{aligned} h_{\alpha\beta}(\mathbf{p}) &= \sum_{\mathbf{R}\mathbf{R}'} \frac{1}{\mathcal{N}} \sum_{\mathbf{k}} e^{i(\mathbf{p} + \mathbf{k}) \cdot (\mathbf{R} + \mathbf{r}_{\alpha} - \mathbf{r}_{\beta}) + i\mathbf{k} \cdot (\mathbf{R}' + \mathbf{r}_{\beta} - \mathbf{r}_{\alpha})} p_{\alpha\beta}(\mathbf{R}) p_{\beta\alpha}(\mathbf{R}') \\ &= \sum_{\mathbf{R}} e^{i\mathbf{p} \cdot (\mathbf{R} + \mathbf{r}_{\alpha} - \mathbf{r}_{\beta})} p_{\alpha\beta}(\mathbf{R}) p_{\beta\alpha}(-\mathbf{R}) \\ &= \sum_{\mathbf{R}} e^{i\mathbf{p} \cdot (\mathbf{R} + \mathbf{r}_{\alpha} - \mathbf{r}_{\beta})} |p_{\alpha\beta}(\mathbf{R})|^2 \end{aligned} \quad (\text{E13})$$

using $p^\dagger(\mathbf{R}) = p(-\mathbf{R})$. We recognize the last line of Eq. (E13) as an expression for the matrix elements of the real space hopping matrix $t_{\alpha\beta}(\mathbf{R} - \mathbf{R}') = |p_{\alpha\beta}(\mathbf{R} - \mathbf{R}')|^2$. This shows that the effective hoppings felt by the bosons are due to the correlation function $p(\mathbf{R})$ of the flat bands. Note that $\text{spec } t_{\alpha\beta}(\mathbf{R} - \mathbf{R}') = \text{spec } |p_{\alpha\beta}(\mathbf{R} - \mathbf{R}')|^2 = \{\text{spec } h(\mathbf{p}) \forall \mathbf{p}\}$. To show that $\epsilon_0(\mathbf{p} = 0)$ is the unique largest eigenvalue of the whole band structure of $h(\mathbf{p})$, the crucial feature is that the hopping elements are non-negative: $|p_{\alpha\beta}(\mathbf{R} - \mathbf{R}')|^2 \geq 0$. Hence we can apply the Perron-Frobenius theorem, which states that a non-negative irreducible matrix has a *unique* largest positive eigenvalue, which we have shown explicitly is ϵ . Because $|p_{\alpha\beta}(\mathbf{R} - \mathbf{R}')|^2$ is non-negative, we must also check that $t_{\alpha\beta}(\mathbf{R} - \mathbf{R}')$ is irreducible to apply the theorem. An irreducible matrix A is one for which $Ae \notin e\forall e$ where e is a basis of any coordinate subspace. Physically, irreducibility is equivalent to the lattice being strongly connected, meaning any two orbitals are connected by a sequence of hoppings $|p_{\alpha\beta}(\mathbf{R} - \mathbf{R}')|^2$. This is *not* the case in a trivial atomic limit where $p_{\alpha\beta}(\mathbf{R} - \mathbf{R}') \propto \delta_{\mathbf{R}\mathbf{R}'}$. Ref. [19] proved nonzero lower bounds on $\|p(\mathbf{R} \neq 0)\|^2$ in terms of real space invariants [33] which are the indices diagnosing obstructed atomic insulators and fragile phases. Excluding certain pathological cases (like a 2D system formed from decoupled 1D chains, or an occupied trivial atomic limit band added with a direct sum into the projector $P(\mathbf{k})$), the results of Ref. [19] show that $t_{\alpha\beta}(\mathbf{R} - \mathbf{R}')$ is strongly connected if the flat bands are in an obstructed, fragile, or stable phase.

We prove a further result on the spectrum of $h(\mathbf{p})$. So far we have shown that $0 \leq \epsilon_\mu(\mathbf{p}) \leq \epsilon$. We now show that the spectral average of the band structure is ϵ^2 :

$$\frac{1}{\mathcal{N}N_L} \sum_{\mathbf{p}\mu} \epsilon_\mu(\mathbf{p}) = \frac{1}{\mathcal{N}N_L} \sum_{\mathbf{p}} \text{Tr } h(\mathbf{p}) = \frac{1}{\mathcal{N}N_L} \sum_{\mathbf{p}\alpha} h_{\alpha\alpha}(\mathbf{p}) = \frac{1}{\mathcal{N}^2 N_L} \sum_{\mathbf{p}\mathbf{k}\alpha} P_{\alpha\alpha}(\mathbf{p} + \mathbf{k}) P_{\alpha\alpha}(\mathbf{k}) = \frac{1}{N_L} \sum_{\alpha} \epsilon^2 = \epsilon^2. \quad (\text{E14})$$

Recalling the many-body energies $E_\mu(\mathbf{p}) = |U|(\epsilon - \epsilon_\mu(\mathbf{p}))$, the many-body density of states $g(E)$ obeys

$$\int_0^{\epsilon|U|} E g(E) dE = \frac{1}{\mathcal{N}} \sum_{\mathbf{p}\mu} E_\mu(\mathbf{p}) = |U|N_L(\epsilon - \epsilon^2) = |U|N_f(1 - \epsilon). \quad (\text{E15})$$

The upper bound of integral in Eq. (E15) is understood to be just below $\epsilon|U|$, where there is a thermodynamically large degeneracy of flat density excitation bands (analogous to the unpaired continuum in the Cooper pair sector).

Our last result concerns a simple transformation of the model under $P(\mathbf{k}) \rightarrow \mathbb{1} - P(\mathbf{k})$, which is equivalent to exchanging the projected and unprojected bands. For simplicity, we assume that all orbitals form an irrep of a single Wyckoff position, e.g. we do not use the bipartite construction in what follows. Note that under $P(\mathbf{k}) \rightarrow \mathbb{1} - P(\mathbf{k})$, we have $N_f \rightarrow N_{orb} - N_f$ and hence $\epsilon \rightarrow 1 - \epsilon$. Now we compute

$$\begin{aligned} h_{\alpha\beta}(\mathbf{p}) &\rightarrow \frac{1}{\mathcal{N}} \sum_{\mathbf{k}} (\delta_{\alpha\beta} - P_{\alpha\beta}(\mathbf{k} + \mathbf{p})) (\delta_{\alpha\beta} - P_{\beta\alpha}(\mathbf{k})) \\ &= \delta_{\alpha\beta} - \delta_{\alpha\beta} \frac{1}{\mathcal{N}} \sum_{\mathbf{k}} P_{\alpha\alpha}(\mathbf{k} + \mathbf{p}) - \delta_{\alpha\beta} \frac{1}{\mathcal{N}} \sum_{\mathbf{k}} P_{\alpha\alpha}(\mathbf{k}) + h_{\alpha\beta}(\mathbf{p}) \\ &= \delta_{\alpha\beta} - 2\epsilon\delta_{\alpha\beta} + h_{\alpha\beta}(\mathbf{p}). \end{aligned} \quad (\text{E16})$$

Thus the many-body energies transform as

$$E_\mu(\mathbf{p}) = |U|(\epsilon - \epsilon_\mu(\mathbf{p})) \rightarrow |U|(1 - \epsilon - (1 - 2\epsilon + \epsilon_\mu(\mathbf{p}))) = |U|(\epsilon - \epsilon_\mu(\mathbf{p})) \quad (\text{E17})$$

and hence are invariant. The energy of the unpaired continuum states does change, however, $\epsilon|U| \rightarrow (1 - \epsilon)|U|$. Because we proved above (Eq. (E9)) that the bound state energies $E_\mu(\mathbf{p}) \leq \epsilon|U|$ are below the unpaired continuum, we see in fact that $E_\mu(\mathbf{p}) \leq \min\{\epsilon|U|, (1 - \epsilon)|U|\}$. This follows by taking $P(\mathbf{k}) \rightarrow \mathbb{1} - P(\mathbf{k})$ and using $E_\mu(\mathbf{p}) \rightarrow E_\mu(\mathbf{p})$, $\epsilon \rightarrow 1 - \epsilon$.

3. Cooper Pair mass and Minimal Quantum Metric

We proved in App. E2 that the many-body spectrum contains a gapless mode $E_{\mu=0}(\mathbf{p} = 0) = 0$. In this section, we use perturbation theory to compute the small \mathbf{p} expansion around this point, yielding the low energy behavior of the bosonic excitations. The result we will prove is $\epsilon_0(\mathbf{p}) = \epsilon - \frac{g_{ij}}{N_L} p_i p_j$ where g_{ij} is the minimal quantum metric (introduced in Ref. [61] and explicitly constructed below) and N_L is the number of orbitals where $P(\mathbf{k})$ is nonzero. We sum over repeated spatial indices i, j in this section. As a result, the many-body energy is

$$E_0(\mathbf{p}) = |U|(\epsilon - \epsilon_0(\mathbf{p})) = |U| \frac{g_{ij}}{N_L} p_i p_j + \dots \quad (\text{E18})$$

which shows the low-lying Goldstone and Cooper pair modes are quadratic. This amounts to a many-body calculation of the Cooper pair mass, which has been previously approximated from the two-body problem[4] and is directly related to the mean-field superfluid weight [1, 15].

Because we have proven that $\epsilon_0(\mathbf{p} = 0)$ is the unique maximal eigenvalue in App. E 2, its small \mathbf{p} corrections can be obtained using non-degenerate perturbation theory. At zeroth order, $h(0)$ has eigenvectors u_μ , with $u_0 = 1/\sqrt{N_L}$ corresponding to the maximal eigenvalue $\epsilon_\mu = \epsilon$. We determine the corrections to $h(0)$ by expanding in \mathbf{p} :

$$h_{\alpha\beta}(\mathbf{p}) = \frac{1}{N} \sum_{\mathbf{k}} P_{\alpha\beta}(\mathbf{k}) P_{\beta\alpha}(\mathbf{k}) + p_i \frac{1}{N} \sum_{\mathbf{k}} \partial_i P_{\alpha\beta}(\mathbf{k}) P_{\beta\alpha}(\mathbf{k}) + \frac{1}{2} p_i p_j \frac{1}{N} \sum_{\mathbf{k}} \partial_{ij} P_{\alpha\beta}(\mathbf{k}) P_{\beta\alpha}(\mathbf{k}) + \dots \quad (\text{E19})$$

Denote $h_{\alpha\beta}^i = \partial_i h_{\alpha\beta}|_{\mathbf{p}=0}$. By time-reversal $h_{\alpha\beta}^*(\mathbf{p}) = h_{\alpha\beta}(-\mathbf{p})$, we expand to first order and find

$$(p_i h_{\alpha\beta}^i)^* = -p_i h_{\alpha\beta}^i, \quad (\text{E20})$$

so $h_{\alpha\beta}^i = -h_{\beta\alpha}^i$ is anti-symmetric because $(h_{\alpha\beta}^i)^* = h_{\beta\alpha}^i$ using Hermiticity. This can also be seen with an integration by parts. This immediately shows that the first order correction to $\epsilon_0(\mathbf{p})$ vanishes because

$$u_0^\dagger h^i u_0 = \frac{1}{N_L} \sum_{\alpha\beta} h_{\alpha\beta}^i = 0. \quad (\text{E21})$$

We now consider the second order correction. There are contributions to the second order correction:

$$\frac{1}{2} p_i p_j \partial_{ij} \epsilon_0(\mathbf{p}) = \frac{1}{2} p_i p_j \left(2\Re \sum_{\mu \neq 0} \frac{u_0^\dagger h^i u_\mu u_\mu^\dagger h^j u_0}{\epsilon - \epsilon_\mu(0)} + \frac{1}{N} \sum_{\mathbf{k}\alpha\beta} \frac{1}{N_L} \partial_{ij} P_{\alpha\beta}(\mathbf{k}) P_{\beta\alpha}(\mathbf{k}) \right) \equiv \frac{1}{2} p_i p_j (A_{ij} + B_{ij}). \quad (\text{E22})$$

The first term A_{ij} is the usual second order correction from a linear perturbation $p_i h^i$, and the second term B_{ij} is simply the expectation value of the second order correction in u_0 . The second term is related to the quantum metric after an integration by parts:

$$\begin{aligned} B_{ij} &= \frac{1}{N_L} \frac{1}{N} \sum_{\mathbf{k}\alpha\beta} \partial_{ij} P_{\alpha\beta}(\mathbf{k}) P_{\beta\alpha}(\mathbf{k}) = -\frac{1}{N_L} \frac{1}{N} \sum_{\mathbf{k}} \text{Tr} \partial_i P(\mathbf{k}) \partial_j P(\mathbf{k}) = -\frac{2}{N_L} g_{ij} \preceq 0, \\ g_{ij} &= \frac{1}{N} \sum_{\mathbf{k}} g_{ij}(\mathbf{k}), \quad g_{ij}(\mathbf{k}) = \frac{1}{2} \text{Tr} \partial_i P(\mathbf{k}) \partial_j P(\mathbf{k}) \end{aligned} \quad (\text{E23})$$

using the convention $\text{Tr} \mathcal{G}_{ij}(\mathbf{k}) = \text{Tr} P(\mathbf{k}) \partial_i P(\mathbf{k}) \partial_j P(\mathbf{k}) = g_{ij}(\mathbf{k}) - \frac{i}{2} f_{ij}(\mathbf{k})$. Note that Ref. [19] proves $\text{Tr} P(\mathbf{k}) \{ \partial_i P(\mathbf{k}), \partial_j P(\mathbf{k}) \} = \text{Tr} \partial_i P(\mathbf{k}) \partial_j P(\mathbf{k})$. Next, we observe that $A_{ij} \succeq 0$ because $\epsilon - \epsilon_\mu(0) \geq 0$. Thus A and B have competing contributions to $\partial_{ij} \epsilon_0(\mathbf{p})$.

Because the spectrum of $h(\mathbf{p})$ is invariant under invariant under $\mathbf{r}_\alpha \rightarrow \mathbf{r}_\alpha + \mathbf{x}_\alpha$, $\frac{1}{2} p_i p_j \partial_{ij} \epsilon_0(\mathbf{p})$ is invariant. However, A_{ij} and B_{ij} are not individually invariant. We now show that there is a unique choice of \mathbf{x}_α , up to a constant, where $A_{ij} = 0$ and the quantum metric alone determines $\partial_{ij} \epsilon_0(\mathbf{p})$. Because $A_{ij} + B_{ij}$ is independent of \mathbf{x}_α , taking $A_{ij} \rightarrow 0$ corresponds to the maximal B_{ij} and hence the minimal g_{ij} for all \mathbf{x}_α .

First we show that there exists \mathbf{x}_α where $A_{ij} = 0$, and then we show such a choice respects the symmetries of the system. Note that we keep \mathbf{r}_α , the physical location of the Wyckoff position, constant.

Returning to Eq. (E22), we recall that $\epsilon - \epsilon_\mu > 0$ and $u_0^\dagger p_i h^i u_\mu u_\mu^\dagger p_j h^j u_0$ is nonnegative. Thus $A_{ij} = 0$ iff $u_\mu^\dagger h^j u_0 = 0$ for all $\mu \neq 0$. Because the u_μ eigenvectors form a complete and orthogonal basis, $u_\mu^\dagger h^j u_0 = 0$ iff $h^j u_0 \propto u_0$. Thus u_0 must be an eigenvector of h^i . For a given choice of orbital locations, this is not guaranteed. However, h^i is not invariant under shifts of orbital location $\mathbf{r}_\alpha \rightarrow \mathbf{r}_\alpha + \mathbf{x}_\alpha$. Using $P_{\alpha\beta}(\mathbf{k}) \rightarrow e^{i\mathbf{k} \cdot (\mathbf{x}_\alpha - \mathbf{x}_\beta)} P_{\alpha\beta}(\mathbf{k})$, the transformation is

$$\begin{aligned} h_{\alpha\beta}^i &= \frac{1}{N} \sum_{\mathbf{k}} \partial_i P_{\alpha\beta}(\mathbf{k}) P_{\beta\alpha}(\mathbf{k}) \rightarrow \frac{1}{N} \sum_{\mathbf{k}} \partial_i P_{\alpha\beta}(\mathbf{k}) P_{\beta\alpha}(\mathbf{k}) + i(x_\alpha^i - x_\beta^i) \frac{1}{N} \sum_{\mathbf{k}} P_{\alpha\beta}(\mathbf{k}) P_{\beta\alpha}(\mathbf{k}) \\ &= h_{\alpha\beta}^i + i(x_\alpha^i - x_\beta^i) h_{\alpha\beta}(0) \end{aligned} \quad (\text{E24})$$

and x_α^i denotes the i th spatial component of \mathbf{x}_α . Note that $h_{\alpha\beta}(0)$ is Hermitian and real, so $i(x_\alpha^i - x_\beta^i) h_{\alpha\beta}(0)$ is Hermitian and anti-symmetric, as is $h_{\alpha\beta}^i$. If $\mathbf{x}_\alpha = \mathbf{x}$ is a constant shift, then $h_{\alpha\beta}^i \rightarrow h_{\alpha\beta}^i$.

Our task is to look for \mathbf{x}_α such that u_0 is an eigenvector of h^i (which guarantees that $A_{ij} = 0$). The eigenvalue equation is

$$\sum_{\beta} (h_{\alpha\beta}^i + i(x_{\alpha}^i - x_{\beta}^i)h_{\alpha\beta}(0))u_0^{\beta} = \lambda u_0^{\alpha} \quad (\text{E25})$$

where λ is the eigenvalue. First we show that if Eq. (E25) condition holds, then $\lambda = 0$. Contracting both sides with $u_0^{\alpha} = 1/\sqrt{N_L}$ gives

$$\lambda = \frac{1}{N_L} \sum_{\alpha\beta} h_{\alpha\beta}^i + i(x_{\alpha}^i - x_{\beta}^i)h_{\alpha\beta}(0) = 0 \quad (\text{E26})$$

because of anti-symmetry in $\alpha\beta$. Then Eq. (E25) reads

$$\begin{aligned} 0 &= \sum_{\beta} h_{\alpha\beta}^j + i \sum_{\beta} (x_{\alpha}^j - x_{\beta}^j)h_{\alpha\beta}(0) \\ 0 &= \sum_{\beta} h_{\alpha\beta}^j + i x_{\alpha}^j \sum_{\beta} h_{\alpha\beta}(0) - i \sum_{\beta} h_{\alpha\beta}(0)x_{\beta}^j \\ \sum_{\beta} h_{\alpha\beta}(0)x_{\beta}^j &= -i \sum_{\beta} h_{\alpha\beta}^j + \epsilon x_{\alpha}^j \\ [(h(0) - \epsilon)x^j]_{\alpha} &= -i \sum_{\beta} h_{\alpha\beta}^j \end{aligned} \quad (\text{E27})$$

where we used the uniform pairing condition $\sum_{\beta} h_{\alpha\beta}(0) = \epsilon$. We now define the vector $-i \sum_{\beta} h_{\alpha\beta}^j = h_{\alpha}^j$ which is real and obeys $\sum_{\alpha} h_{\alpha}^j = 0$, so it is orthogonal to the uniform eigenvector u_0 . Because $h(0)$ has a unique eigenvector u_0 with eigenvalue ϵ (see Eq. (E10)), $(h(0) - \epsilon)$ is invertible up to the u_0 eigenspace. This means x_{α}^j is uniquely determined up to constant shifts because $u_0^{\alpha} \propto 1$. Thus we obtain x_{α}^j up to constant shifts by applying the pseudo-inverse[77] $(h(0) - \epsilon)^{+}$:

$$\begin{aligned} x_{\alpha}^j &= [-i(h(0) - \epsilon)^{+} h^j u_0 \sqrt{N_L}]_{\alpha}, \quad [h^j u_0 \sqrt{N_L}]_{\alpha} = \sum_{\beta} h_{\alpha\beta}^j \\ \mathbf{x}_{\alpha} &= [i(\epsilon - h(0))^{+} (\nabla h(\mathbf{p})|_{\mathbf{p}=0}) u_0 \sqrt{N_L}]_{\alpha}. \end{aligned} \quad (\text{E28})$$

The pseudo-inverse of a Hermitian matrix is very simple. For a hermitian matrix h with eigenvalues ϵ_{μ} and eigen-decomposition $h = \sum_{\mu} \epsilon_{\mu} p_{\mu}$, the pseudo-inverse is $h^{+} = \sum_{\mu} \epsilon_{\mu}^{+} p_{\mu}$ where p_{μ} is the projector onto the ϵ_{μ} eigenspace, $\epsilon^{+} = 1/\epsilon$ if $\epsilon \neq 0$, and $\epsilon^{+} = 0$ otherwise. Hence $h h^{+} = h^{+} h$ acts as the identity on the nonzero eigenspaces and 0 otherwise.

Having proven in Eq. (E28) that orbitals shifts \mathbf{x}_{α} always exist for which $A_{ij} = 0$, we now show that \mathbf{x}_{α} preserve the space group symmetries $g \in G$. In particular, this will show that orbitals at high-symmetry Wyckoff positions, whose location is fixed by symmetry, are necessarily the choices where $A_{ij} = 0$. In this case, the minimal quantum metric is the quantum metric evaluated in the \mathbf{r}_{α} convention Eq. (A1).

To prove this result, we need the action of the space group symmetries on $h(\mathbf{p})$. We prove in App. E 4 that

$$\Gamma[g] h(\mathbf{p}) \Gamma^{\dagger}[g] = h(g^{-1} \mathbf{p}), \quad g \in G \quad (\text{E29})$$

where the representation $\Gamma_{\alpha\beta}[g] = |D_{\alpha\beta}[g]|$ is a permutation matrix. It follows that

$$\Gamma[g] \nabla h(\mathbf{p}) \Gamma^{\dagger}[g] = \nabla h(g^{-1} \mathbf{p}) = g^{-1} \nabla h|_{g^{-1} \mathbf{p}}. \quad (\text{E30})$$

Evaluating Eq. (E30) at $\mathbf{p} = 0$ gives $\Gamma[g] \nabla h|_{\mathbf{p}=0} \Gamma^{\dagger}[g] = g^{-1} \nabla h|_{\mathbf{p}=0}$. Then

$$\begin{aligned} g^{-1} \mathbf{x}_{\alpha} &= [i(\epsilon - h(0))^{+} (g^{-1} \nabla h(\mathbf{p})|_{\mathbf{p}=0}) u_0]_{\alpha} \\ &= [i(\epsilon - h(0))^{+} \Gamma[g] (\nabla h(\mathbf{p})|_{\mathbf{p}=0}) \Gamma^{\dagger}[g] u_0]_{\alpha} \\ &= \sum_{\beta} \Gamma_{\alpha\beta}[g] [i(\epsilon - h(0))^{+} (\nabla h(\mathbf{p})|_{\mathbf{p}=0}) [g] u_0]_{\beta} \\ &= \sum_{\beta} \Gamma_{\alpha\beta}[g] \mathbf{x}_{\beta} \end{aligned} \quad (\text{E31})$$

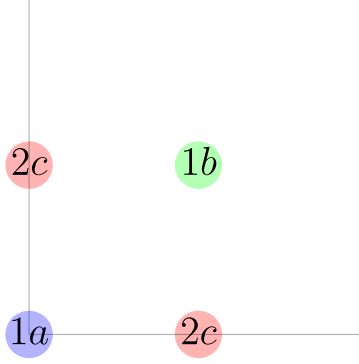


FIG. 5. Unit cell of the wallpaper group $p4mm$ generated by C_4 and translations (we take $\mathbf{a}_1 = (1, 0)$, $\mathbf{a}_2 = (0, 1)$ for ease). There are three maximal Wyckoff positions $1a = (0, 0)$, $1b = (1/2, 1/2)$, $2c = \{(0, 1/2), (1/2, 0)\}$. The site-symmetry groups are $G_{1a} = 4mm$, $G_{1b} = 4mm$, $G_{2c} = 2mm$. In all cases, the rotations of the site-symmetry groups are enough to pin $\mathbf{x}_\alpha = 0$.

where we used $\Gamma[g]h(0)\Gamma^\dagger[g] = h(0)$ and $\Gamma[g]u_0 = u_0$ because $\Gamma[g]$ is a permutation matrix and u_0 is the uniform eigenvector. Thus if two orbitals are related by a symmetry g , their \mathbf{x}_α that guarantee the minimal metric are also related by g . With Eq. (E31), we can prove that $\mathbf{x}_\alpha = 0$ if the site symmetry group G_x of the Wyckoff position x contains a symmetry h such that $h\mathbf{v} \neq \mathbf{v}$ for all $\mathbf{v} \neq 0$ and $\Gamma[h] = \mathbb{1}$. As an example, h can be any nontrivial rotation at a maximal Wyckoff position. In this case

$$h\mathbf{x}_\alpha = \sum_{\beta} \Gamma_{\alpha\beta}[h]\mathbf{x}_\beta = \mathbf{x}_\alpha, \quad (\text{E32})$$

but by assumption, the only solution to $h\mathbf{x}_\alpha = \mathbf{x}_\alpha$ is $\mathbf{x}_\alpha = 0$. We give two examples in space group $p4mm$ (see Fig. 5). (1) Consider an s (or p) orbital at the $2c = \{\frac{1}{2}\hat{x}, \frac{1}{2}\hat{y}\}$ position. The site symmetry group is $G_{2c} = 2mm$ consisting of C_2 reflection and mirrors. The s orbitals transform in a 1D irrep, so $\Gamma[C_2] = 1$. Thus $-\mathbf{x}_\alpha = C_2\mathbf{x}_\alpha = \mathbf{x}_\alpha$, so $\mathbf{x}_\alpha = 0$. (2) Consider p_x, p_y orbitals at the $1b = \frac{1}{2}\hat{x} + \frac{1}{2}\hat{y}$ position. The representation of C_4 is $D[C_4] = i\sigma_2$ (the p_x, p_y orbitals are rotated into each other), so $\Gamma[C_4] = \sigma_1$. Then $\Gamma[C_2] = 1$ and $-\mathbf{x}_\alpha = C_2\mathbf{x}_\alpha = \mathbf{x}_\alpha$ as before. We remark that if the orbitals are not at a maximal Wyckoff position (such as the 6j position in App. F), the symmetries allow \mathbf{x}_α to be nonzero.

4. Space Group Symmetry and Representations of the Boson Bands

Because $h(\mathbf{p})$ is a single-particle Hamiltonian, its bands can display nontrivial topology. In fact, we will show that topological quantum chemistry can be applied to $h(\mathbf{p})$ to prove a number of nontrivial statements about the possible band decompositions and symmetry representations. To bring this formalism to bear, we must first work out the symmetries of $h(\mathbf{p})$. We denote the $N_L \times N_L$ representations of the symmetries of $h_{\alpha\beta}(\mathbf{p})$ by $\Gamma[g]$.

First we show that $h(\mathbf{p})$ has a bosonic time-reversal symmetry with representation $\Gamma[\mathcal{T}] = K$. We check

$$h_{\alpha\beta}^*(\mathbf{p}) = \frac{1}{\mathcal{N}} \sum_{\mathbf{k}} P_{\alpha\beta}^*(\mathbf{p} + \mathbf{k}) P_{\beta\alpha}^*(\mathbf{k}) = \frac{1}{\mathcal{N}} \sum_{\mathbf{k}} P_{\alpha\beta}(\mathbf{k}) P_{\beta\alpha}(\mathbf{p} + \mathbf{k}) = \frac{1}{\mathcal{N}} \sum_{\mathbf{k}} P_{\alpha\beta}(\mathbf{k} - \mathbf{p}) P_{\beta\alpha}(\mathbf{k}) = h_{\alpha\beta}(-\mathbf{p}). \quad (\text{E33})$$

We also need to check the embedding matrices. Using $P(\mathbf{k} + \mathbf{G}) = V[\mathbf{G}]P(\mathbf{k})V^\dagger[\mathbf{G}]$ where $V_{\alpha\beta}[\mathbf{G}] = \delta_{\alpha\beta}e^{-i\mathbf{r}_\alpha \cdot \mathbf{G}}$ is the embedding matrix and \mathbf{G} is a reciprocal lattice vector (see the Appendix of Ref. [19]), we compute

$$h_{\alpha\beta}(\mathbf{p} + \mathbf{G}) = \frac{1}{\mathcal{N}} \sum_{\mathbf{k}} P_{\alpha\beta}(\mathbf{p} + \mathbf{G} + \mathbf{k}) P_{\beta\alpha}(\mathbf{k}) = \frac{1}{\mathcal{N}} \sum_{\mathbf{k}} e^{-i\mathbf{G} \cdot \mathbf{r}_\alpha} P_{\alpha\beta}(\mathbf{p} + \mathbf{k}) e^{i\mathbf{G} \cdot \mathbf{r}_\beta} P_{\beta\alpha}(\mathbf{k}) = [V(\mathbf{G})h(\mathbf{p})V^\dagger(\mathbf{G})]_{\alpha\beta} \quad (\text{E34})$$

which is the same as the transformation of the electron Hamiltonian. The embedding matrix contains the location \mathbf{r}_α of the orbital basis in the lattice. Since the embedding matrix $V[\mathbf{G}]$ of $h(\mathbf{p})$ is the same as the initial electron Hamiltonian (see Eq. (A7)), we find that the orbitals of the effective boson tight-binding model are located at the same position as the electron orbitals. The representations of the orbitals, however, may be different.

To study the spatial symmetries, we recall that $D[g]P(\mathbf{k})D^\dagger[g] = P(g\mathbf{k})$ (see Eq. (A17)). In indices, we have

$$\begin{aligned} h_{\alpha\beta}(g\mathbf{p}) &= \frac{1}{\mathcal{N}} \sum_{\mathbf{k}} P_{\alpha\beta}(g\mathbf{p} + \mathbf{k}) P_{\beta\alpha}(\mathbf{k}) = \frac{1}{\mathcal{N}} \sum_{\mathbf{k}} P_{\alpha\beta}(g\mathbf{p} + g\mathbf{k}) P_{\beta\alpha}(g\mathbf{k}) \\ &= \frac{1}{\mathcal{N}} \sum_{\mathbf{k}, \kappa\kappa' \lambda\lambda'} D_{\alpha\kappa}[g] P_{\kappa\kappa'}(\mathbf{p} + \mathbf{k}) D_{\beta\kappa'}^*[g] D_{\beta\lambda}[g] P_{\lambda\lambda'}(\mathbf{k}) D_{\alpha\lambda'}^*[g] \\ &= \frac{1}{\mathcal{N}} \sum_{\mathbf{k}, \kappa\kappa' \lambda\lambda'} D_{\alpha\kappa}[g] D_{\alpha\lambda'}^*[g] P_{\kappa\kappa'}(\mathbf{p} + \mathbf{k}) P_{\lambda\lambda'}(\mathbf{k}) D_{\beta\kappa'}^*[g] D_{\beta\lambda}[g]. \end{aligned} \quad (\text{E35})$$

We now need the following fact which we prove momentarily: in every point group, there exists a choice of basis where

$$D_{\alpha\kappa}[g] D_{\alpha\lambda'}^*[g] = \delta_{\lambda\kappa} |D_{\alpha\lambda}[g]|^2, \quad g \in G. \quad (\text{E36})$$

To understand Eq. (E36), we see that each column of $D[g]$ can only have a single non-zero element. Because $D[g]$ is unitary, this element must be a complex phase. Thus Eq. (E36) is equivalent to the statement that $D[g]$ is a complex permutation matrix. This is trivially satisfied if there is a single orbital per unit cell. More generally, a group with this property, that there exists a basis where all irreps are complex permutation matrices, is called a monomial group. It was recently proven that all spinless point groups in 2D and 3D are monomial [85]. Because $D[g]$ are spinless representations of the point group (or little group) of the Γ point $\mathbf{p} = 0$, Eq. (E36) holds. Conveniently, all the representation matrices given on the Bilbao crystallographic server https://www.cryst.ehu.es/cgi-bin/cryst/programs/representations_point.pl?tipogruppo=spg are in the complex permutation matrix form so there is only one nonzero entry per row. However, recall that our convention in App. A 2 a is to take $D[\mathcal{T}]$ to act as the identity on the orbital index. It is now convenient to define

$$D_{\alpha\kappa}[g] D_{\alpha\lambda'}^*[g] = \delta_{\lambda\kappa} |D_{\alpha\lambda}[g]|^2 = \delta_{\lambda\kappa} |D_{\alpha\lambda}[g]| \equiv \delta_{\lambda\kappa} \Gamma_{\alpha\lambda}[g], \quad \Gamma_{\alpha\beta}[g] = |D_{\alpha\beta}[g]| \quad (\text{E37})$$

where $\Gamma[g]$, which are real permutation matrices, are the representations of $g \in G$ on $h(\mathbf{p})$. This follows from Eqs. (E35) and (E37):

$$\begin{aligned} h_{\alpha\beta}(g\mathbf{p}) &= \frac{1}{\mathcal{N}} \sum_{\mathbf{k}, \lambda\lambda'} D_{\alpha\lambda}[g] D_{\alpha\lambda'}^*[g] P_{\lambda\lambda'}(\mathbf{p} + \mathbf{k}) P_{\lambda'\lambda}(\mathbf{k}) D_{\beta\lambda'}^*[g] D_{\beta\lambda}[g] \\ &= \frac{1}{\mathcal{N}} \sum_{\mathbf{k}, \lambda\lambda'} \Gamma_{\alpha\lambda}[g] P_{\lambda\lambda'}(\mathbf{p} + \mathbf{k}) P_{\lambda'\lambda}(\mathbf{k}) \Gamma_{\beta\lambda'}[g] \\ &= [\Gamma[g] h(\mathbf{p}) \Gamma^\dagger[g]]_{\alpha\beta}. \end{aligned} \quad (\text{E38})$$

In this way, we have shown that $h(\mathbf{p})$ possess all the space group symmetries of the electron Hamiltonian, but in a “bosonized” form. Because $\Gamma[g]$ are all real permutation matrices, we can think of the boson orbitals as those obtained from replacing all electron orbitals with s orbitals. We emphasize that this result holds on the UPC lattices we have constructed, where the orbitals form an irrep of a single Wyckoff position (App. A 2).

Because $\Gamma[g]$ is real, it is obvious that $\Gamma[\mathcal{T}]$ commutes with all spatial operators, so the topology of the Cooper pair bound states is classified by time-reversal symmetric space groups with $\Gamma[\mathcal{T}]^2 = +1$. There is an additional constraint on the spectrum: we proved that $u_0^\alpha(\mathbf{p} = 0) = 1/\sqrt{N_L}$. But $\Gamma[g]$ is a permutation matrix, so $\Gamma[g]u_0(\mathbf{p} = 0) = u_0(\mathbf{p} = 0)$ and hence the irrep of the $\epsilon_0(\mathbf{p})$ band at $\mathbf{p} = 0$ is always the trivial irrep. We now show that in the higher Cooper pair bands and at nonzero momenta, the Cooper pair wavefunction can (and will) exhibit other pairing symmetries.

Using the representation matrices $\Gamma[g]$, we can compute the action of g on the many-body Cooper pair creation operators. From Eq. (D44), we first derive

$$\begin{aligned} g\eta_{\mathbf{p},\mu}^\dagger g^\dagger &= \frac{1}{\sqrt{\mathcal{N}}} \sum_{\mathbf{k}\alpha\alpha'} \frac{u_\mu^\alpha(\mathbf{p})}{\sqrt{\epsilon_\mu(\mathbf{p})}} \bar{c}_{g\mathbf{p}+g\mathbf{k},\alpha',\uparrow}^\dagger D_{\alpha'\alpha}^\dagger[g] \bar{c}_{-g\mathbf{k},\alpha'',\downarrow}^\dagger D_{\alpha''\alpha}^\downarrow[g] \\ &= \frac{1}{\sqrt{\mathcal{N}}} \sum_{\mathbf{k}\alpha\alpha'} \frac{1}{\sqrt{\epsilon_\mu(\mathbf{p})}} \bar{c}_{g\mathbf{p}+\mathbf{k},\alpha',\uparrow}^\dagger D_{\alpha'\alpha}[g] D_{\alpha''\alpha}^*[g] u_\mu^\alpha(\mathbf{p}) \bar{c}_{-\mathbf{k},\alpha'',\downarrow}^\dagger \\ &= \frac{1}{\sqrt{\mathcal{N}}} \sum_{\mathbf{k}\alpha\alpha'} \frac{1}{\sqrt{\epsilon_\mu(g\mathbf{p})}} \bar{c}_{g\mathbf{p}+\mathbf{k},\alpha',\uparrow}^\dagger \delta_{\alpha'\alpha''} \Gamma_{\alpha'\alpha}[g] u_\mu^\alpha(\mathbf{p}) \bar{c}_{-\mathbf{k},\alpha'',\downarrow}^\dagger \end{aligned} \quad (\text{E39})$$

where we used that $D[g] = D^\dagger[g] = D^\downarrow[g]^*$ by \mathcal{T} and S_z . Now we use the space group symmetries of $h(\mathbf{p})$ such that $\epsilon_\mu(g\mathbf{p}) = \epsilon_\mu(\mathbf{p})$ and $\sum_\alpha \Gamma_{\alpha'\alpha}[g] u_\mu^\alpha(\mathbf{p}) = \sum_{\mu'} u_{\mu'}^{\alpha'}(g\mathbf{p}) B_{\mu'\mu}^g(\mathbf{p})$ where $[B^g(\mathbf{p})]_{\mu'\mu} = u_{\mu'}^\dagger(g\mathbf{p}) \Gamma[g] u_\mu(\mathbf{p})$ is the sewing

matrix of the bands [25]. If $\epsilon_\mu(\mathbf{p}) \neq \epsilon_{\mu'}(\mathbf{p})$, then $B_{\mu'\mu}^g(\mathbf{p}) = 0$ and thus

$$g\eta_{\mathbf{p},\mu}^\dagger g^\dagger = \frac{1}{\sqrt{\mathcal{N}}} \sum_{\mathbf{k}\alpha\mu'} \frac{u_{\mu'}^\alpha(g\mathbf{p})}{\sqrt{\epsilon_\mu(g\mathbf{p})}} B_{\mu'\mu}^g(\mathbf{p}) \bar{c}_{g\mathbf{p}+\mathbf{k},\alpha,\uparrow}^\dagger \bar{c}_{-\mathbf{k},\alpha,\downarrow}^\dagger = \sum_{\mu'} \eta_{g\mathbf{p},\mu'}^\dagger B_{\mu'\mu}^g(\mathbf{p}) . \quad (\text{E40})$$

At the high symmetry points, $B_g(\mathbf{p})$ is the representation matrix of the bands of $h(\mathbf{p})$, and hence is determined by the irreps of the Cooper pair bands. Hence, the symmetry and topology of the single-particle boson Hamiltonian $h(\mathbf{p})$ is detectable through $B_g(\mathbf{p})$ in the many-body states. We emphasize that although the bound states Cooper pairs are always spin-singlets, they can have nontrivial symmetry representations (p -wave, d -wave, etc) due to their multi-orbital nature. This is perhaps unfamiliar because *with only spin indices*, a Cooper pair wavefunction which is odd under $\mathbf{p} \rightarrow -\mathbf{p}$ must be a spin triplet because the spin indices are anti-symmetrized, for example. In contrast, we have shown here that the low-energy Cooper pair bound states, which are spin-singlets, can have be odd under $\mathbf{p} \rightarrow -\mathbf{p}$ since their orbital indices are anti-symmetrized even though their spin indices are symmetric.

5. Topology of the Boson Bands

Let us review the constraints placed on the bands of $h(\mathbf{p})$. First, we chose the electron orbitals to be irreps of a single Wyckoff position in order to guarantee the UPC (App. A 2), and we showed that the orbitals of the boson Hamiltonian $h(\mathbf{p})$ are at the same Wyckoff position determined by $V[\mathbf{G}]$ in Eq. (E34). (Note that in the bipartite crystalline lattice construction, the Wyckoff position of the boson Hamiltonian is that of the (larger) L sublattice.) However, the electron orbitals transform in the representation $D[g]$ whereas the boson orbitals transform in the representation $\Gamma[g]$ (Eq. (E38)). Since $\Gamma_{\alpha\beta}[g] = |D_{\alpha\beta}[g]|$, the orbitals of $h(\mathbf{p})$ are effectively s orbitals. $h(\mathbf{p})$ also possesses spinless time-reversal (see Eq. (E33)). Lastly, we proved that the lowest energy state at the gamma point $\mathbf{p} = 0$ is always the trivial (s) irrep.

We now use Topological Quantum Chemistry [26] to determine the momentum space irreps which are induced from the boson orbitals satisfying the constraints in the previous paragraph. Because the symmetry of the Cooper pair wavefunction at a given \mathbf{p} is determined by the induced momentum space irreps, we can completely classify the possible pairing symmetries and Cooper pair band connectivities in every space group.

First we make the momentum space irreps explicit. Consider a high symmetry momentum \mathbf{p} satisfying $g\mathbf{p} = \mathbf{p} + \mathbf{G}$ where \mathbf{G} is a reciprocal lattice vector. Then $h(\mathbf{p})$ commutes with $V^\dagger[\mathbf{G}]\Gamma[g]$ and the Cooper pair wavefunctions at \mathbf{p} transform in an irrep of the little group operators $V^\dagger[\mathbf{G}]\Gamma[g]$ (see the Appendix of Ref. [19]). By computing the irreps $V^\dagger[\mathbf{G}]\Gamma[g]$ for a given model, one can determine the possible pairing symmetries. The Bilbao Crystallographic server has tabulated all such irreps for every Wyckoff position and space group. For instance, in the kagome model in App. D 4c (see Fig. 6), we computed the irreps at the gamma point to be Γ_1 (a s -wave 1D irrep) and Γ_5 (a 2D d -wave irrep, angular momentum ± 2). This is because the little group of the gamma point contains the operator $\Gamma[C_6]$ which is a 3×3 permutation matrix with eigenvalues $1, e^{\pm \frac{2\pi i}{3}}$. From the Bilbao Crystallographic server, we observe that the K point has irreps K_1 (s -wave) and K_3 (d -wave), and the M point has irreps M_1 (s -wave) and $M_3 \oplus M_4$ (p -wave). Note that the s -wave irrep at Γ is at zero energy, so physically this is the mode that condenses, leading to the eta-pairing groundstates over zero momentum and zero angular momentum. However at higher temperature, the higher energy branch is also populated.

The global structure of the Cooper pair bands in momentum space is also determined by topological quantum chemistry. In general, a set of bands in momentum space can only be gapped if the irreps obey a set of compatibility relations [80]. To apply these compatibility relations to the Cooper pair bands, we recall that the Cooper pair orbitals are induced from a single Wyckoff position, the Cooper bands form an elementary band representation (EBR). If the Wyckoff position is non-maximal, then in general the Cooper pair bands will be trivially decomposable: they can be separated into gapped atomic bands. If the Wyckoff position is maximal (like the $3c$ kagome position in $G = p6mm$), then there are two possibilities: the EBR could be indecomposable meaning that all Cooper pair bands are connected, or the EBR could be decomposable. If the EBR is decomposable, it can be split into disconnected groups of bands, and necessarily at least one band in this decomposition is topological [87, 88]. The Bilbao crystallographic server tabulates these properties for all EBRs, and explicitly writes the possible irreps of the split EBR. Finally, there is an additional constraint due to time-reversal symmetry which prevents stable topological bands [49] in one, two, and three dimensions. Thus if a branch of a split EBR has a nonzero symmetry indicator (which would diagnose stable topology if the band were gapped everywhere), there must be a Weyl node in the spectrum which prevents the bands from being gapped everywhere [26, 92, 93]. However, the Cooper pair bands can be gapped with nontrivial topology if the split EBR has a decomposition into fragile topological bands.

Using the Bilbao Crystallographic server, we exhaustively tabulate every EBR in the 230 space groups which is decomposable and obeys the constraints in the first paragraph of App. E 5 (notably, that there are s orbitals on the

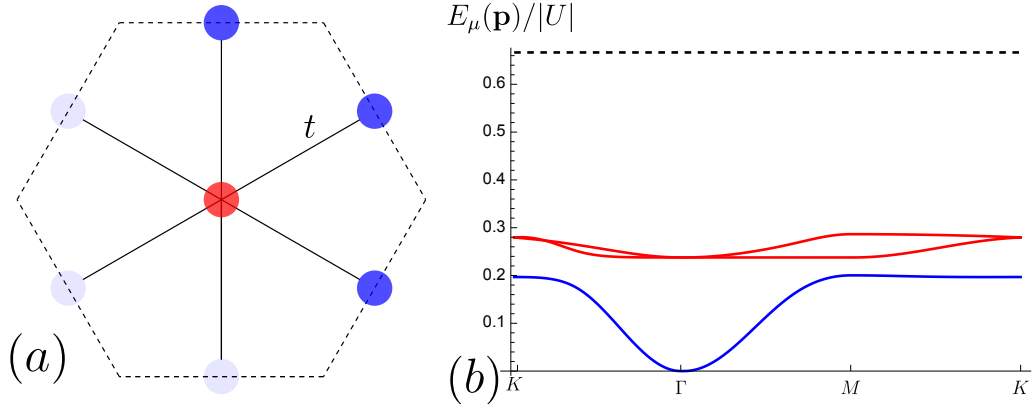


FIG. 6. Cooper pair band structure of the Hamiltonian Eq. (D63) on the kagome sites. ((a)) in App. D 4 c. (b) The band representation computed in App. D 4 c is $\mathcal{B}_1 = \Gamma_1 + K_1 + M_1$ for the low-energy blue band, and $\mathcal{B}_2 = \Gamma_5 + K_3 + M_3 \oplus M_4$ for the higher energy pair of red bands.

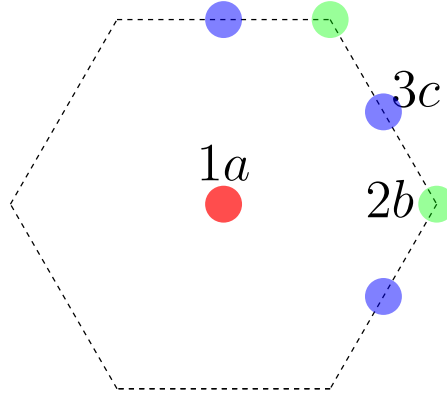


FIG. 7. We show the maximal Wyckoff positions in $p6$ and $p6mm$. The $1a$ position forms a triangular lattice, the $2b$ position forms a hexagonal lattice, and the $3c$ position forms a kagome lattice. The site symmetry groups of the positions are $G_{1a} = 6, G_{2b} = 3, G_{3c} = 2$.

Wyckoff position). We leave a complete study of the magnetic space groups to other work.

To illustrate the method, we first consider the 2D wallpaper groups with spinless time-reversal symmetry. Almost every Wyckoff position is indecomposable, meaning that the bands are all connected through high symmetry points in the BZ. Of the 17 spinless wallpaper groups, only $p61'$ and $p6mm1'$ have decomposable bands induced from the trivial irrep at a maximal Wyckoff position. In both cases, this Wyckoff position is the $3c$ position (see Fig. 7) which has site symmetry group $G_{3c} = 2 = \{1, C_2\}$. Putting s or p electron orbitals at the $3c$ position yields the Cooper pair representations $\Gamma[C_2] = \mathbb{1}$ and $\Gamma[C_6] = P_3$ where P_3 is the permutation matrix exchanging the 3 sites. This is the representation of an s -orbital at the $3c$ position, denoted $A_{3c} \uparrow G$. From the Bilbao crystallographic server we find that in $G = p61'$ (the $1'$ denotes time-reversal), there are two possible band decompositions

$$\begin{aligned} A_{3c} \uparrow p61' &= \Gamma_1 \oplus \Gamma_3 \Gamma_5 + K_1 \oplus K_2 K_3 + M_1 \oplus M_2 \oplus M_2 \\ &= \begin{cases} (\Gamma_1 + K_1 + M_1) + (\Gamma_3 \Gamma_5 + K_2 K_3 + 2M_2) \\ (\Gamma_1 + K_1 + M_2) + (\Gamma_3 \Gamma_5 + K_2 K_3 + M_1 \oplus M_2) \end{cases} \end{aligned} \quad (\text{E41})$$

where the parentheses denote which bands are connected. Both decompositions contain a single band with a Γ_1 irrep (the trivial) irreps, which is the quadratic band at low energy. The two higher bands are connected and gapped from the low energy band. The momentum space irreps are defined

$$\begin{array}{c|cc} 61' & 1 & C_6 \\ \hline \Gamma_1 & 1 & 1 \\ \Gamma_3 \Gamma_5 & 2 & -1 \end{array}, \quad \begin{array}{c|cc} 3 & 1 & C_3 \\ \hline K_1 & 1 & 1 \\ K_2 K_3 & 2 & -1 \end{array}, \quad \begin{array}{c|cc} m & 1 & M_x \\ \hline M_1 & 1 & 1 \\ M_2 & 1 & -1 \end{array}. \quad (\text{E42})$$

We now consider the topology of the two branches in Eq. (E41). We observe that the $\Gamma_1 + K_1 + M_1$ band is $A_{1a} \uparrow p61'$ and hence is a trivial atomic band. Its complement $\Gamma_3\Gamma_5 + K_2K_3 + 2M_2 = A_{3c} \uparrow G \ominus A_{1a} \uparrow G$ is fragile topological. This is an instance of the general result that gapping band induced from a maximal Wyckoff position must result in topology [87, 88]: since the lower band is trivial, the higher two bands must be topological. The other allowed decomposition has a $\Gamma_1 + K_1 + M_2$ band. Using the Smith normal form [82], we compute the symmetry indicator $\theta = m(\Gamma_2) + m(M_2) \bmod 2$, which is the number of odd inversion eigenvalues mod 2. We observe that $\theta = 1$ for $\Gamma_1 + K_1 + M_2$, indicating it must have Weyl nodes connecting it to the other bands.

We systematize this information in the following table. W.P. stands for the Wyckoff position of the orbitals. The η irreps column denotes the orbital of $h(\mathbf{p})$ of the site symmetry group of the Wyckoff position (physically it is always an s orbital, but is denoted with different symbols in different space groups), and e^- irrep denotes the possible electron orbitals that yield the bosonic orbital through $\Gamma[g] = |D_{\alpha\beta}[g]|$. # numbers the possible decompositions and θ is the symmetry indicator, which results in Weyl nodes due to $\Gamma[\mathcal{T}]$. Our classification enumerates the topology of the Cooper pair bands (the first entry corresponds to the gapless quadratic band). When the band is trivial, its atomic representation is given. Otherwise fragile topology or topologically protected Weyl nodes are indicated.

G	name	W.P.	η^\dagger irreps (e^- irreps)	#	θ	Classification
16	$p6$				$\theta = m(\Gamma_2) + m(M_2) \bmod 2 \in \mathbb{Z}_2$	
		3c	$A (A, B)$	1	0, 0	$A_{1a} \uparrow G$, fragile
		3c	$A (A, B)$	2	1, 1	Weyl, Weyl
17	$p6mm$				none	
		3c	$A_1 (A_1, A_2, B_1, B_2)$	1		$A_{1a} \uparrow G$, fragile

We see that in 2D, the only cases with decomposable bands at maximal Wyckoff positions are in $p6$ and $p6mm$. In all other groups and maximal Wyckoff positions, the Cooper pair bands are connected. In the decomposable cases listed above, only the higher energy bands can be fragile topological.

Performing an exhaustive search 3D, we find 22 space groups containing decomposable bands with a trivial irrep at the Γ point. In the case where the symmetry indicator is zero, we check whether the band is fragile or atomic. They are enumerated in the following table. There are many cases where the low-lying Cooper pair band has topologically protected Weyl nodes. We also highlight $G = Fd\bar{3}c$, space group 228, where the only allowed decomposition is into fragile bands.

G	name	W.P.	η irreps (e^- irreps)	#	θ	Classification
147	$P\bar{3}$				$(\mathbb{Z}_2, \mathbb{Z}_4)$	
		3e	$A_g (A_g, A_u)$	1	(0, 0), (0, 0)	$A_g^{1a} \uparrow G$, fragile
				2	(0, 1), (0, 3)	Weyl, Weyl
				3	(1, 3), (1, 1)	Weyl, Weyl
				4	(1, 0), (1, 0)	Weyl, Weyl
		3f	$A_g (A_g, A_u)$	1	(0, 3), (0, 1)	Weyl, Weyl
				2	(0, 0), (0, 0)	$A_g^{1b} \uparrow G$, fragile
				3	(1, 2), (1, 2)	Weyl, Weyl
				4	(1, 3), (1, 1)	Weyl, Weyl
148	$R\bar{3}$				$(\mathbb{Z}_2, \mathbb{Z}_4)$	
		9d	$A_g (A_g, A_u)$	1	(1, 3), (1, 1)	Weyl, Weyl
				2	(0, 0), (0, 0)	$A_g^{3b} \uparrow G$, fragile
				3	(1, 2), (1, 2)	Weyl, Weyl
				4	(0, 3), (0, 3)	Weyl, Weyl
		9e	$A_g (A_g, A_u)$	1	(0, 0), (0, 0)	$A_g^{3a} \uparrow G$, fragile
				2	(1, 1), (1, 3)	Weyl, Weyl
				3	(1, 3), (1, 1)	Weyl, Weyl
				4	(1, 0), (1, 0)	Weyl, Weyl
162	$P\bar{3}1m$				\mathbb{Z}_2	
		3f	$A_g (A_g, A_u, B_g, B_u)$	1	0	$A_{1g}^{1a} \uparrow G$, fragile
		3g	$A_g (A_g, A_u, B_g, B_u)$	1	0	$A_{1g}^{1b} \uparrow G$, fragile

163	$P\bar{3}1c$				\mathbb{Z}_2	
		6g	$A_g (A_g, A_u)$	1 2 3 4	1, 1 0, 0 1, 1 0, 0	Weyl, Weyl fragile, fragile Weyl, Weyl $A_g^{2b} \uparrow G$, fragile
164	$P\bar{3}m1$				\mathbb{Z}_2	
		3e	$A_g (A_g, A_u, B_g, B_u)$	1	0, 0	$A_{1g}^{1a} \uparrow G$, fragile
		3f	$A_g (A_g, A_u, B_g, B_u)$	1	0, 0	$A_{1g}^{1b} \uparrow G$, fragile
165	$P\bar{3}c1$				\mathbb{Z}_2	
		6e	$A_g (A_g, A_u)$	1 2	1, 1 0, 0	Weyl, Weyl $A_g^{2b} \uparrow G$, fragile
166	$R\bar{3}m$				\mathbb{Z}_2	
		9d	$A_g (A_g, A_u, B_g, B_u)$	1	0, 0	$A_{1g}^{3b} \uparrow G$, fragile
		9e	$A_g (A_g, A_u, B_g, B_u)$	1	0, 0	$A_{1g}^{3a} \uparrow G$, fragile
167	$R\bar{3}c$				\mathbb{Z}_2	
		18d	$A_g (A_g, A_u)$	1 2	1, 1 0, 0	Weyl, Weyl $A_g^{6b} \uparrow G$, fragile
168	$P6$				\mathbb{Z}_2	
		3c	$A (A, B)$	1 2	0, 0 1, 1	$A^{1a} \uparrow G$, fragile Weyl, Weyl
175	$P6/m$				$(\mathbb{Z}_2, \mathbb{Z}_2, \mathbb{Z}_2)$	
		3f	$A_g (A_g, A_u, B_g, B_u)$	1 2	(0, 0, 0), (0, 0, 0) (0, 1, 1), (0, 1, 1)	$A_g^{1a} \uparrow G$, fragile Weyl, Weyl
		3g	$A_g (A_g, A_u, B_g, B_u)$	1 2	(0, 0, 0), (0, 0, 0) (0, 1, 1), (0, 1, 1)	$A_g^{1b} \uparrow G$, fragile Weyl, Weyl
176	$P6_3/m$				\mathbb{Z}_2	
		6g	$A_g (A_g, A_u)$	1 1	1, 1 0, 0	Weyl, Weyl $A_g^{2b} \uparrow G$, fragile
177	$P622$				none	
		3f	$A_1 (A_1, B_1, B_2, B_3)$	1		$A_1^{1a} \uparrow G$, fragile
		3g	$A_1 (A_1, B_1, B_2, B_3)$	1		$A_1^{1b} \uparrow G$, fragile
183	$P6mm$				none	
		3c	$A_1 (A_1, A_2, B_1, B_2)$	1		$A_1^{1a} \uparrow G$, fragile
184	$P6cc$				\mathbb{Z}_2	
		3c	$A (A, B)$	1 2	0, 0 1, 1	$A_1^{2a} \uparrow G$, fragile Weyl, Weyl
191	$P6/mmm$				none	
		3f	$A_g (A_g, A_u, B_{1g}, B_{1u}, B_{2g}, B_{2u})$	1		$A_{1g}^{1a} \uparrow G$, fragile
		3g	$A_g (A_g, A_u, B_{1g}, B_{1u}, B_{2g}, B_{2u})$	1		$A_{1g}^{1b} \uparrow G$, fragile
192	$P6/mcc$				\mathbb{Z}_2	
		6f	$A_1 (A_1, B_1, B_2, B_3)$	1	0, 0	$A_1^{2a} \uparrow G$, fragile
		6g	$A_g (A_g, A_u, B_g, B_u)$	1 2	0, 0 1, 1	$A_1^{2a} \uparrow G$, fragile Weyl, Weyl
193	$P6_3/mcm$				none	
		6f	$A_g (A_g, A_u, B_g, B_u)$	1		$A_{1g}^{2b} \uparrow G$, fragile
194	$P6_3/mmc$				none	
		6g	$A_g (A_g, A_u, B_g, B_u)$	1		$A_{1g}^{2a} \uparrow G$, fragile

202	$Fm\bar{3}$				none	
		24d	$A_g (A_g, A_u)$	1 2		$A_g^{4a} \uparrow G$, fragile $A_g^{4b} \uparrow G$, fragile
209	$F432$				none	
		24d	$A_1 (A_1, B_1)$	1 2		$A_1^{4a} \uparrow G$, fragile, $T_2^{4b} \uparrow G$ $A_1^{4b} \uparrow G$, fragile, $T_2^{4a} \uparrow G$
225	$Fm\bar{3}m$				none	
		24d	$A_g (A_g, A_u, B_{1g}, B_{1u})$	1 2		$A_{1g}^{4a} \uparrow G$, fragile $A_{1g}^{4b} \uparrow G$, fragile
228	$Fd\bar{3}c$				none	
		48d	$A (A, B)$	1		fragile, fragile

We use the explicit formulae in Ref. [114] for the symmetry indicators [84, 90, 91] in the above groups using the Smith normal form[82]. The results are below. The notation is the same as on the Bilbao Crystallographic Server.

G	name	Symmetry Indicator θ
147	$P\bar{3}$	$(\mathbb{Z}_2, \mathbb{Z}_4)$
		$m(M_1^+) + m(\Gamma_1^+) \pmod{2}$
		$m(A_1^+) - 2m(A_2^+ A_3^+) - m(L_1^+) + m(M_1^+) - m(\Gamma_1^+) + 2m(\Gamma_2^+ \Gamma_3^+) \pmod{4}$
148	$R\bar{3}$	$(\mathbb{Z}_2, \mathbb{Z}_4)$
		$m(T_1^+) + m(L_1^+) \pmod{2}$
		$m(F_1^+) - m(L_1^+) + m(T_1^+) + 2m(T_2^+ T_3^+) - m(\Gamma_1^+) + 2m(\Gamma_2^+ \Gamma_3^+) \pmod{4}$
162	$P\bar{3}1m$	\mathbb{Z}_2
		$m(A_1^-) + m(A_3^-) + m(\Gamma_1^-) + m(\Gamma_3^-) + m(L_2^+) + m(M_2^+) \pmod{2}$
163	$P\bar{3}1c$	\mathbb{Z}_2
		$m(A_3) + m(\Gamma_1^-) + m(\Gamma_3^+) + m(M_2^+) \pmod{2}$
164	$P\bar{3}m1$	\mathbb{Z}_2
		$m(A_1^-) + m(A_3^-) + m(\Gamma_1^-) + m(\Gamma_3^+) + m(L_2^+) + m(M_2^+) \pmod{2}$
165	$P\bar{3}c1$	\mathbb{Z}_2
		$m(A_3) + m(\Gamma_1^-) + m(\Gamma_3^+) + m(M_2^+) \pmod{2}$
166	$R\bar{3}m$	\mathbb{Z}_2
		$m(F_2^+) + m(L_2^+) + m(T_1^-) + m(T_3^+) + m(\Gamma_1^-) + m(\Gamma_3^+) \pmod{2}$
167	$R\bar{3}c$	\mathbb{Z}_2
		$m(F_2^+) + m(\Gamma_2^+) + m(\Gamma_3^-) \pmod{2}$
168	$P6$	\mathbb{Z}_2
		$m(A_1) + m(M_1) \pmod{2}$
175	$P6/m$	$(\mathbb{Z}_2, \mathbb{Z}_2, \mathbb{Z}_2)$
		$m(A_1^+) + m(A_1^-) + m(\Gamma_1^+) + m(M_1^-) \pmod{2}$
		$m(A_1^+) + m(A_1^-) + m(M_1^+) + m(M_1^-) \pmod{2}$
		$m(A_1^+) + m(A_1^-) + m(A_2^+) + m(\Gamma_1^+) + m(L_2^+) + m(M_1^-) \pmod{2}$
176	$P6_3/m$	\mathbb{Z}_2
		$m(M_1^+) + m(\Gamma_1^+) \pmod{2}$
177	$P622$	none
183	$P6mm$	none
184	$P6cc$	\mathbb{Z}_2
		$m(A_3 A_4) + m(M_3) \pmod{2}$
191	$P6/mmm$	none
192	$P6/mcc$	\mathbb{Z}_2

		$m(A_5) + m(\Gamma_1^-) + m(\Gamma_3^+) + m(\Gamma_5^-) + m(\Gamma_6^-) + m(M_2^+) + m(M_3^+) \bmod 2$
193	$P6_3/mcm$	none
194	$P6_3/mmc$	none
202	$Fm\bar{3}$	none
209	$F432$	none
225	$Fm\bar{3}m$	none
228	$Fd\bar{3}c$	none

Appendix F: Ten Band Model for Twisted Bilayer Graphene

In this section, we put forward a variation of the ten band model discussed in Ref. 37. Our ten band model captures the flat band irreps of twisted bilayer graphene via an S -matrix construction consisting of 6 orbitals in the L sublattice and 4 orbitals in the \tilde{L} sublattice, yielding two flat bands. However, we compute the Wilson loop[36, 115] of the flat bands in our model and find it has winding number 2, instead of winding number 1 as in the Bistritzer-MacDonald Hamiltonian [36, 37, 39]. In contrast, the model of Ref. [37], however, in the larger lattice has orbitals at both the $1a$ and $3f$ positions, and thus does not satisfy uniform pairing because the orbitals at the different Wyckoff positions are not related by symmetry.

To remedy this issue we propose a modified S -matrix which instead has in the L lattice s orbitals in the $6j$ position, which are related by $C_{6z}\mathcal{T}$ and hence have uniform pairing. The \tilde{L} lattice possesses p_x, p_y orbitals at the $2c$ positions (the hexagon). In SSG 177.151, the irreps induced by the two sublattices read

$$E_{2c} \uparrow G = 2\Gamma_3 + (2K_1 \oplus K_2K_3) + (2M_1 \oplus 2M_2) \quad (F1)$$

$$A_{6j} \uparrow G = (\Gamma_1 \oplus \Gamma_2 \oplus 2\Gamma_3) + (2K_1 \oplus 2K_2K_3) + (3M_1 \oplus 3M_2) \quad (F2)$$

$$\mathcal{B}_{FB} = (\Gamma_1 \oplus \Gamma_2) + K_2K_3 + (M_1 \oplus M_2). \quad (F3)$$

The irreps of the flat band correctly match the irreps carried by the flat bands in twisted bilayer graphene, and thus these two bands must be topological. Note that as this is a lattice model, one cannot correctly implement the particle-hole symmetry that protects the strong topology in TBG [116]. The real-space Hamiltonian involves only NN hopping and NNN hopping between s and p orbitals, and there are only four complex independent parameters:

$$\begin{aligned} H_{\text{kin}}^{\nu,\sigma} = & \sum_{\mathbf{R}} t_{NN,x}^{\nu,\sigma} c_{\mathbf{R},1,\sigma,\nu}^\dagger d_{\mathbf{R},p_x,1,\sigma,\nu} + t_{NN,y}^{\nu,\sigma} c_{\mathbf{R},1,\sigma,\nu}^\dagger d_{\mathbf{R},p_y,1,\sigma,\nu} \\ & + t_{NNN,x}^{\nu,\sigma} c_{\mathbf{R},1,\sigma,\nu}^\dagger d_{\mathbf{R}-\mathbf{a}_2,p_x,2,\sigma,\nu} + t_{NNN,y}^{\nu,\sigma} c_{\mathbf{R},1,\sigma,\nu}^\dagger d_{\mathbf{R}-\mathbf{a}_2,p_y,2,\sigma,\nu} + (p6') + (H.c.) \end{aligned} \quad (F4)$$

where σ denotes the spin and ν denotes the valley, giving four identical copies of the kinetic Hamiltonian. Here the c orbitals belong to the L sublattice, and are labeled $\alpha = 1 \dots 6$, labeling each of the $6j$ positions, while the d orbitals belong to the \tilde{L} sublattice and are labeled $\beta = \{p_x, 1\}, \{p_y, 1\}, \{p_x, 2\}, \{p_y, 2\}$, labeling the $2c$ positions. In addition to the spin degree of freedom, the TBG model has a valley degree of freedom, ν , from the modes arising from the Dirac cones from the K and K' points in the BZ. $p6'$ indicates that the appropriate symmetry-related terms are added to yield the full tight-binding Hamiltonians. We find that the choice of parameters

$$\begin{aligned} t_{NN,x}^{\nu=+1,\sigma=\uparrow} &= 76.50 + 2.69i, t_{NN,y}^{\nu=+1,\sigma=\uparrow} = -14.64 + 35.81i, \\ t_{NNN,x}^{\nu=+1,\sigma=\uparrow} &= 12.17 - 7.44i, t_{NNN,y}^{\nu=+1,\sigma=\uparrow} = 5.47 - 5.45i \end{aligned} \quad (F5)$$

yields an excellent fit of the low-lying bands to the BM model, as depicted in Fig. 8(b). The lattice vectors are $\mathbf{a}_1 = (-\frac{\sqrt{3}}{2}, -\frac{1}{2})a_0$, $\mathbf{a}_2 = (\frac{\sqrt{3}}{2}, -\frac{1}{2})a_0$, where a_0 is the unit cell length.

The main difference between this ten-band model and previous models arises from the addition of the valley degree of freedom. The most natural Hubbard-type interaction would be one that includes all spin and valleys summed together in the density:

$$H = \frac{|U|}{2} \sum_{\mathbf{R},\alpha} \left(\sum_{\nu,\sigma} \bar{n}_{\mathbf{R},\alpha,\sigma,\nu} \right)^2. \quad (F6)$$

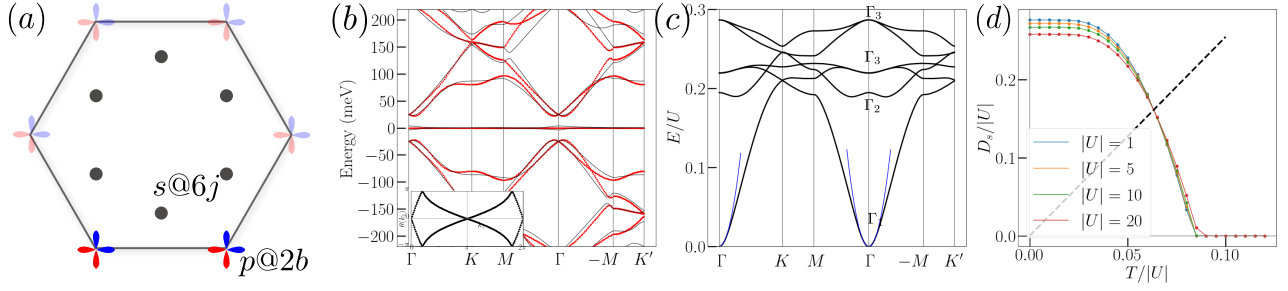


FIG. 8. We summarize the 10-band UPC model of TBG. (a) shows the electron orbitals of the model in the unit cell, (b) shows the single-particle bands with the Wilson loop over the flat bands inset, (c) shows the Cooper pair spectrum, and (d) shows the mean-field superfluid weight at finite temperature.

However, we find that this interaction is not tractable with our eta-pairing formalism. Instead, however, the slightly different interaction

$$H = \frac{|U|}{2} \sum_{\mathbf{R}, \alpha} (\bar{S}_{\mathbf{R}, \alpha, \nu\sigma=+1}^z)^2 + (\bar{S}_{\mathbf{R}, \alpha, \nu\sigma=-1}^z)^2, \quad (\text{F7})$$

where the spin-valley operators $\bar{S}_{\mathbf{R}, \alpha, \nu\sigma}^z$ are defined as

$$\bar{S}_{\mathbf{R}, \alpha, \nu\sigma=+1}^z = \bar{n}_{\mathbf{R}, \alpha, \nu=+1, \sigma=\uparrow} - \bar{n}_{\mathbf{R}, \alpha, \nu=-1, \sigma=\downarrow} \quad (\text{F8})$$

$$\bar{S}_{\mathbf{R}, \alpha, \nu\sigma=-1}^z = \bar{n}_{\mathbf{R}, \alpha, \nu=+1, \sigma=\downarrow} - \bar{n}_{\mathbf{R}, \alpha, \nu=-1, \sigma=\uparrow}, \quad (\text{F9})$$

can be recast into an eta-pairing problem. So long as $U(1)$ valley, $U(1)$ spin, and \mathcal{T} are preserved, there are two eta-pairing operators that commute with the interaction Hamiltonian

$$\eta_{+1}^\dagger = \sum_{\mathbf{k}, m} \gamma_{\mathbf{k}, m, \nu=+1, \sigma=\uparrow}^\dagger \gamma_{-\mathbf{k}, m, \nu=-1, \sigma=\downarrow}^\dagger \quad (\text{F10})$$

$$\eta_{-1}^\dagger = \sum_{\mathbf{k}, m} \gamma_{\mathbf{k}, m, \nu=+1, \sigma=\downarrow}^\dagger \gamma_{-\mathbf{k}, m, \nu=-1, \sigma=\uparrow}^\dagger. \quad (\text{F11})$$

This spin-valley-polarized model splits into two eta-pairing models, each giving the Cooper pair spectrum shown in Fig. 1(c). The two Hamiltonians are labeled by spin-valley, $\nu\sigma = +1$ and $\nu\sigma = -1$, and are

$$H^{\nu\sigma=+1} = \sum_{\sigma\nu=+1} H_{\text{kin}}^{\nu, \sigma} + \frac{|U|}{2} \sum_{\mathbf{R}, \alpha} (\bar{S}_{\mathbf{R}, \alpha, \nu\sigma=+1}^z)^2 \quad (\text{F12})$$

$$H^{\nu\sigma=-1} = \sum_{\sigma\nu=-1} H_{\text{kin}}^{\nu, \sigma} + \frac{|U|}{2} \sum_{\mathbf{R}, \alpha} (\bar{S}_{\mathbf{R}, \alpha, \nu\sigma=-1}^z)^2. \quad (\text{F13})$$

We now deduce the irreducible representations of the Cooper pair bands. Let us focus on the $\nu\sigma = +1$ sector. As argued and rigorously proved in App. E, the Cooper pairs themselves transform like s orbitals induced from the larger sublattice L , which in this case is the $6j$ position. We offer here an intuitive argument for why this must be so. Consider an *unprojected* Cooper pair operator at site \mathbf{R} and flavor α , in the larger sublattice L :

$$\eta_{\mathbf{R}, \alpha}^\dagger = c_{\mathbf{R}, \alpha, \uparrow}^\dagger c_{\mathbf{R}, \alpha, \downarrow}^\dagger. \quad (\text{F14})$$

Let us assume there is one orbital per position (at least in the larger sublattice L), so that the crystalline symmetry g is a permutation matrix up to a phase: the orbital α is located at position \mathbf{x}_α , and under g this is mapped to orbital β located at position $\mathbf{x}_\beta = g\mathbf{x}_\alpha$. Under a crystalline symmetry g , this operator transforms as

$$g\eta_{\mathbf{R}, \alpha}^\dagger g^{-1} = g c_{\mathbf{R}, \alpha, \uparrow}^\dagger c_{\mathbf{R}, \alpha, \downarrow}^\dagger g^{-1} \quad (\text{F15})$$

$$= \sum_{\beta, \beta'} D[g]_{\alpha\beta} D^*[g]_{\alpha\beta'} c_{g\mathbf{R}, \beta, \uparrow}^\dagger c_{g\mathbf{R}, \beta', \downarrow}^\dagger \quad (\text{F16})$$

$$= \eta_{g\mathbf{R}, \beta}^\dagger, \quad \mathbf{x}_\beta = g\mathbf{x}_\alpha. \quad (\text{F17})$$

	1	C_{3z}	C_{2x}
Γ_1	1	1	1
Γ_2	1	1	-1
Γ_3	2	-1	0

TABLE IV. Irreps of the group 32 which is the unitary subgroup of $6'22'$, the little group of the Gamma point in twisted bilayer graphene.

Any phases introduced in the permutation matrix D is canceled by the complex conjugate from the time-reversed D arising from the opposite spin. Thus, these η operators transform as s orbitals. When projecting into the flat bands, the orbitals belonging to the smaller sublattice \tilde{L} possess no wavefunction weight, and so those bands do not participate in the Cooper pair Hamiltonian, leaving s orbitals in the larger L sublattice.

In our TBG model, these irreps read

$$A_{6j} \uparrow G = (\Gamma_1 \oplus \Gamma_2 \oplus 2\Gamma_3) + (2K_1 \oplus 2K_2K_3) + (3M_1 \oplus 3M_2). \quad (\text{F18})$$

The $6j$ position is non-maximal, so the bands form a composite representation which can in principle be separated into gapped bands. The Γ_1 irrep is the zero-energy Cooper pair which has s -wave symmetry. The Γ_2 irrep is odd under C_{2x} and is of p_z orbital character. The Γ_3 irrep is formed from angular momentum ± 1 states under the C_{3z} operator, and so is of p_x, p_y orbital character (see Table F below).

Appendix G: Mean-field superfluid weight in degenerate flat bands

In this section, we derive the mean-field superfluid weight of a set of N_f degenerate isolated flat bands with uniform pairing. We take $e, \hbar, k_B = 1$. In this section only, we use bra-ket notation for the single-particle eigenstates since we are working at the mean-field level. Our calculation is straightforward generalization of the $N_f = 1$ case demonstrated in Ref. [61]. The result agrees with prior work (Ref. [17]) on degenerate flat bands, but correctly accounts for the minimal quantum metric in the self-consistent mean-field solution [61].

We describe our system with the attractive mean-field approximated Hubbard model

$$H = \sum_{\mathbf{k}} \mathbf{c}_{\mathbf{k}}^\dagger H_{\text{BdG}}(\mathbf{k}) \mathbf{c}_{\mathbf{k}} + \sum_{\mathbf{k}} \text{Tr} \tilde{h}^\dagger(\mathbf{k}) - N_{orb} \mathcal{N} \mu - \mathcal{N} \sum_{\alpha} \frac{|\Delta_{\alpha}|^2}{U}, \quad (\text{G1})$$

$$H_{\text{BdG}}(\mathbf{k}) = \begin{pmatrix} \tilde{h}^\dagger(\mathbf{k}) - \mu \mathbb{1}_{N_{orb}} & \Delta \\ \Delta^\dagger & -\tilde{h}^\dagger(\mathbf{k}) + \mu \mathbb{1}_{N_{orb}} \end{pmatrix}, \quad (\text{G2})$$

where μ is the chemical potential, \tilde{h}^σ is the single-particle hopping matrix for spin σ and $\mathbf{c}_{\mathbf{k}} = (c_{\mathbf{k}, \alpha=1, \uparrow}, \dots, c_{\mathbf{k}, \alpha=N_{orb}, \uparrow}, c_{-\mathbf{k}, \alpha=1, \downarrow}, \dots, c_{-\mathbf{k}, \alpha=N_{orb}, \downarrow})$. The matrix $\Delta = \text{diag}(\Delta_1, \dots, \Delta_{N_{orb}})$ contains the mean-field order parameters $\Delta_{\alpha} = \Delta_{i\alpha} = U \langle c_{\mathbf{R}\alpha\downarrow} c_{\mathbf{R}\alpha\uparrow} \rangle$, where $c_{\mathbf{R}\alpha\sigma}$ destroys a particle with spin σ at orbital α in the unit cell \mathbf{R} . We assume the order parameters are independent of the unit cell. Since we have shown in App. D that the lowest energy gap is s -wave, zero momentum, and has the wavefunction $\propto \sum_{\mathbf{R}, \alpha} \tilde{c}_{\mathbf{R}, \alpha, \uparrow}^\dagger \tilde{c}_{\mathbf{R}, \alpha, \downarrow}^\dagger$, we expect our mean-field ansatz to accurately capture this Cooper pair branch.

The superfluid weight for this Hamiltonian is given by [61] (where $\partial_i = \partial/\partial k_i$)

$$[D_s]_{ij} = \frac{1}{\mathcal{N} V_c} \sum_{\mathbf{k}, ab} \frac{n_F(E_a) - n_F(E_b)}{E_b - E_a} [\langle \psi_a | \partial_i \tilde{H}_{\mathbf{k}} | \psi_b \rangle \langle \psi_b | \partial_j \tilde{H}_{\mathbf{k}} | \psi_a \rangle - \langle \psi_a | (\partial_i \tilde{H}_{\mathbf{k}} \gamma^z + \delta_i \Delta) | \psi_b \rangle \langle \psi_b | (\partial_j \tilde{H}_{\mathbf{k}} \gamma^z + \delta_j \Delta) | \psi_a \rangle] - \frac{1}{V_c} C_{ij}, \quad (\text{G3})$$

and

$$\partial_i \tilde{H}_{\mathbf{k}} = \begin{pmatrix} \left. \frac{\partial \tilde{h}^\dagger(\mathbf{k}')}{\partial k'_i} \right|_{\mathbf{k}'=\mathbf{k}} & 0 \\ 0 & \left. \frac{\partial \tilde{h}^\dagger(\mathbf{k}')^*}{\partial k'_i} \right|_{\mathbf{k}'=-\mathbf{k}} \end{pmatrix}, \quad \delta_i \Delta = \begin{pmatrix} 0 & \left. \frac{d\Delta}{dq_i} \right|_{\mathbf{q}=0} \\ \left. \frac{d\Delta^\dagger}{dq_i} \right|_{\mathbf{q}=0} & 0 \end{pmatrix}, \quad C_{ij} = \frac{1}{U} \sum_{\alpha} \left. \frac{d\Delta_{\alpha}}{dq_i} \frac{d\Delta_{\alpha}^*}{dq_j} \right|_{\mathbf{q}=0} + \text{H.c.} \quad (\text{G4})$$

The vector \mathbf{q} in the derivatives $d\Delta_\alpha/dq_i$ corresponds to the insertion of an electromagnetic field with $\mathbf{A} \sim \mathbf{q}$, which changes the self-consistent order parameters as $\Delta_{i\alpha} \rightarrow \Delta_{i\alpha} e^{2i\mathbf{q} \cdot (\mathbf{R} + \mathbf{r}_\alpha)}$. The Fermi distribution is $n_F(E) = 1/(1 + e^{\beta E})$, where $\beta = 1/T$ is the inverse temperature. The eigenvalues and eigenvectors of H_{BdG} are E_a and $|\psi_a\rangle$ respectively, and $\gamma_z = \sigma_z \otimes \mathbb{1}_{N_{orb}}$, where σ_i are the Pauli matrices. The coefficient $[n_F(E_a) - n_F(E_b)]/(E_b - E_a)$ should be understood as $-\partial n_F(E)/\partial E$ when $E_a = E_b$. The total volume of the system is $\mathcal{N}V_c$ where V_c is the volume of a unit cell.

We will focus on the superfluid weight for a set of degenerate flat bands \mathcal{B} with energy $\epsilon_{\bar{m}}$ (\bar{m} denotes a flat band) in a system with time-reversal symmetry ($\tilde{h}^\dagger(\mathbf{k}) = [\tilde{h}^\dagger(-\mathbf{k})]^*$) and uniform pairing. Due to time-reversal symmetry, there always exists a choice of intra-unit-cell orbital positions which guarantees that the derivatives of the order parameters at $\mathbf{q} = \mathbf{0}$ vanish [61]. With the uniform pairing condition, these positions are given by Eq. (E28). Let us assume that this is the chosen set of positions, so that the superfluid weight of Eq. G3 simplifies to

$$[D_s]_{ij} = \frac{1}{V_c \mathcal{N}} \sum_{\mathbf{k}, ab} \frac{n_F(E_a) - n_F(E_b)}{E_b - E_a} [\langle \psi_a | \partial_i \tilde{H}_{\mathbf{k}} | \psi_b \rangle \langle \psi_b | \partial_j \tilde{H}_{\mathbf{k}} | \psi_a \rangle - \langle \psi_a | \partial_i \tilde{H}_{\mathbf{k}} \gamma^z | \psi_b \rangle \langle \psi_b | \partial_j \tilde{H}_{\mathbf{k}} \gamma^z | \psi_a \rangle], \quad (\text{G5})$$

This can be expressed in terms of the dispersion relations and Bloch functions of the bands by expressing the eigenvectors of H_{BdG} as $|\psi_a\rangle = \sum_{m=1}^{N_{orb}} (w_{+,am} |+\rangle \otimes |m_{\mathbf{k}}\rangle + w_{-,am} |-\rangle \otimes |m_{\mathbf{k}}\rangle)$, where $|m_{\mathbf{k}}\rangle$ is the eigenvector of $\tilde{h}^\dagger(\mathbf{k})$ with eigenvalue $\epsilon_{m,\mathbf{k}}$. We denote the eigenvectors of σ_z with eigenvalues ± 1 by $|\pm\rangle$. With these definitions, Eq. (G5) can be rewritten as

$$[D_s]_{ij} = \frac{1}{V_c \mathcal{N}} \sum_{\mathbf{k}} \sum_{mn} C_{pq}^{mn} [j_i(\mathbf{k})]_{mn} [j_j(\mathbf{k})]_{pq}, \quad (\text{G6})$$

$$C_{pq}^{mn} = 4 \sum_{ab} \frac{n_F(E_a) - n_F(E_b)}{E_b - E_a} w_{+,am}^* w_{+,bn} w_{-,bp}^* w_{-,aq}, \quad (\text{G7})$$

$$\begin{aligned} [j_i]_{mn} &= \langle m_{\sigma,\mathbf{k}} | \partial_i \tilde{h}^\sigma(\mathbf{k}) | n_{\sigma,\mathbf{k}} \rangle \\ &= \delta_{mn} \partial_i \epsilon_{m,\mathbf{k}} + (\epsilon_{m,\mathbf{k}} - \epsilon_{n,\mathbf{k}}) \langle \partial_i m_{\mathbf{k}} | n_{\mathbf{k}} \rangle. \end{aligned} \quad (\text{G8})$$

In a system with uniform pairing, we can make the ansatz $\Delta = \Delta \mathbb{1}$, and $H_{\text{BdG}} = \sum_{\mathbf{k}} \sum_{m=1}^{N_{orb}} [(\epsilon_m - \mu)^2 \sigma^z + \Delta^2 \sigma^x] \otimes |m\rangle \langle m|$, where the momentum dependence of $\epsilon_m(\mathbf{k})$ and $|m_{\mathbf{k}}\rangle$ is suppressed. The eigenvalues of H_{BdG} are then $\pm E_m = \pm \sqrt{(\epsilon_m - \mu)^2 + \Delta^2}$, and the corresponding eigenfunctions are $|\psi_m^+\rangle = (u_m |+\rangle + v_m |-\rangle) \otimes |m\rangle$ and $|\psi_m^-\rangle = (-v_m |+\rangle + u_m |-\rangle) \otimes |m\rangle$, where (again suppressing the momentum dependence)

$$u_m = \frac{1}{\sqrt{2}} \sqrt{1 + \frac{\epsilon_m - \mu}{E_m}}, \quad v_m = \frac{1}{\sqrt{2}} \sqrt{1 - \frac{\epsilon_m - \mu}{E_m}}. \quad (\text{G9})$$

As Eq. G8 shows, all contributions to the superfluid weight which involve $[j_i^\sigma]_{mn}$ with $m, n \in \mathcal{B}$ vanish (because $\epsilon_m(\mathbf{k}) = \epsilon_n(\mathbf{k}) = \epsilon_{\bar{m}}$ for the degenerate flat bands) vanish. Thus the superfluid weight reduces to the geometric contribution

$$\begin{aligned} [D_s]_{ij} &= \frac{2|\Delta|^2}{V_c \mathcal{N}} \sum_{\mathbf{k}} \sum_{m \in \mathcal{B}} \sum_{n \notin \mathcal{B}} \left[\frac{\tanh(\beta E_{\bar{m}}/2)}{E_{\bar{m}}} - \frac{\tanh(\beta E_n/2)}{E_n} \right] \frac{\epsilon_n - \epsilon_{\bar{m}}}{\epsilon_n + \epsilon_{\bar{m}} - 2\mu} (\langle \partial_i m | n \rangle \langle n | \partial_j m \rangle + \text{H.c.}) \\ &+ \frac{|\Delta|^2}{V_c \mathcal{N}} \sum_{\mathbf{k}} \sum_{\substack{m \neq n \\ m, n \notin \mathcal{B}}} \left[\frac{\tanh(\beta E_m/2)}{E_m} - \frac{\tanh(\beta E_n/2)}{E_n} \right] \frac{\epsilon_n - \epsilon_m}{\epsilon_n + \epsilon_m - 2\mu} (\langle \partial_i m | n \rangle \langle n | \partial_j m \rangle + \text{H.c.}). \end{aligned} \quad (\text{G10})$$

Let W_n be the band gap between the bands in \mathcal{B} and the n th band. We now assume that $W_n \gg |\epsilon_{\bar{m}} - \mu|$ and $W_n \gg |\Delta|$ for all $n \notin \mathcal{B}$, and the superfluid weight reduces to [117]

$$[D_s]_{ij} = \frac{4\Delta^2}{V_c} \frac{\tanh(\beta E_{\bar{m}}/2)}{E_{\bar{m}}} g_{ij}, \quad (\text{G11})$$

where $g_{ij} = (1/\mathcal{N}) \sum_{\mathbf{k}} \sum_{m \in \mathcal{B}} \sum_{n \notin \mathcal{B}} \text{Re} \langle \partial_i m | n \rangle \langle n | \partial_j m \rangle$ is the integral of the quantum metric of the set of bands \mathcal{B} . Since we assumed above that the derivatives of the order parameters are zero, this is in fact the minimal quantum metric [61].

At $T = 0$, the filling and the pairing gap are given by

$$N_f \mathcal{N} \nu = \sum_{\mathbf{k}} v^2 \text{Tr} P_{\mathbf{k}} = N_f \mathcal{N} v^2 \quad (\text{G12})$$

$$\Delta_\alpha = \Delta = \frac{|U|}{\mathcal{N}} \sum_{\mathbf{k}} uv [P_{\mathbf{k}}]_{\alpha\alpha} = \epsilon |U| \sqrt{\nu(1-\nu)}, \quad (\text{G13})$$

with $\epsilon = N_f/N_L$, where N_L is the number of orbitals where the flat band states have a nonzero weight. We have used that $v = v_{\bar{m}}, u = u_{\bar{m}}$ are independent of \mathbf{k} and \bar{m} for a flat band (see Eq. Eq. (G9)) and that $\text{Tr } P = N_f$. Noticing that $|\Delta|/E_{\bar{m}} = 2uv = 2\sqrt{\nu(1-\nu)}$, we get the zero-temperature superfluid weight

$$[D_s]_{ij} = 8 \frac{|U|^\epsilon}{V_c} \nu(1-\nu) g_{ij}. \quad (\text{G14})$$